



# Variable-Speed Power-Turbine for the Large Civil Tilt Rotor

*Mark Suchezky and G. Scott Cruzen  
Williams International Co. LLC*

## NASA STI Program . . . in Profile

Since its founding, NASA has been dedicated to the advancement of aeronautics and space science. The NASA Scientific and Technical Information (STI) program plays a key part in helping NASA maintain this important role.

The NASA STI Program operates under the auspices of the Agency Chief Information Officer. It collects, organizes, provides for archiving, and disseminates NASA's STI. The NASA STI program provides access to the NASA Aeronautics and Space Database and its public interface, the NASA Technical Reports Server, thus providing one of the largest collections of aeronautical and space science STI in the world. Results are published in both non-NASA channels and by NASA in the NASA STI Report Series, which includes the following report types:

- **TECHNICAL PUBLICATION.** Reports of completed research or a major significant phase of research that present the results of NASA programs and include extensive data or theoretical analysis. Includes compilations of significant scientific and technical data and information deemed to be of continuing reference value. NASA counterpart of peer-reviewed formal professional papers but has less stringent limitations on manuscript length and extent of graphic presentations.
- **TECHNICAL MEMORANDUM.** Scientific and technical findings that are preliminary or of specialized interest, e.g., quick release reports, working papers, and bibliographies that contain minimal annotation. Does not contain extensive analysis.
- **CONTRACTOR REPORT.** Scientific and technical findings by NASA-sponsored contractors and grantees.

- **CONFERENCE PUBLICATION.** Collected papers from scientific and technical conferences, symposia, seminars, or other meetings sponsored or cosponsored by NASA.
- **SPECIAL PUBLICATION.** Scientific, technical, or historical information from NASA programs, projects, and missions, often concerned with subjects having substantial public interest.
- **TECHNICAL TRANSLATION.** English-language translations of foreign scientific and technical material pertinent to NASA's mission.

Specialized services also include creating custom thesauri, building customized databases, organizing and publishing research results.

For more information about the NASA STI program, see the following:

- Access the NASA STI program home page at <http://www.sti.nasa.gov>
- E-mail your question via the Internet to [help@sti.nasa.gov](mailto:help@sti.nasa.gov)
- Fax your question to the NASA STI Help Desk at 443-757-5803
- Telephone the NASA STI Help Desk at 443-757-5802
- Write to:  
NASA Center for AeroSpace Information (CASI)  
7115 Standard Drive  
Hanover, MD 21076-1320



# Variable-Speed Power-Turbine for the Large Civil Tilt Rotor

*Mark Suchezky and G. Scott Cruzen  
Williams International Co. LLC*

Prepared under Contract NNC10BA15B

National Aeronautics and  
Space Administration

Glenn Research Center  
Cleveland, Ohio 44135

This report contains preliminary findings,  
subject to revision as analysis proceeds.

Trade names and trademarks are used in this report for identification  
only. Their usage does not constitute an official endorsement,  
either expressed or implied, by the National Aeronautics and  
Space Administration.

*Level of Review:* This material has been technically reviewed by NASA technical management OR expert reviewer(s).

Available from

NASA Center for Aerospace Information  
7115 Standard Drive  
Hanover, MD 21076-1320

National Technical Information Service  
5301 Shawnee Road  
Alexandria, VA 22312

Available electronically at <http://www.sti.nasa.gov>

# Contents

1.0 Introduction .....	1
Nomenclature .....	2
2.0 VSPT Concept Development .....	2
2.1 Figure of Merit .....	2
2.2 Efficiency Prediction Technique .....	4
2.3 Structural Constraints .....	5
2.4 Exhaust Constraint.....	5
2.5 List of Analytical Studies .....	6
2.6 Flow Path Selection: Cx/U .....	6
2.7 Work Coefficient .....	11
2.8 3–D Design Execution.....	17
2.9 Loss System Validation via CFD .....	19
2.10 Turbine Blade Incidence Study .....	19
2.11 Thin Turbine Blade Incidence Study.....	21
2.12 Third Stage Combined Incidence Study.....	24
2.13 Airfoil Leading Edge Geometry .....	27
3.0 VSPT LCTR Mission Performance Modeling .....	32
4.0 Development of a Cost-Effective Approach to an LCTR-Relevant VSPT Component Experiment .....	34
4.1 Experimental Test Plan and Instrumentation List .....	36
4.2 VSPT Component Experiment Program Plan, Schedule, and ROM Cost.....	38
5.0 Conclusions .....	40
Appendix A.—NPSS Outputs.....	43
Appendix B.—Definitions .....	51
Appendix C.—FlowPath Details.....	53
Appendix D.—Four Stage CFD Analysis.....	63
D.1 Stage 1 .....	64
D.2 Stage 2 .....	65
D.3 Stage 3 .....	67
D.4 Stage 4 .....	68
Appendix E.—Meanline Results for Four Stage: High Loading 1 .....	73
Appendix F.—Disk Sizing.....	75
Appendix G.—Efficiency and Reaction Definitions .....	77
Appendix H.—NPSS Output for Critical Mission Point .....	79
References.....	89

## List of Tables

Table 2.1—LCTR Mission Segments.....	3
Table 2.2.—Fuel Burn Comparison for High and Low CX/U Designs.....	10
Table 2.3.—Three-Stage Turbine Results.....	14
Table 2.4.—Four-Stage Turbine Segment Fuel Burn .....	16
Table 3.1.—Critical Mission Points.....	32
Table 4.1.—NASA GRC Single-Spool Turbine Test Facility Capabilities.....	34
Table 4.2.—Proposed Map/Test Plan .....	37
Table 4.3.—Proposed Instrumentation List for VSPT Component Experiment.....	38
Table A.1.—Sea level static (MRP) 100 percent NPT .....	43
Table A.2.—2,000 altitude, +45 °F day, hover (not at maximum power) 100 percent NPR.....	45

Table A.3.—Cruise mission 1, 303.4 kn, 28,000 altitude, +0 °F day, Initial cruise power level, 100 percent NPR rpm/650 rotor tip speed.....	47
Table A.4.—Cruise mission 1, 303.4 kn, 28,000 altitude, +0 °F day, Initial cruise power level, 54 percent NPR rpm/350 rotor tip speed—NO multispeed gearbox.....	49
Table H.1.—65 Percent Design Speed Take Off .....	80
Table H.2.—65 Percent Design Speed Climb.....	81
Table H.3.—65 Percent Design Speed Cruise .....	82
Table H.4.—75 Percent Design Speed Take Off .....	83
Table H.5.—75 Percent Design Speed Climb.....	84
Table H.6.—75 Percent Design Speed Cruise .....	85
Table H.7.—85 Percent Design Speed Take Off .....	86
Table H.8.—85 Percent Design Speed Climb.....	87
Table H.9.—85 Percent Design Speed Cruise .....	88

## List of Figures

Figure 1.1—NASA LCTR Concept.....	1
Figure 2.1.—LCTR Mission Profile .....	3
Figure 2.2—Falcon Meanline Code Interface.....	4
Figure 2.3.—Airfoil Shapes .....	7
Figure 2.4.—Low CX/U Design Velocity Triangles .....	8
Figure 2.5.—High CX/U Design Velocity Triangles.....	8
Figure 2.6.—Comparison of High and Low CX/U Flowpaths .....	9
Figure 2.7.—Design Speed Selection for High and Low CX/U Designs .....	11
Figure 2.8.—Work Coefficient Versus Flow Coefficient.....	12
Figure 2.9.—Work Coefficient Versus Flow Coefficient.....	12
Figure 2.10.—Comparison of Three Stage and Four Stage Turbine Flowpaths.....	13
Figure 2.11.—Turbine Design Speed Selection.....	14
Figure 2.12.—Smith Correlation for Three Turbines .....	15
Figure 2.13.—Four-Stage Turbine Flowpath.....	15
Figure 2.14.—Design Speed Versus Segment Fuel Burn .....	16
Figure 2.15.—Smith Correlation for Four Study Turbines .....	16
Figure 2.16.—Airfoil Stacking .....	18
Figure 2.17.—FoilGen Output.....	18
Figure 2.18.—Third Stage extracted from full simulation to investigate off-design performance.....	19
Figure 2.19.—Efficiency Comparisons for Four Turbine Designs.....	20
Figure 2.20.—A Simple Turbine Blade Cascade.....	22
Figure 2.21.—A sample thin blade cascade.....	22
Figure 2.22.—Blade Profile Modifications.....	23
Figure 2.23.—Thin turbine blade geometry compared to nominal.....	24
Figure 2.24.—Third Stage Speed Study composed of Three airfoils .....	25
Figure 2.25.—Third Stage Performance .....	25
Figure 2.26.—Third Vane Pressure Loss.....	26
Figure 2.27.—Vane Velocity Vectors.....	26
Figure 2.28.—Fixed geometry LE slats. Used with permission from Zenith Aircraft Company, Mexico, Missouri, 65265-0650. ....	28
Figure 2.29.—Typical Turbine Airfoil Leading Edge Profile .....	28
Figure 2.30.—Third Blade Mean, surface curvature smoothed.....	29
Figure 2.31.—Third Blade mid span static pressure distribution .....	30
Figure 2.32.—Smoothed third Blade Efficiency Trend with Speed .....	31

Figure 2.33.—Separation bubble visualization.....	32
Figure 3.1.—VSPT Total Mission Fuel Burn for Three Williams International Designs .....	33
Figure 4.1.—Schematic of Recommended Engine Configuration for LCTR.....	35
Figure 4.2.—VSPT Test Article Mated to NASA-GC Single Spool Turbine Test Facility .....	36
Figure 4.3.—Proposed Schedule for VSPT Experiment.....	39
Figure B.1.—Turbine AN <sub>2</sub> and Rim Speed Definitions .....	51
Figure C.1.—High Cx/U Four Stage .....	53
Figure C.2.—Low Cx/U Four Stage .....	54
Figure C.3.—Three Stage .....	55
Figure C.4.—Four Stage High Loading (1) .....	56
Figure C.5.—Four Stage High Loading (2) .....	57
Figure C.6.—SixStage High Cx/U.....	58
Figure C.7.—Three Stage B.....	59
Figure C.8.—Four Stage C .....	60
Figure C.9.—Smith Curve of All Turbines.....	61
Figure C.10.—Design Speed Comparison: All Turbines.....	61
Figure F.1.—Approximate Disk Size .....	75



## 1.0 Introduction

The Large Civil Tilt-Rotor (LCTR) is part of NASA's Heavy Lift Systems Investigation. This proposed 90 passenger aircraft would offload short to medium range air traffic from large airports and/or runways. Due to its vertical takeoff and landing capability, only a helipad would be needed within existing airport infrastructure (Figure 1.1).

The proposed vehicle has four turbo-shaft engines powering two rotors. Each engine is to develop 7,500 hp for a total 30,000 hp. The mission would require high rotor rpm at sea level take off (650 ft/s tip speed) and significantly lower rpm at cruise (350 ft/s tip speed) (Ref. 1). That is, the cruise rpm of the main rotors is 54 percent of the SLTO rpm. This requirement comes from the fact that the main rotors are more efficient at low rpm during the altitude cruise but require high rpm during sea level take-off (SLTO). The turboshaft engines will drive the main rotors through a gearbox enabling the high rpm power turbines (PT) to spin the low rpm (103 to 191 rpm) main rotors. Each main rotor is driven by two engines. There are two possible methods for achieving the required rpm sweep.

1. Two (or higher) gear-ratio transmission: with the power turbine operating at near constant rpm.
2. Fixed gear-ratio transmission: with the power turbine experiencing the full 54 to 100 percent speed range.

For method 1, the complexity of designing a flight weight, 15,000 hp transmission (two engines X 7,500 hp each), while obtaining high life and reliability is a formidable task. The method for changing gears (ex. torque converter, clutch, etc.) would also need to be addressed. This method is not within the scope of this study and will not be further considered.



Figure 1.1—NASA LCTR Concept

## Nomenclature

AN <sup>2</sup>	See Appendix B
C <sub>m</sub> /U	Flow Coefficient
C <sub>x</sub> /U	Flow Coefficient
Δh <sub>0</sub> /U <sup>2</sup>	Work Coefficient
FOM	Figure of Merit
h <sub>0</sub>	Total Enthalpy
LCTR	Large Civil Tilt-Rotor
LE	Leading Edge
η	Efficiency (see Appendix G)
NPSS	Numerical Propulsion System Simulator
PT	Power Turbine
SLTO	Sea Level Take Off
TE	Trailing Edge
U	Wheel Speed (usually associated with midspan)
VSPT	Variable Speed Power Turbine

## 2.0 VSPT Concept Development

### 2.1 Figure of Merit

In this study various techniques are investigated to improve efficiency and off-design characteristics of a power turbine operating in the LCTR mission. The relative performance of each design modification needs to be assessed using some form of figure of merit (FOM). The FOM chosen for this study is overall fuel burn during the mission. The overall mission profile is not well established at this time so a fictitious but representative mission needs to be assumed. Based on the work of Snyder and Thurman (Ref. 1), a study engine simulation was generated using the Numerical Propulsion System Simulator (NPSS). This simulation software has the ability to predict engine performance throughout the flight envelope based on performance maps of the individual engine components. Four output points were generated from this model and made available for this study. These four flight conditions are:

#### Point 1

SLTO;	100% PT Speed,	100ft,	0.0 Mach,	Std. Day
-------	----------------	--------	-----------	----------

#### Point 2

Climb;	100% PT Speed,	2,000ft	0.0 Mach	+45 °F
--------	----------------	---------	----------	--------

#### Point 3

Start Cruise;	100% PT Speed	28,000ft	0.51 Mach	Std. Day
---------------	---------------	----------	-----------	----------

#### Point 4

Cruise;	54% PT Speed	28,000ft	0.51 Mach	Std. Day
---------	--------------	----------	-----------	----------

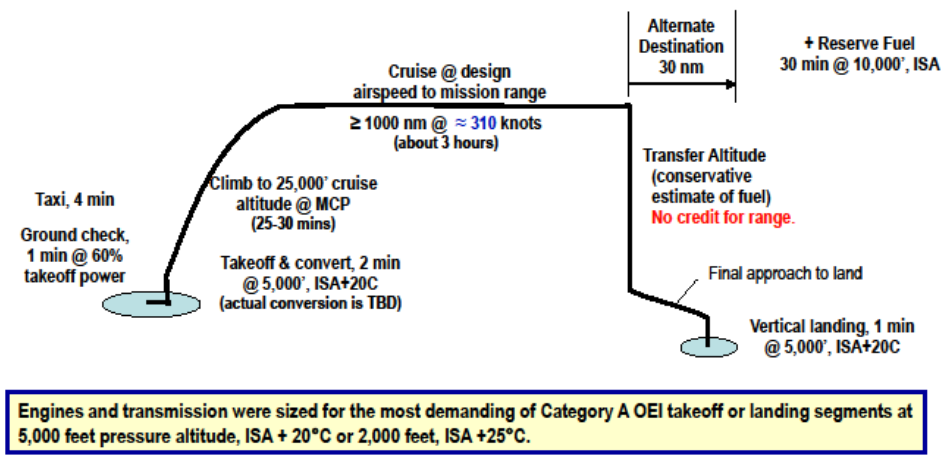
A detailed output from the NPSS cycle model is included in Appendix A. These four points are the only points currently available from the model and therefore a mission made up of only these four points was assumed. The actual mission will deviate significantly from this mission, but this mission is used as a starting point (Table 2.1).

This mission was made to mimic the mission shown in Figure 2.1, provided by C. Snyder of NASA at contract start.

TABLE 2.1—LCTR MISSION SEGMENTS

Point	Description	Δtime	Cycle PT	Power	Wf	PT	Fuel Burned	
		Minutes	ETA	hp	lbm/hr	Speed	lbm	
1	SLTO;100% PT Speed,100ft,0.0 Mach, Std. Day	2	0.85	7500	2581.28	100.0%	86.0	
2	Climb;100% PT Speed,2,000ft0.0 Mach+45°F	2	0.8266	4639.6	1761.6	100.0%	58.7	
3	Start Cruise;100% PT Speed 28,000ft 0.51Mach Std. Day	30	0.8485	2651.5	836.01	100.0%	418.0	
4	Cruise;54% PT Speed 28,000ft 0.51 Mach Std. Day	180	0.7859	2345.4	805.23	54.0%	2415.7	
3	Start Cruise;100% PT Speed 28,000ft 0.51Mach Std. Day	30	0.8485	2651.5	836.01	100.0%	418.0	
2	Climb;100% PT Speed,2,000ft0.0 Mach+45°F	2	0.8266	4639.6	1761.6	100.0%	58.7	
TOTALS		246	Minutes				3455.2	lbm
		-or-						
		4	hours					
		6	minutes					

 **LCTR Mission Profile (“similar” to Regional aircraft)**



*Mission fuel is cruise-dominated.  
 Propulsion system weight and overall fuel efficiency are critical.*

Figure 2.1.—LCTR Mission Profile

Unfortunately, cycle points such as idle and taxi were not available to use in this cycle so there is some error introduced. The mission used in this study (Table 2.1) includes a long cruise segment of 3 hr with ½ hr of climb condition before and after. There is also some high power SLTO time at the beginning and end of the mission to simulate vertical takeoff and landing.

Given the cycle predicted fuel burns at each condition and the assumed duration of each segment, the fuel burned can be integrated. (Eq. (1))

$$W_{fuel} = \sum_{seg=1}^{nseg} \dot{W}_{fuel} \times \Delta Time \tag{1}$$

Table 2.1 shows that the predicted fuel burn would be 3455.2 lbm of fuel per engine over the 4 hr and 6 min flight. Because all of the power to drive the main rotors comes from the power turbine, the fuel burn at any condition will be proportional to PT efficiency. Therefore we can evaluate the impact of predicted PT efficiencies ( $\eta_{PT}$ ) throughout the mission by scaling the fuel flows by the ratio of predicted  $\eta_{PT}$  to cycle  $\eta_{PT}$ .

$$W_{fuel} = \sum_{seg=1}^{nseg} \frac{\eta_{predicted}}{\eta_{cycle}} \dot{W}_{fuel} \times \Delta Time \quad (2)$$

Using this technique, a prediction for  $\eta_{PT}$  can be input into Equation (2) for each of the four cycle points and an overall mission fuel burn can be calculated. Comparing the new predicted fuel burn back to the cycle prediction (3455.2 lbm) yields the FOM used in this study.

## 2.2 Efficiency Prediction Technique

Efficiency predictions are made by the use of a ‘meanline’ analysis. The meanline used is proprietary to Williams International and is referred to as ‘MeanTurb’. MeanTurb is a row by row analysis tool that tracks the mean particle through each airfoil row. All three components of velocity are modeled which makes the tool very general and can be used for axial, mixed flow, or radial turbines. The velocity triangles are solved with the loss system, cooling flows (if applicable), gas properties, and seal leakages all converged simultaneously. The solution technique is to solve each blade row independently and then use small-change effects (Jacobian matrix) and Newton’s Method to close on continuity, angular momentum, and energy. The loss system used in this study is a combination of various public domain loss systems (Kacker and Okapuu (Ref. 4) and Moustapha, Kacker and Tremblay (Ref. 5)) with modifications based on Williams International experience.

The technique used to predict turbine efficiency is two parts. The first part is referred to as ‘design mode’. In this phase a simpler design-mode meanline called “Falcon” is used. This meanline is different from MeanTurb in that you specify mass-flow, power, pressure reaction and airfoil loading coefficient (Zweifel). The velocity triangles are calculated using nearly the same loss system as MeanTurb with several simplifying assumptions. Falcon is wrapped with a graphical user interface which allows for intuitive design as well as optimization functionality. Figure 2.2 is a screen shot of the interface.

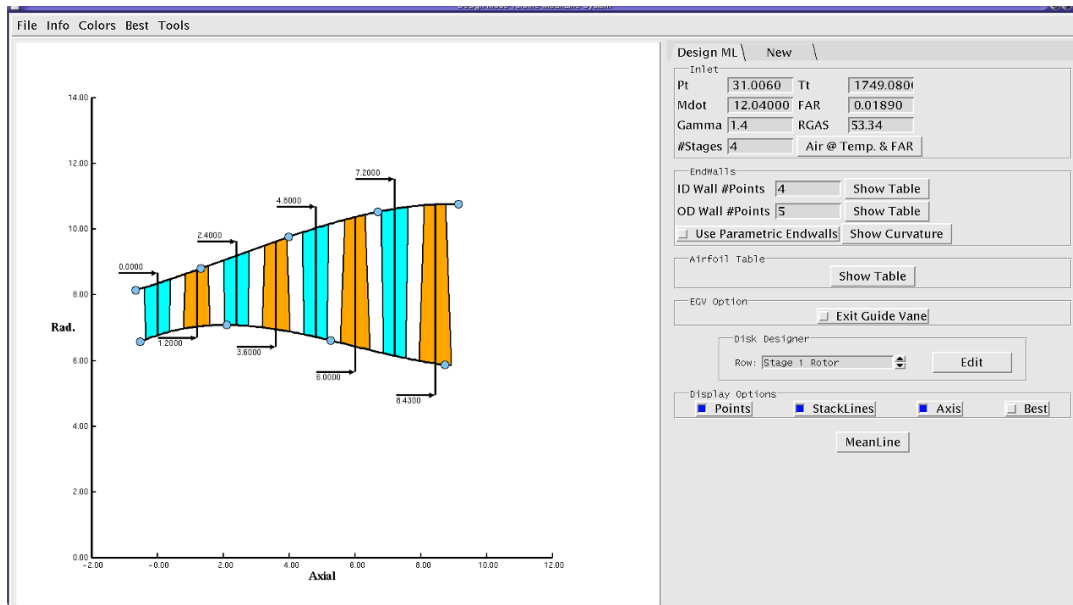


Figure 2.2—Falcon Meanline Code Interface

The second part of the efficiency prediction process begins after a satisfactory design has been produced in Falcon. Falcon writes out an off-design input file for MeanTurb. At this point the geometry is assumed fixed and parameters such as power, work split, reaction, mass-flow and efficiency are outputs of MeanTurb. One important point in this study is that the LE metal angles are assumed fixed so the impact of off-incidence design is captured in the MeanTurb calculations.

### 2.3 Structural Constraints

The 100 percent speed condition must be structurally viable. This study used aggressive  $AN^2$  and Rim Speed limits of 60. E9 in<sup>2</sup>·rpm<sup>2</sup> and 1200 ft/s respectively as upper limits. (See Appendix B for definitions.) The most challenging structural design will be the last stage blade which will have the largest span and highest pull stress. Fortunately it is also the coolest airfoil which aids in creep rupture life. Although challenging, these limits should be achievable for a long life application. After designing several flowpaths to this criterion, a sanity check calculation was performed. A meanline analysis was run for Point 1 (the hottest and fastest of the four performance conditions used) with the inlet temperature raised by 100 °F to simulate deterioration and hot day operation. The average blade pull-stress was estimated at 68 ksi and metal temperature at 1190 °F. Based on proprietary material databases, there are several commercially available alloys capable of >20,000 hr of useful life at these conditions. Over-speed protection in the event of a gearbox or coupling failure has not been addressed. It is possible that failure analysis may require more structural conservatism.

### 2.4 Exhaust Constraint

Choosing the exit annulus area determines the exit Mach number from the turbine (last blade, absolute frame of reference). The four cycle points given have nozzle (tail pipe) exit Mach numbers of about 0.27. This very low exit Mach number corresponds to a design philosophy of extracting as much energy out of the power turbine as possible and achieving nearly no thrust from the nozzle. Achieving such low exit Mach numbers at the exit of a gas turbine is difficult and results in large, heavy turbines operating at low rpm. It is more advantageous to design to an exit Mach number of .4 to .55 and diffuse through the exhaust system. For the purposes of this study, Mach numbers in this range will be used. In a more formal detailed design, a trade study between nozzle exit Mach number, turbine weight, exhaust system weight and fuel burn should be performed to find the best overall system trade.

It can be shown that the combination of the structural and exhaust constraints sets the turbine rpm and the last stage flowpath. That is: picking a Mach number exiting the turbine sets the turbine exit annulus area because of continuity (although swirl angle and boundary layer blockage play a role). Then, with  $AN^2$  already chosen, the rpm falls out. (See Appendix B for more information)

$$A = \text{function}(PT, TT, Mdot, Mach, Swirl) \quad (3)$$

$$\text{rpm} = \sqrt{\frac{AN^2}{A}} \quad (4)$$

The Rim Speed can be used to calculate the last blade trailing edge hub radius:

$$\text{Rim Speed(ft/s)} = \text{Radius}_{\text{Hub}} \text{ (in.)} / 12. * \text{rpm} * \pi / 30. \quad (5)$$

Then the trailing edge tip radius can be determined by the annulus area.

$$\text{Radius}_{\text{Tip}} = \sqrt{\frac{A}{\pi} + \text{Radius}_{\text{Hub}}^2} \quad (6)$$

From the above relations it is clear that selecting structural criteria and an exit Mach number uniquely defines the exit of the turbine and the rpm. In a more detailed engine design exercise, the front of the power turbine would need to mate to the exit of the previous turbine which would further define the

flowpath. In this work, no special attention is given to the proceeding turbine. Detailed design of the overall turbine section is out of scope.

## 2.5 List of Analytical Studies

Several analytical studies have been performed to gain confidence and reduce risk in designing a power turbine capable of nearly a 2X speed variation while maintaining acceptable efficiency levels.

1. Flow Path Selection
  - a. CX/U
  - b. Work Coefficient
  - c. Number of Stages
2. Loss System Validation via CFD
3. Incidence Tolerant Design
  - a. LE Shape
  - b. Airfoil Thickness

## 2.6 Flow Path Selection: Cx/U

Turbine Flow Coefficient, commonly referred to as Cx/U, is the ratio of through-flow velocity to mean wheel speed. Often Cx/U is referred to as axial velocity over wheel speed but in this study the radial velocity is taken into account. The meridional velocity is used instead and defined as:

$$V_{\text{meridional}} \equiv \sqrt{V_{\text{axial}}^2 + V_{\text{radial}}^2} \quad (7)$$

For the purposes of this study, Cx/U and Cm/U will be used synonymously and is defined as:

$$C_m / U = C_x / U \equiv \frac{\sqrt{V_{\text{axial}}^2 + V_{\text{radial}}^2}}{\omega \bar{r}} \quad (8)$$

where:

- all values are calculated at the TE plane of the turbine blade
- $\bar{r}$  equals the average of the hub and tip radius of the blade TE

The Flow Coefficient, Cx/U is a good indicator of the velocity triangles. Low Cx/U designs are characterized by high turning and relatively low velocity whereas high Cx/U designs tend towards low turning (camber) and higher velocities. The airfoil shapes can be dramatically different as shown in Figure 2.3.

The off-incidence loss generated at the LE of an airfoil is a function of two factors: 1) Loss Coefficient and 2) Inlet dynamic head. Low CX/U designs have lower LE Mach number but higher swings in incidence. High CX/U designs have lower excursions in incidence but always operate at higher inlet Mach number. Therefore it is reasonable to assume that there is an optimum CX/U for off incidence performance. Figure 2.4 and Figure 2.5 show a simplified example of velocity triangle for Low versus High CX/U designs.

For the VSPT, the corrected speed variation is from 54 to 100 percent. This implies that the wheel speed (U) varies from 54 to 100 percent but velocity triangle analysis shows that the Cx is nearly constant. Therefore, CX/U is approximately inversely proportional to speed.

Two flowpaths were generated to look at the impact of CX/U on mission fuel burn. The design philosophy was to follow the structural and exhaust constraints as given in the previous section and build turbine flowpaths that have good cruise velocity triangles and airfoil loadings. Once the flowpaths are established, MeanTurb is run to investigate the off design characteristics. Very good cruise performance (>90 percent) is achieved with four stage turbines. See Figure 2.6.

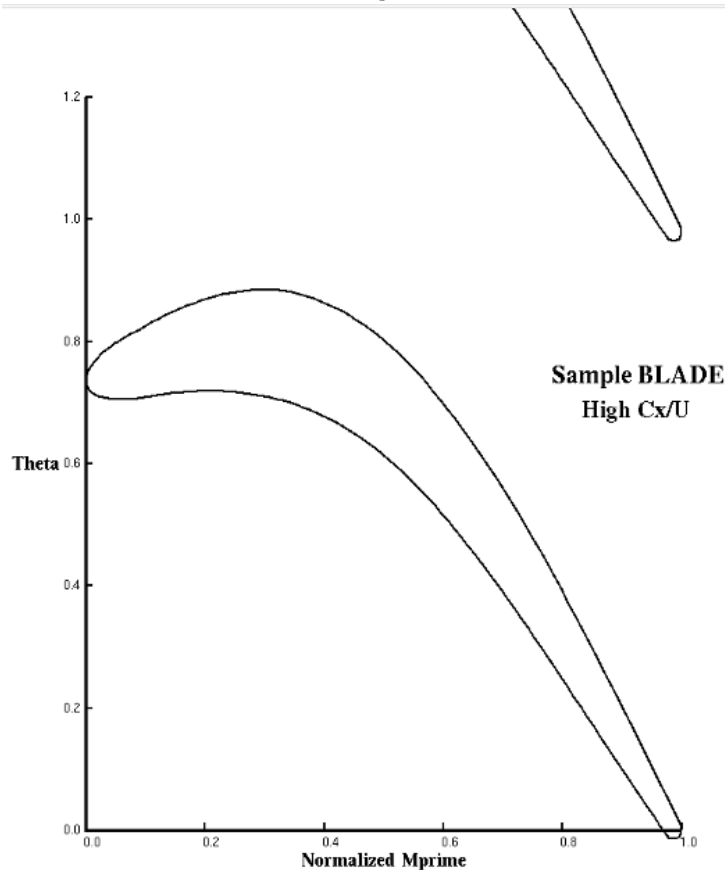
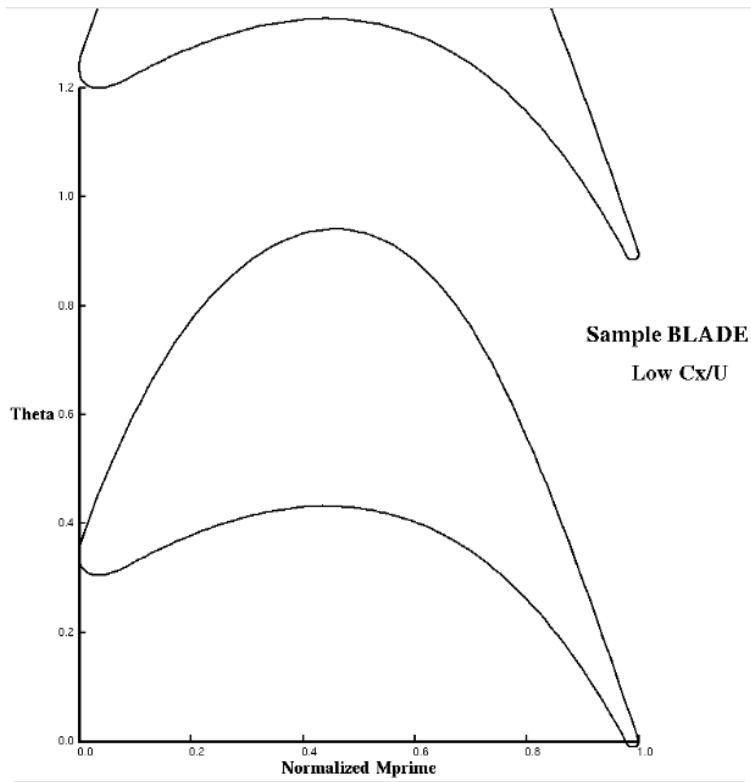


Figure 2.3.—Airfoil Shapes

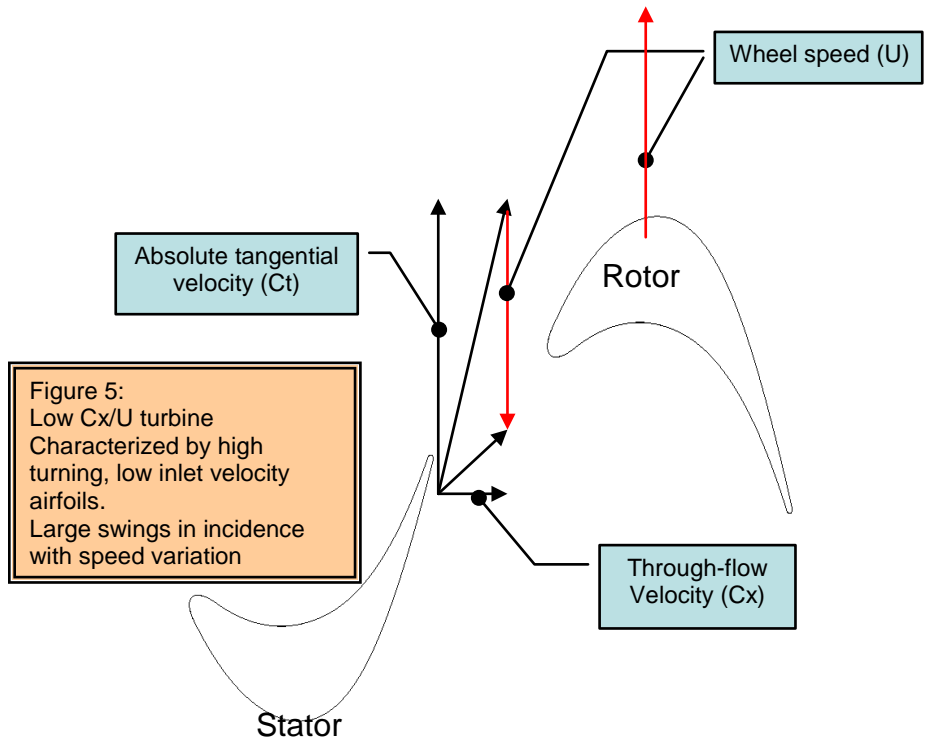


Figure 2.4.—Low  $C_x/U$  Design Velocity Triangles

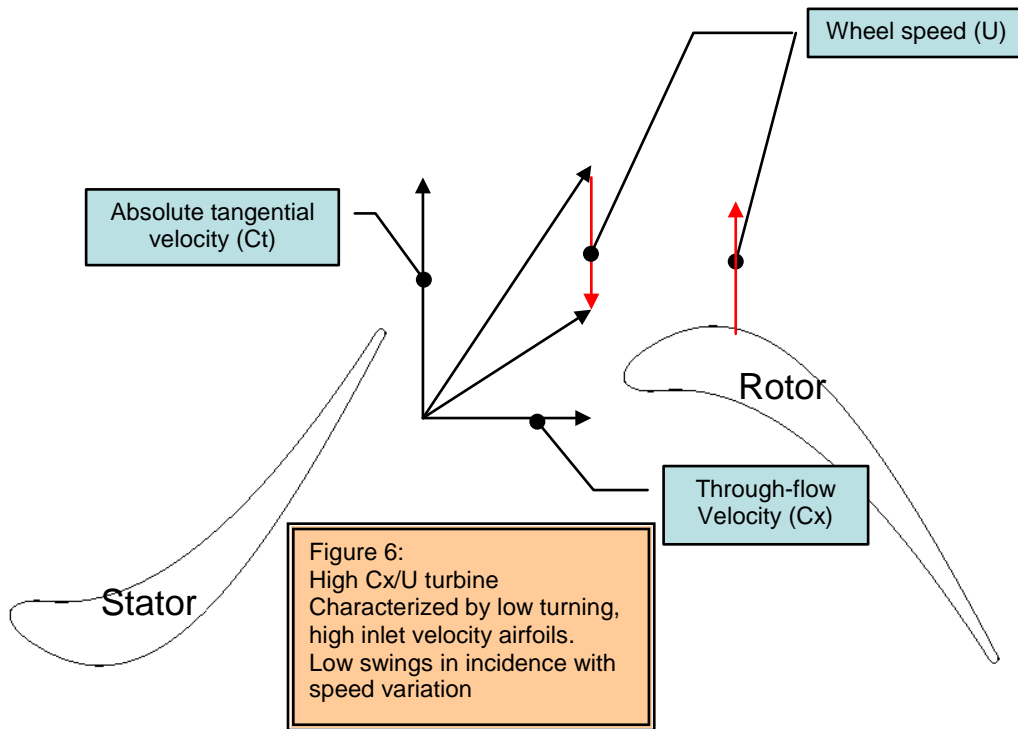


Figure 2.5—High  $C_x/U$  Design Velocity Triangles

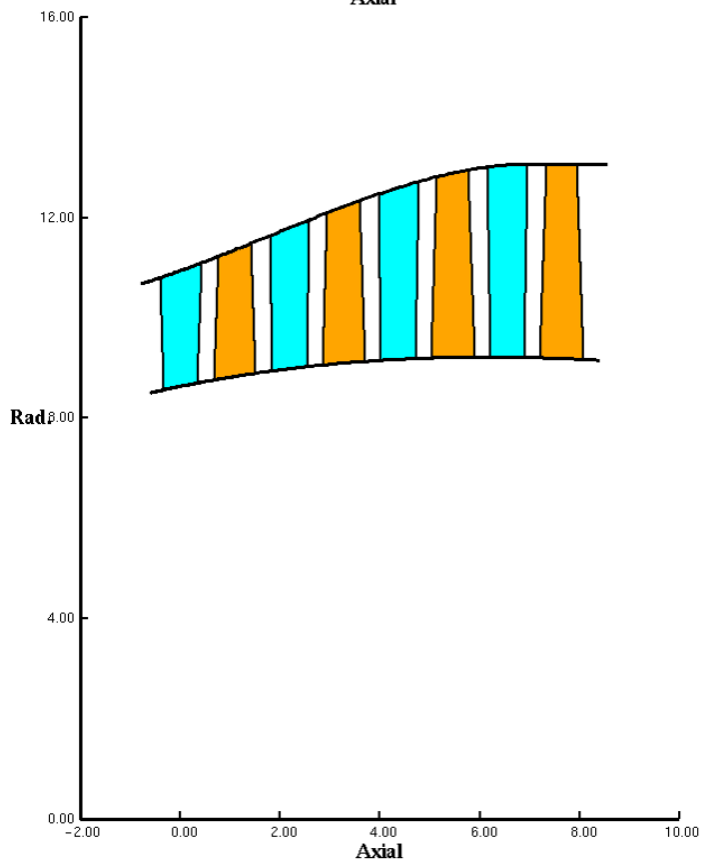
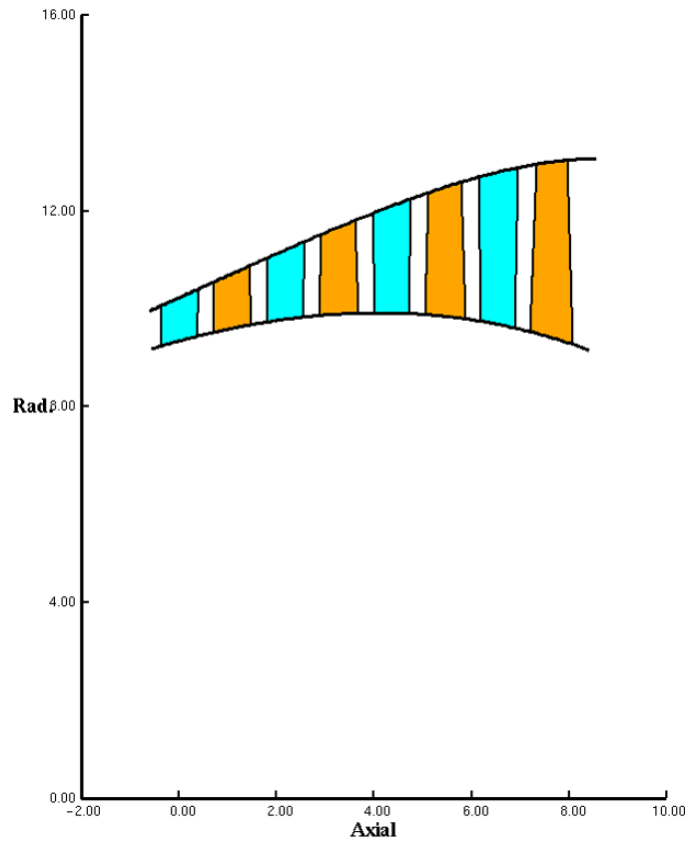


Figure 2.6.—Comparison of High and Low CX/U Flowpaths

If the turbines in Figure 2.6 were designed for the low speed cruise condition (54 percent speed), they would have predicted efficiencies of 91.4 and 90.2 percent respectively when operating at that design point. Unfortunately, each of these turbines is predicted to have an efficiency of 69.3 percent when operating at the high speed cruise condition (100 percent speed). Likewise, if the two turbines were designed for the 100 percent speed condition, the efficiencies would be 92.8 and 91.4 percent respectively. These turbines both would have very low efficiencies (<58 percent) when operating at the 54 percent speed conditions. Of course, these off-design efficiency predictions are highly dependent on the empirical loss system used in the meanline prediction system. Nonetheless, a compromised design point somewhere between 54 and 100 percent would most likely be a good compromise. A method for determining the optimal design point was developed. Four design speeds were chosen: 54, 69, 85 and 100 percent speed. A preliminary design was produced for each of these turbines at each of these speeds. This preliminary design process sets the LE metal angles and blade counts for the velocity triangles corresponding to that speed. Each of these designs was then run off-design using MeanTurb to the four different mission points in order to predict the efficiency. The resulting efficiencies are available in Table 2.2. For each of these designs, the resulting efficiencies for points 1, 2, 3, and 4 were used in Equation (2) (via spread sheet) and the overall impact to mission fuel burn was calculated, the results of which are also included in Table 2.2.

The results of Table 2.2 are plotted in Figure 2.7. From this plot, the best design practice is to pick a design point that is compromised between the low speed and high speed cruise but favoring the low speed cruise condition. An unexpected outcome of this study is the fact that both the High CX/U design and the Low CX/U design optimize at about the same speed and result in about the same overall fuel burn. Neither design philosophy appears to have an advantage. There is no compelling evidence from this study that CX/U (in of itself) is a determining factor in the design of this type of turbine.

TABLE 2.2.—FUEL BURN COMPARISON FOR HIGH AND LOW CX/U DESIGNS

**High CX/U**

<b>% Speed</b>	<b>Design RPM</b>	<b>Fuel Burn%</b>	<b>ETA 1</b>	<b>ETA 2</b>	<b>ETA 3</b>	<b>ETA 4</b>
53.8	8045	-3.29	73.34	68.62	69.34	91.39
69.2	10343	-7.88	88.33	84.71	84.12	88.62
84.6	12642	1.41	92.95	90.84	90.63	74.87
100.0	14941	23.20	91.25	91.58	92.80	57.42

**Low CX/U**

<b>% Speed</b>	<b>Design RPM</b>	<b>Fuel Burn%</b>	<b>ETA 1</b>	<b>ETA 2</b>	<b>ETA 3</b>	<b>ETA 4</b>
53.8	8045	-2.22	69.98	66.62	69.30	90.20
69.2	10343	-7.80	87.58	83.60	82.85	89.14
84.6	12642	-1.84	92.00	89.60	89.44	78.75
100.0	14941	24.30	89.29	89.78	91.43	57.00

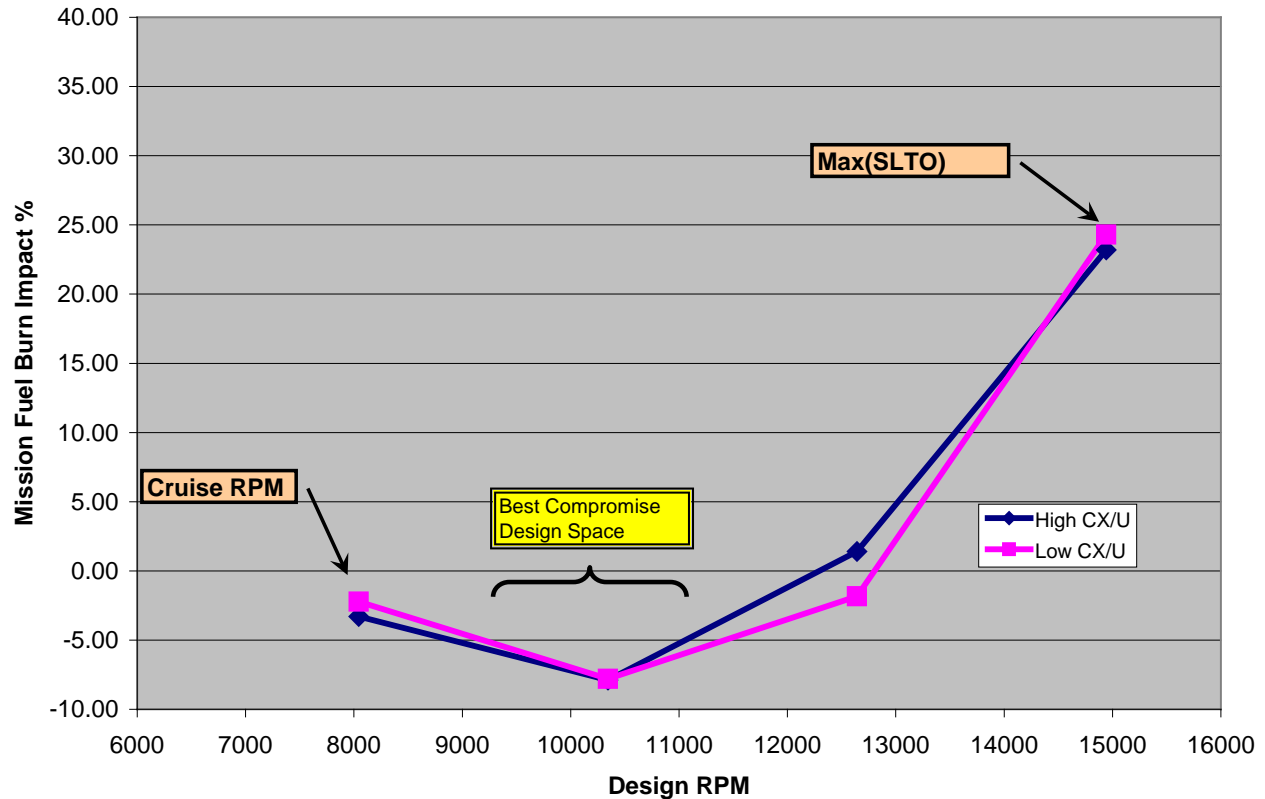


Figure 2.7.—Design Speed Selection for High and Low CX/U Designs

## 2.7 Work Coefficient

The Work Coefficient ( $\Delta h_0/U^2$ ) is a dimensionless parameter relating the turbine work to the mean wheel speed of the turbine. The use of Work Coefficient (Wcoeff) combined with Flow Coefficient (Cx/U) was popularized by Smith (Ref. 6) with his correlation of turbine efficiency using both parameters. Smith showed that there was an optimum relationship between the two parameters. There is no indication that Smith's 1965 correlation considered turbines operating far off-design so it is not obvious whether his correlation is helpful in determining optimum velocity triangles for the LCTR power turbine application when operating at its full range of speeds. The Smith correlation was presented (Ref. 6) as a plot and Figure 2.8 is a reproduction produced by digitizing the figure in his paper.

Assuming the LCTR power turbine is designed at the 54 percent cruise condition, then as the turbine transitions from 54 to 100 percent speed, the Flow Coefficient (Cx/U) and Work Coefficient ( $\Delta h_0/U^2$ ) change considerably. MeanLine and cycle analysis confirm that  $\Delta h_0/U^2$  is nearly proportional to  $1/\text{rpm}^2$  and Cx/U is nearly proportional to  $1/\text{rpm}$ . Therefore the Wcoeff increases by  $1/.54^2$  or 3.4 times when the rotor speed drops from 100 to 54 percent rpm. Likewise the Cx/U increases by a corresponding factor of  $1/.54$  or 1.85. If Smith's correlation indicates optimum relationships between these two parameters, it is reasonable to assume that it may provide some guidance in designing a turbine that transitions over a large swing in these parameters. The two turbines in the Cx/U study were placed on the Smith correlation in Figure 2.9.

### Smith Correlation

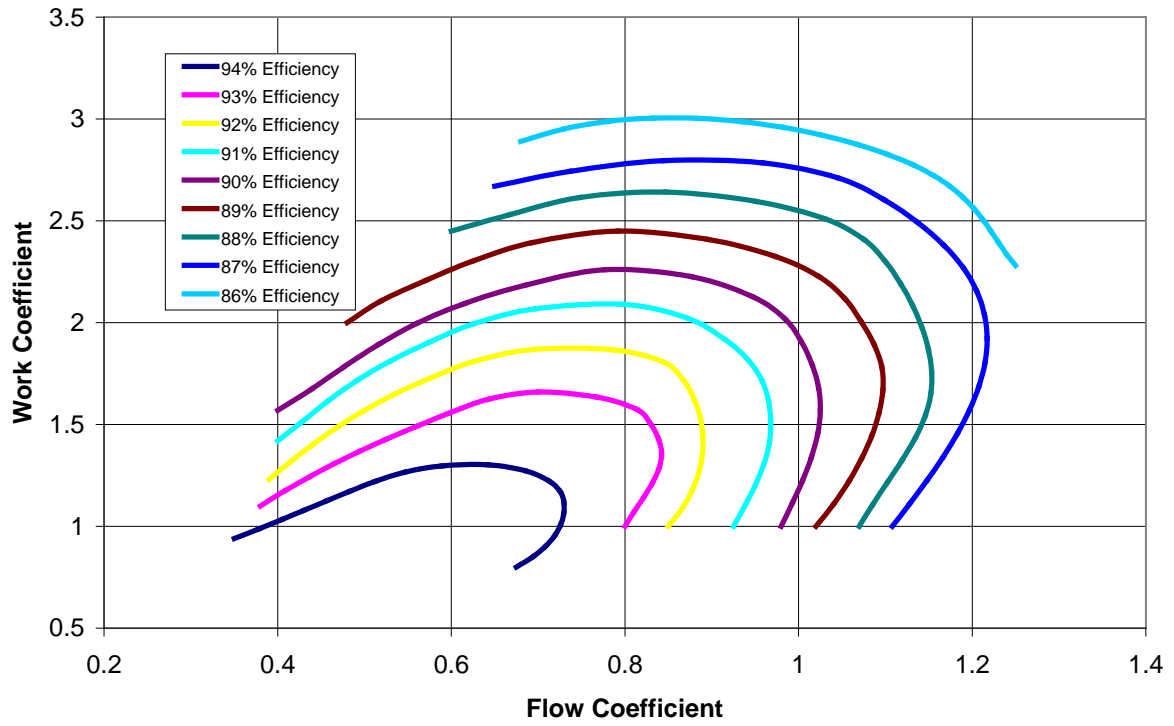


Figure 2.8.—Work Coefficient Versus Flow Coefficient

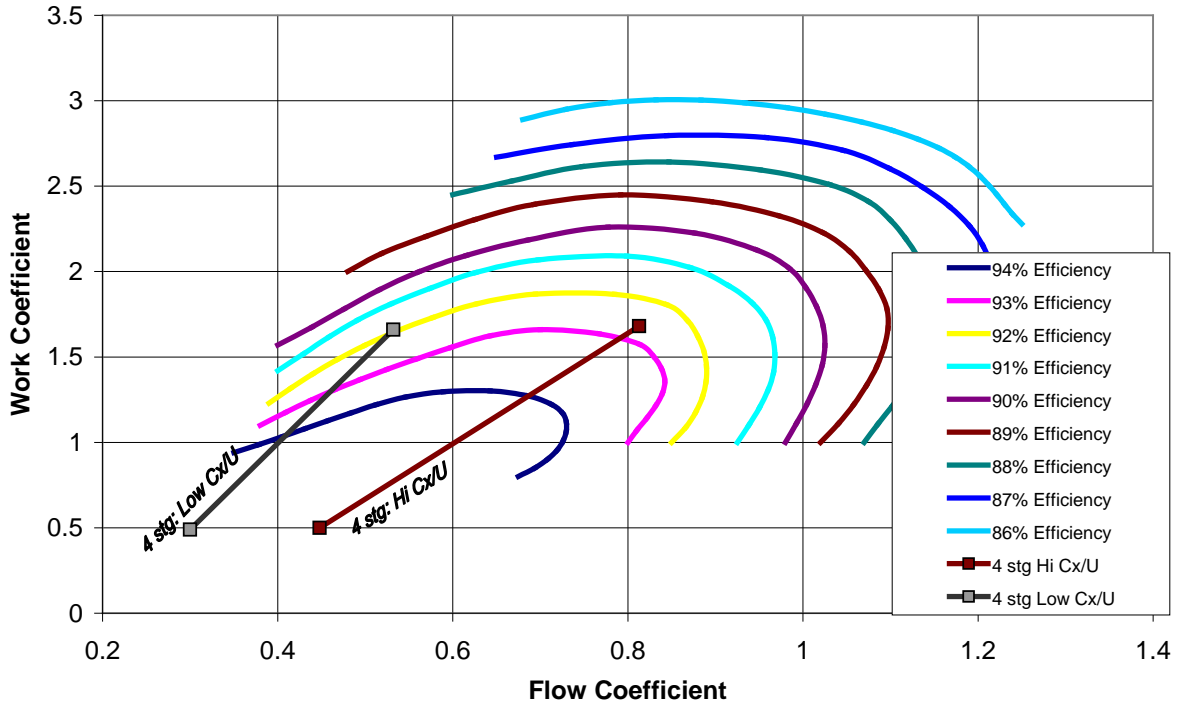


Figure 2.9.—Work Coefficient Versus Flow Coefficient

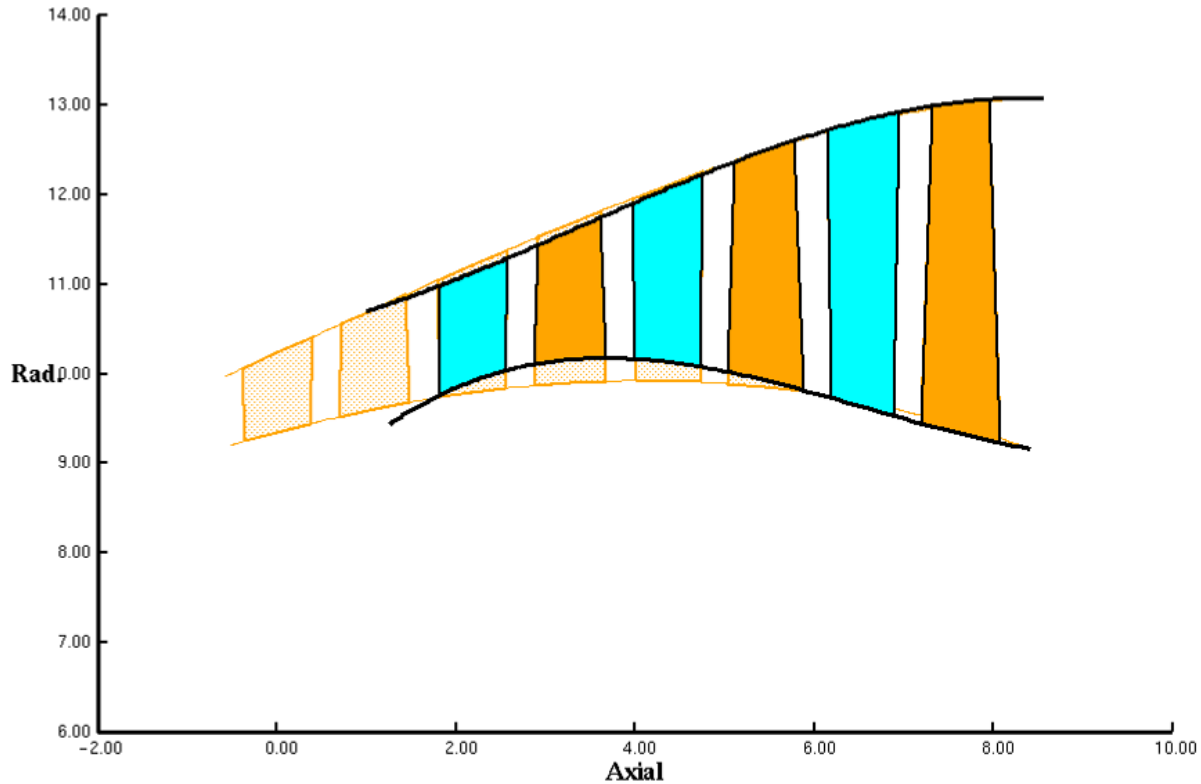


Figure 2.10.—Comparison of Three Stage and Four Stage Turbine Flowpaths

From this plot, the high  $C_x/U$  flowpath is shown to transition through the heart of the efficiency islands while the low  $C_x/U$  is in a non-optimum part of the correlation.

Both flowpaths developed in the  $C_x/U$  study have similar Work Coefficients which drop to very low levels when the rotor rpm is at 100 percent. These low levels are outside of normal gas turbine design experience. Another study was conducted to investigate the impact of running to higher Work coefficients in order to assure operation within the traditional design space. A new flowpath was generated by removing the first stage but holding the same rpm and about the same overall radius of the last three stages. This Three Stage turbine has the same power and speed as the two four stage turbines already analyzed but the average work per stage is higher (by the ratio of 4/3). Figure 2.10 compares the Three Stage turbine with the High  $C_x/U$  four stage design from the previous study.

The same process of picking four design speeds, calculating efficiency at each of the four mission points, and integrating the fuel burn across the mission was performed with the Three Stage design. Table 2.3 documents the results and Figure 2.11 plots the Three Stage turbine results against the results of the Four Stage  $C_x/U$  study.

The Three Stage does not show a predicted improvement in overall fuel burn relative to the lower work four stage designs, but it does show a significantly different trend. Figure 2.11 shows that the Three stage turbine is more forgiving than any of the Four Stage designs in choosing the design speed. It also indicates that the optimal design speed is closer to the SLTO rpm which is different than the previous two designs and is not the expected result. In Figure 2.12, the Three Stage turbine is shown on the Smith Correlation compared to the two Four Stage designs. The Three Stage falls between the two Four Stage designs. If the Smith Correlation were a good indicator of off-design capability, then it could be expected that the Three Stage design would have off-design performance characteristics between the two Four Stage designs: which it clearly does not.

The large difference in character between the Three Stage and Four Stage designs begs the question as to what makes the Three Stage so different. The difference in Work Coefficient appears to have played

a significant role. At 54 percent speed, the Work coefficient of the Three Stage turbine is about 2.1 which is well within design experience. Designing to higher Work Coefficient may further improve performance. Higher Work Coefficients are generally more challenging to design because they result in higher airfoil turnings and Mach numbers. The practical limit is approximately 3.0, above which the design becomes very challenging. To assess whether higher Work Coefficient is better for overall mission fuel burn, a High Work Four Stage turbine was designed (Figure 2.13). The Work Coefficient at the 54 percent cruise speed was set at 2.83 and the Flow Coefficient was set to 1.0 in an attempt to stay in the center of the Smith Correlation. After the same process of picking four design speeds, calculating efficiencies, and integrating mission fuel burn, this design proved to be the best out of a total of 8 flowpaths that were examined (Table 2.4). The flowpath is reduced in radius relative to the designs presented so far, making it smaller and lighter, which is an added benefit. (Figure 2.14)

The fuel burn calculation versus speed plot for this turbine is shown in Figure 2.14.

The corresponding Smith Curve correlation is shown in Figure 2.15.

TABLE 2.3.—Three-STAGE TURBINE RESULTS

**3 Stage**

% Speed	Design RPM	Fuel Burn%	ETA 1	ETA 2	ETA 3	ETA 4
53.8	8045	-1.11	70.57	66.14	67.52	89.72
69.2	10343	-4.51	78.24	74.89	74.04	89.63
84.6	12642	-7.19	93.53	91.76	91.60	84.44
100.0	14941	-6.36	92.35	92.49	93.53	66.26

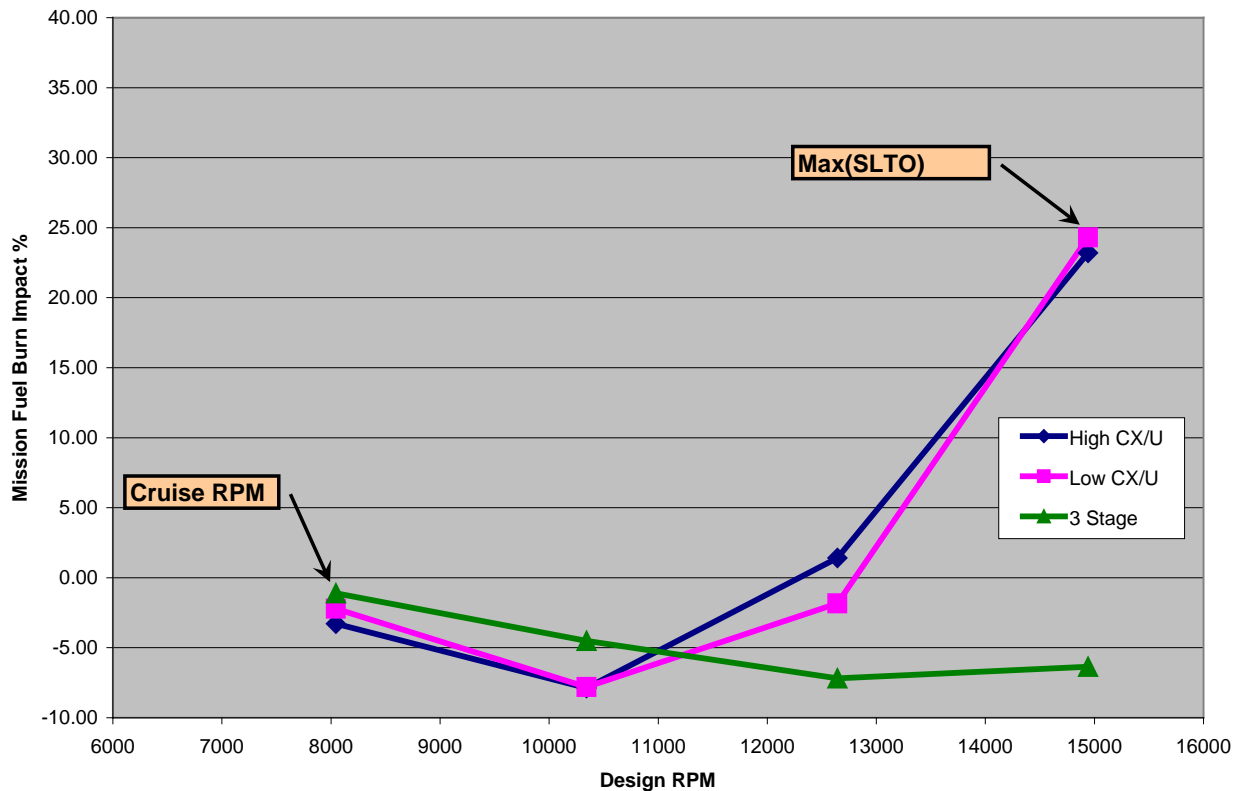


Figure 2.11.—Turbine Design Speed Selection

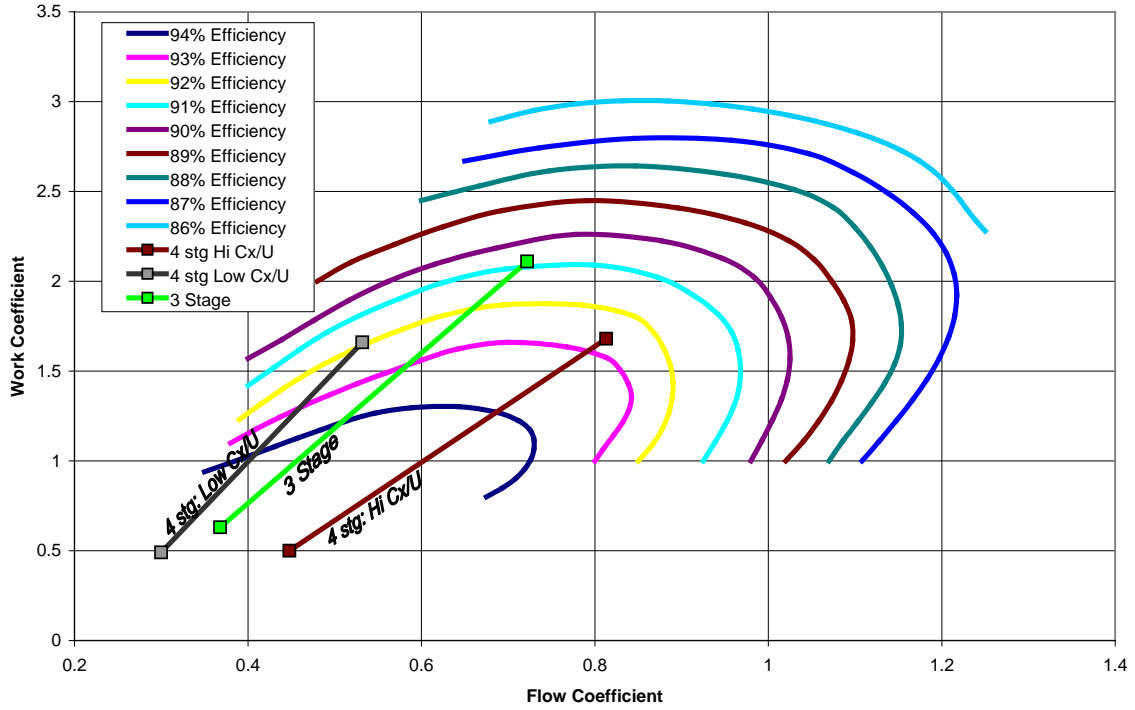


Figure 2.12.—Smith Correlation for Three Turbines

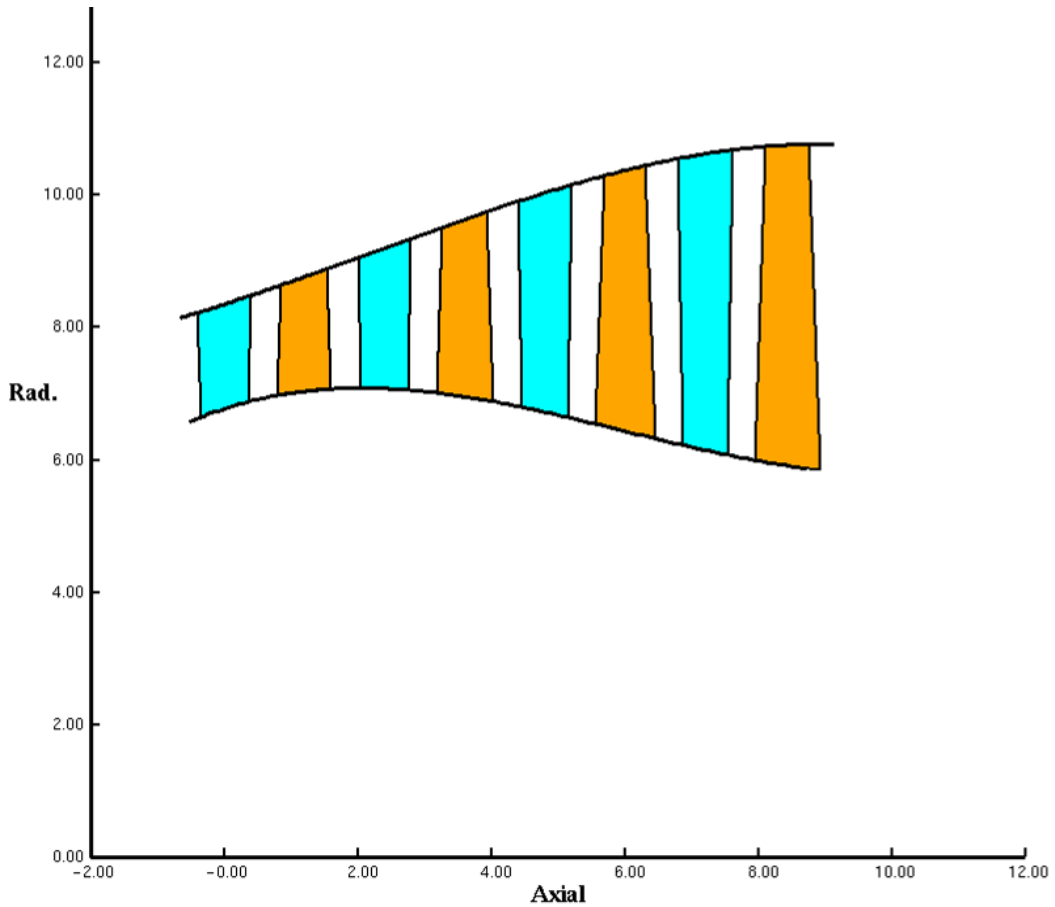


Figure 2.13.—Four-Stage Turbine Flowpath

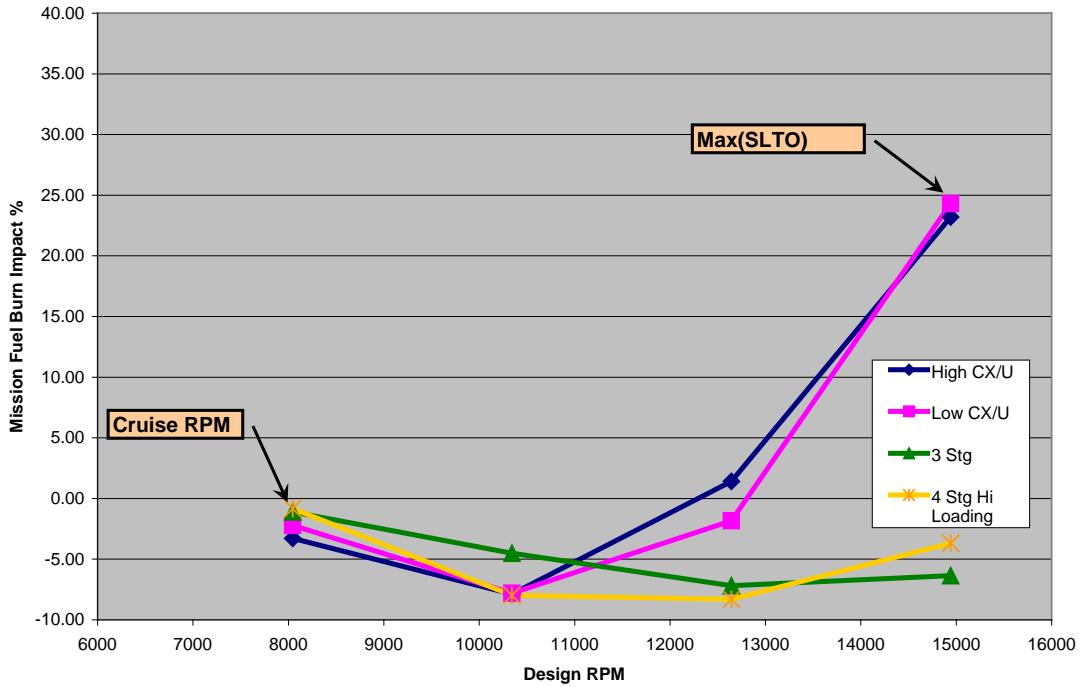


Figure 2.14.—Design Speed Versus Segment Fuel Burn

TABLE 2.4.—FOUR-STAGE TURBINE SEGMENT FUEL BURN  
4 Stg Hi Loading (1)

% Speed	Design RPM	Fuel Burn%	ETA 1	ETA 2	ETA 3	ETA 4
53.8	8045	-0.84	78.77	71.42	69.10	87.45
69.2	10343	-7.98	90.15	87.28	87.13	87.37
84.6	12642	-8.31	93.67	92.32	92.37	85.64
100.0	14941	-3.68	93.96	93.59	94.26	79.31

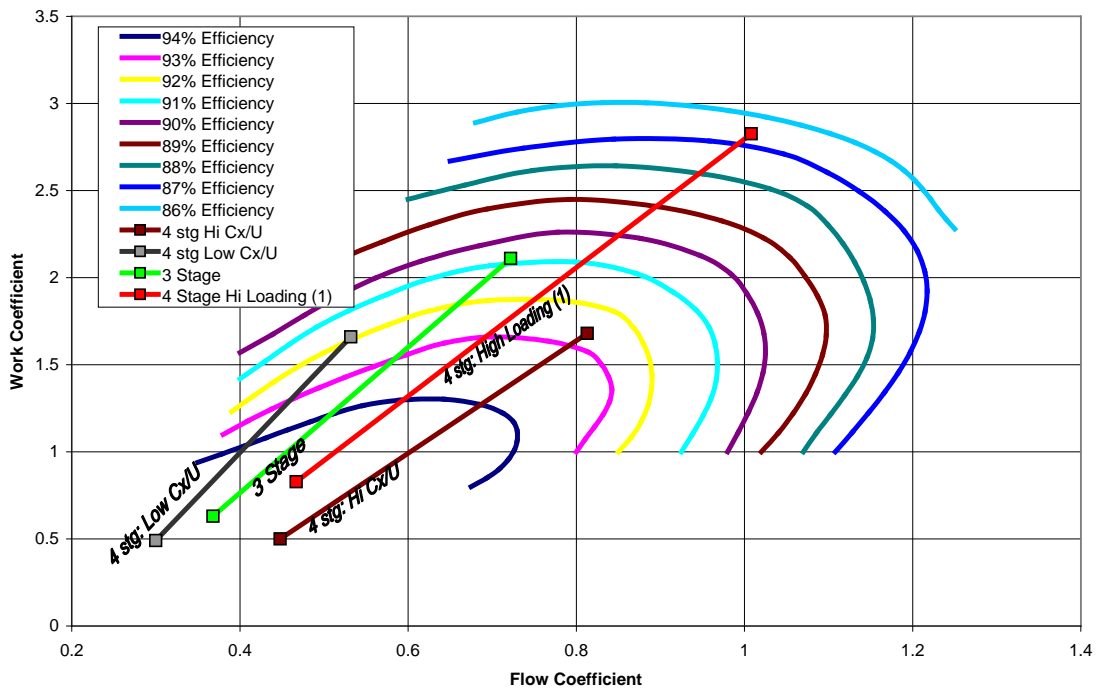


Figure 2.15.—Smith Correlation for Four Study Turbines

A complete description of the 8 flowpaths examined in this study is provided in Appendix C.

This flowpath (Four Stage: High Loading 1) emerges from the flowpath study as having the best potential to minimize mission fuel burn. This conclusion is based on the assumption that the meanline loss model and, more specifically, the off-design loss model adequately predict the efficiency characteristics through a significant range in incidence and loading. Presumably, the design is centered in the design space such that the turbine will not rapidly lose performance as speed and loading change throughout the flight envelope. In order to gain confidence in this conclusion, a 3-D design was executed at 75 percent speed (11174 rpm) and investigated in various CFD simulations. Appendix D contains both the 3-D and 1-D analysis summaries for the design conditions. An additional summary of the meanline predictions for 54 and 100 percent design speed is presented in Appendix E. This is provided to illustrate the large impact of the full speed variation and its implication to the design velocity triangles.

## 2.8 3-D Design Execution

Airfoils were designed consistent with the chosen flowpath (Four Stage: High Loading 1). The design was executed at 75 percent speed, i.e., 11174 rpm. The basic methodology for executing the 3-D design was as follows:

- Each of the 8 airfoils is designed by stacking three 2-D design sections, i.e., a hub section, a mean section and a tip section. (Figure 2.16)
- Each 2-D section is manually designed in an interactive design tool called “FoilGen”. (Figure 2.17) FoilGen has a variety of tools that allow for simple structural analysis, 2-D aerodynamics, 3-D stacking and airfoil internal core validation if applicable.
- Design iterations are passed through an in-house 3-D solver called VORTEX. VORTEX has an inviscid mode with an empirical loss model which aids in establishing the correct velocity triangles in the absence of viscous effect. This solver runs fast enough to execute several design iterations per day.
- Designs are validated via viscous simulation. VORTEX can be run with the full Navier Stokes equations turned on. The turbulence model is the  $\kappa\text{-}\omega$  model with integration to the walls (no wall functions). A steady state mixing plane assumption was used at the interface between stators and rotors.

The full Four Stage design was executed at 75 percent speed which is consistent with Figure 2.14. This places the design point approximately half way between the cruise (54 percent speed) and the SLTO (100 percent speed) conditions. The airfoil geometry was not refined to a final status for all 8 airfoils, but only to a satisfactory level for further study. The third Stage was chosen as a representative stage for more in-depth analysis. The third Stage design was pulled out and further refined (Figure 2.18). Calculations were performed using boundary conditions from the full Four stage calculation. A detailed review of the full four stage 3-D CFD run is documented in Appendix D.

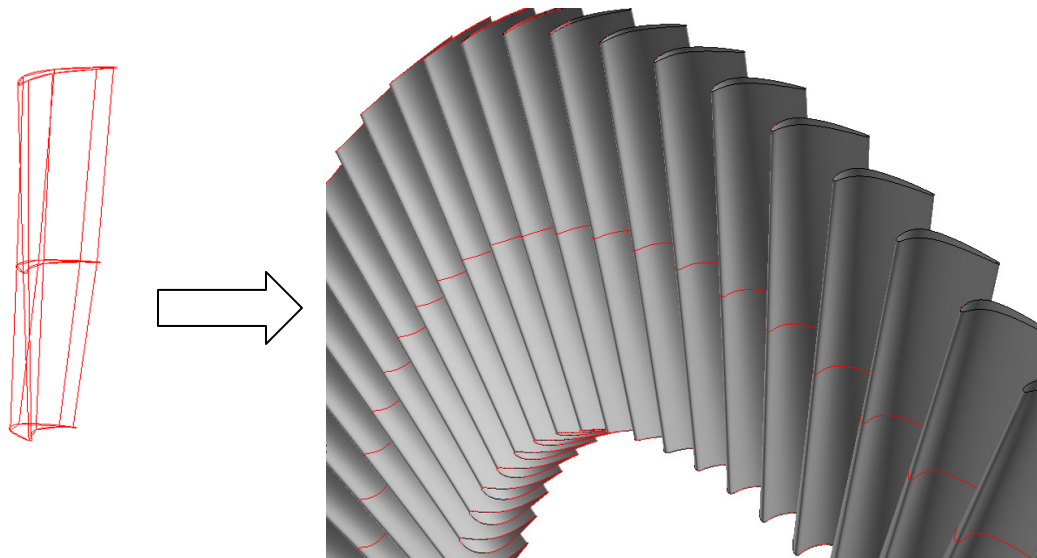


Figure 2.16.—Airfoil Stacking

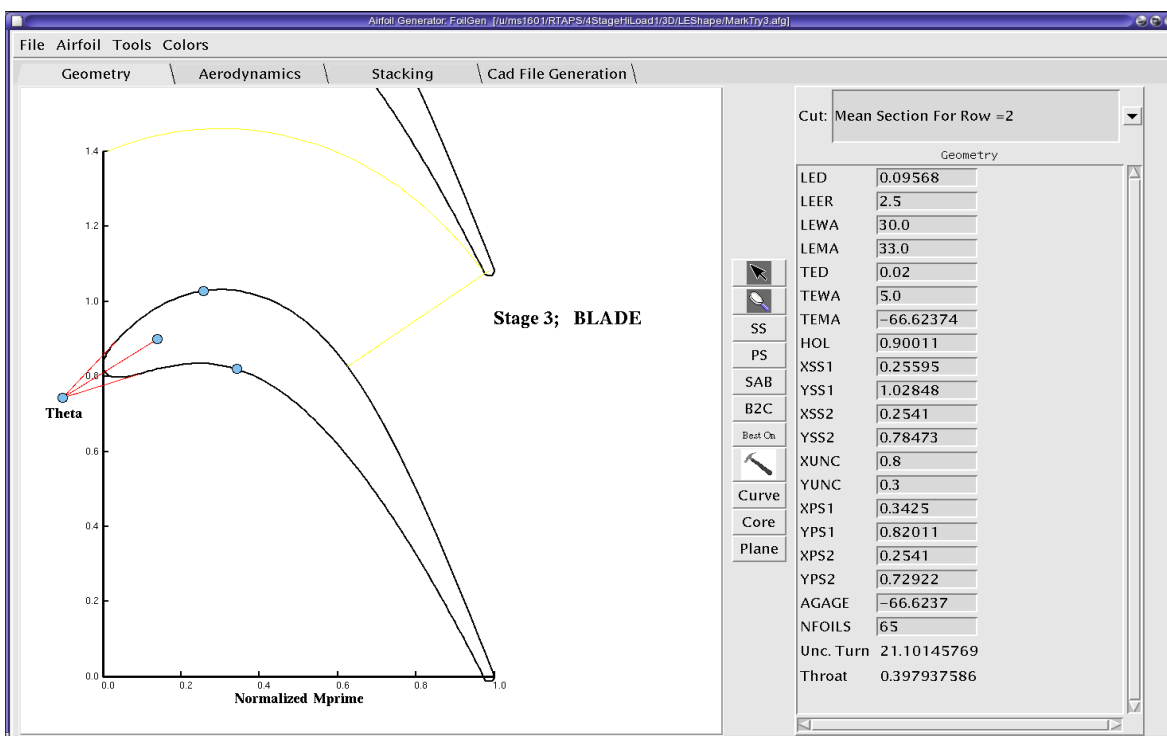


Figure 2.17.—FoilGen Output

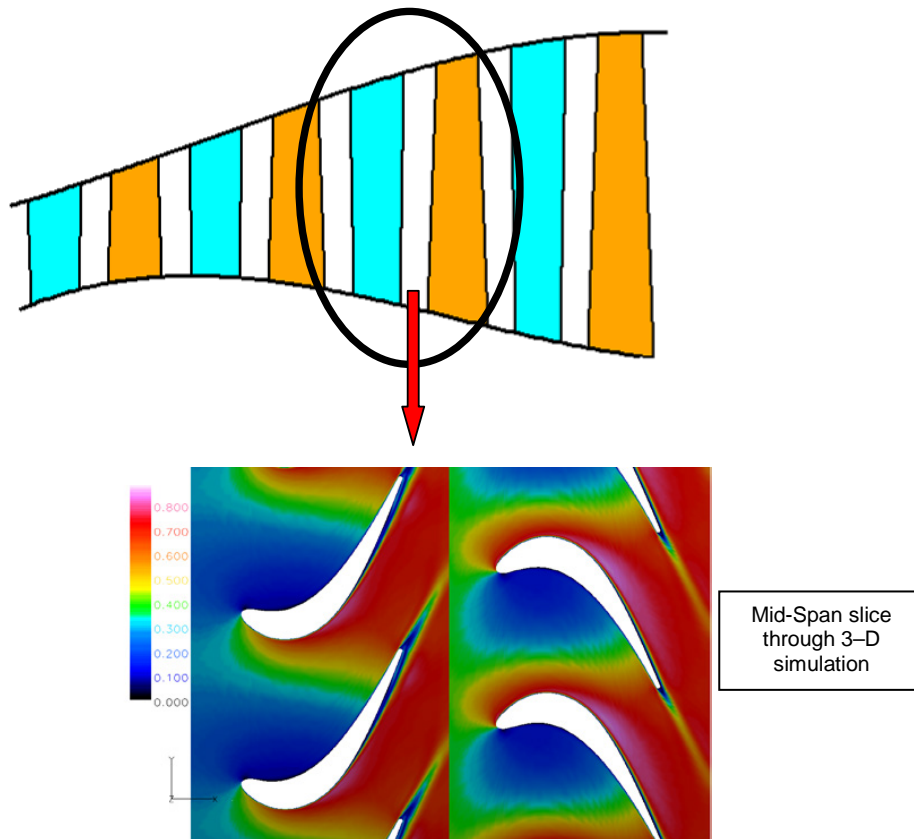


Figure 2.18.—Third Stage extracted from full simulation to investigate off-design performance

## 2.9 Loss System Validation via CFD

The optimum flowpath selected for this turbine and the choice of design speed relies on the off-design predictive capability of the meanline analysis. In order to assess the validity of this model, various CFD models were exercised. The third stage vane and blade were chosen as a representative set of airfoils. Two separate studies were performed. The first study addresses the incidence tolerance of the third blade and the other adds the vane and assesses the third stage together. The blade study was performed with two different blade thicknesses.

## 2.10 Turbine Blade Incidence Study

The third stage vane and blade were run together through a series of CFD runs. All CFD runs are based on steady state assumptions using mixing planes to account for time averaging between stationary and rotating frames. The inlet conditions (Total Pressure, Total Temperature, and gas angles) to the third vane were held fixed and the exit static pressure from the third blade was also fixed. The CFD was then run over a sweep of rpm. This analysis will simulate the incidence and loading sweeps that the blade would undergo throughout the operating envelope while the vane remains fixed at design point. The meanline was run exactly the same way to predict the efficiency changes as the speed changes. Both the meanline and the CFD assume no leakage flows, cooling flows or tip clearance. The meanline has a real gas model while the CFD runs assume ideal gas. The CFD confirms the large incidence swing and loading changes that are expected as the rpm is varied. Four different CFD simulations were performed; each one was swept through the speed range. All four simulations predict better incidence tolerance than the meanline correlation. This result is particularly satisfying because the meanline prediction was better

than the cycle simulation. If actual incidence tolerance is better than the meanline characteristic, than overall engine performance should surpass the NPSS simulation.

The four CFD simulations used are:

1. VORTEX (Williams International proprietary solver).  $\kappa\text{-}\omega$  turbulence model, integrated through boundary layers to the wall.
2. FLUENT (ANSYS, Inc.)  $\kappa\text{-}\epsilon$  realizable, using wall functions
3. FLUENT  $\kappa\text{-}\omega$  turbulence model, transitional flow model
4. FLUENT  $\kappa\text{-}\omega$  turbulence model, SST

All FLUENT calculations used a density based, implicit solver while VORTEX used a density based explicit solver. FLUENT version 6.3 was used.

Figure 2.19 compares the meanline prediction and the four CFD runs. Inside of the design speed range, all four CFD simulations predict flatter efficiency trends than the meanline. There is considerable variability in the predicted level of efficiency among the FLUENT turbulence models. VORTEX and the Std,  $\kappa\text{-}\omega$  SST model are very similar and close to the meanline level. The transitional flow model for  $\kappa\text{-}\omega$  predicts unrealistically low efficiency even at the design point. VORTEX was run to a more broad speed range to search for an incidence cliff. It did reveal a very rapid fall off in efficiency at 40 percent speed when the loading was high enough to cause suction side separations. At that condition, the efficiency fall off was more rapid than predicted by the meanline.

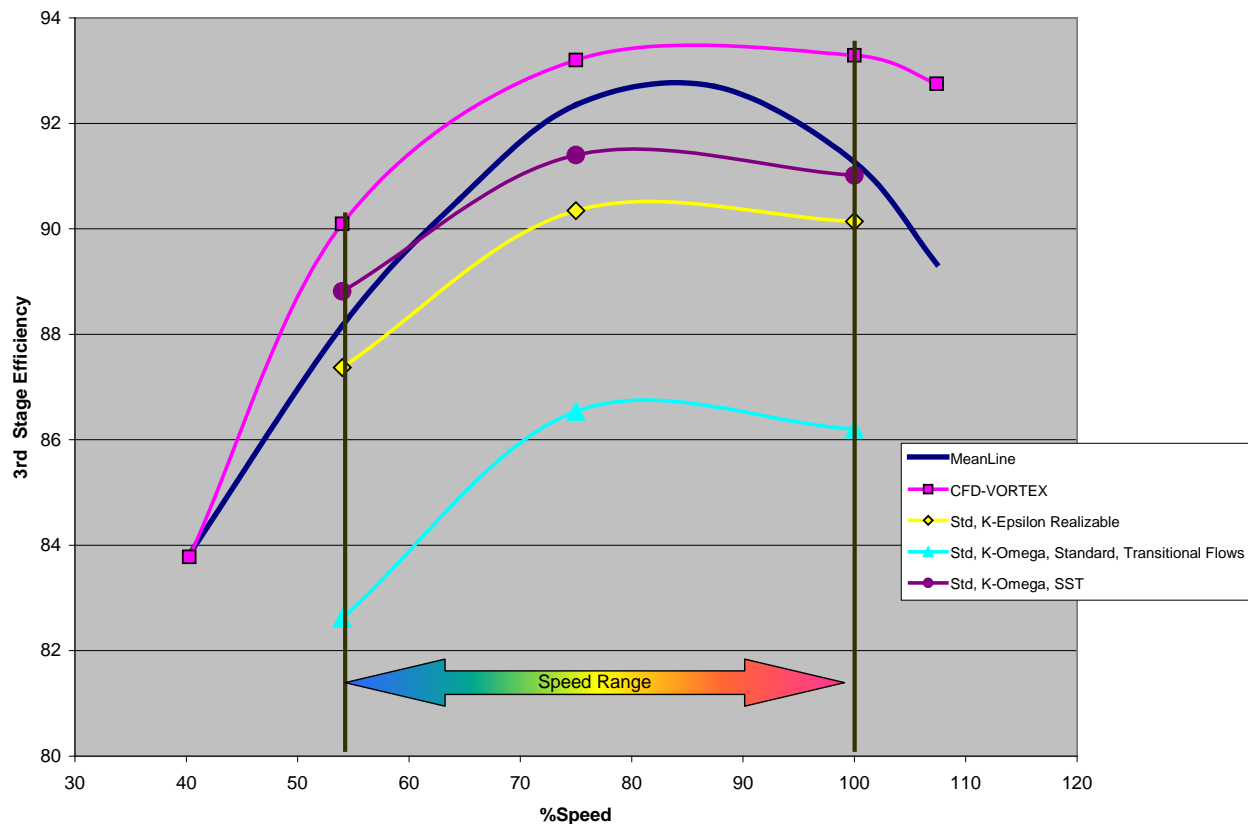


Figure 2.19.—Efficiency Comparisons for Four Turbine Designs

Figure 2.19 is good testimony to the fact that CFD is still paced by the lack of fidelity in turbulence modeling. The level of efficiency predicted by various turbulence models is significant. However, all four models predict a very similar efficiency trend with speed. The results give some confidence that the design may meet its incidence tolerance goals but is not adequate to completely mitigate risk. If it were necessary to choose between a fixed speed turbine and a variable speed turbine, a turbine rig test would still be recommended to determine if this design can truly meet the incidence tolerance goals. Another observation from Figure 2.19 is that the turbine blade is more tolerant to negative incidence than positive. This would lead us to move the design speed lower (higher camber airfoils) and allow the turbine to run off-design further on the negative side than the positive.

## 2.11 Thin Turbine Blade Incidence Study

Traditional airfoil design philosophy would indicate that larger leading edge diameters are more incidence tolerant than smaller diameters. While this is well established for airfoils in a free-stream, it is not nearly so obvious for airfoil cascades where the internal flow between the airfoils is more like channel flow than external flow. When a cascade airfoil has a larger LE diameter, the entire airfoil must be thicker. Thicker airfoils have higher through flow velocities and therefore (by intuition) generate more viscous scrubbing losses. Although this statement seems straight forward and logical, the high camber inherent in gas turbine blades complicates the situation.

Consider the airfoil shown in Figure 2.20. The throat of the airfoil cascade spans from the TE of one airfoil to the suction side of an adjacent airfoil. The passage between the two airfoils is bounded by the suction side of one airfoil and the pressure side of the adjacent. This passage controls the through-flow Mach numbers of the gas as it passes through the airfoils. It is desirable for this passage to be separation free and as low loss as possible. In this figure, the design philosophy is to produce a smooth, converging passage through the airfoil to the throat. To illustrate this passage convergence, a line of the same dimension as the throat is shown in orange. It is swept forward in the direction of the green line perpendicular to the suction side resulting in the orange trace. This gives a visual cue to the convergence through the passage as well as how the airfoil pressure side can impact the channel convergence.

Now consider the airfoil shown in Figure 2.21. This cascade has the same suction side as Figure 2.22 but a pressure side that results in a thinner airfoil. The airfoil passage now has a non-smooth area distribution through the channel. After the leading edge of the airfoil, the pressure side diffuses and then converges to the airfoil throat. Experience with this type of cascade would predict pressure side separation and reattachment as sketched in light grey. If the resulting separation bubble is large enough, the resulting blockage may result in through-flow Mach numbers similar to the airfoil in Figure 2.20. Separation bubbles that occur at relatively low velocities and are followed by strong acceleration generally do not generate high pressure loss. However, in the case of a rotating blade, the low momentum fluid trapped in a separation bubble can be centrifugally pumped outward due to the high rotational acceleration field. This can cause much higher loss than in the case of a stationary airfoil.

A study was executed to determine if a thin blade could potentially improve overall fuel burn by lowering through-flow velocity or would a separation bubble out-weigh any perceived benefit. Again the third stage was used as a representative stage. The blade was redesigned to be thinner but still maintain the same suction side as the nominal blade.

Figure 2.22 shows visually the change made to the blade. The brown line in the background indicates the nominal blade pressure side.

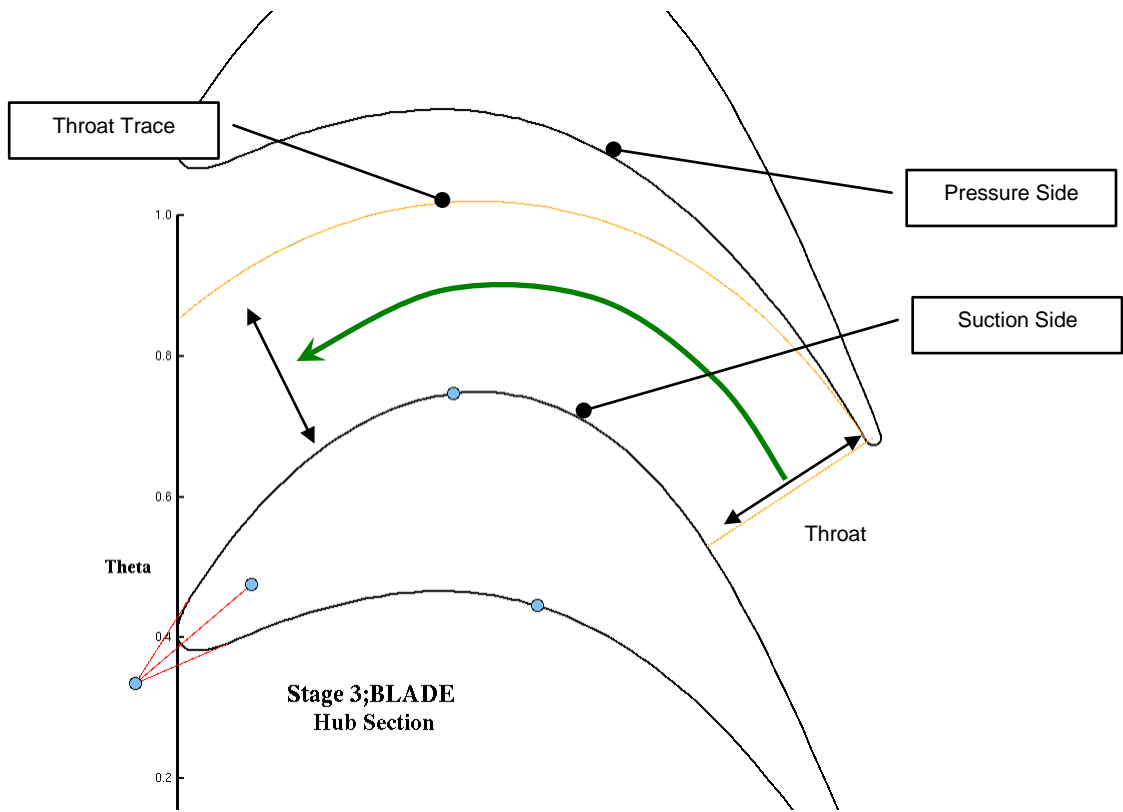


Figure 2.20.—A Simple Turbine Blade Cascade

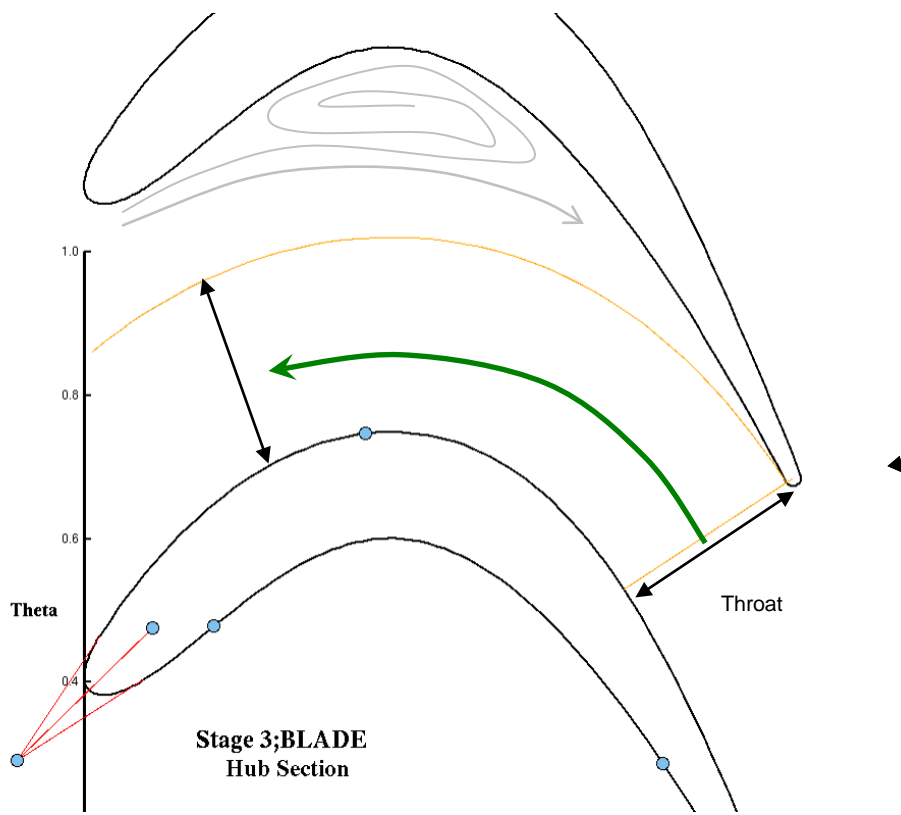


Figure 2.21.—A sample thin blade cascade

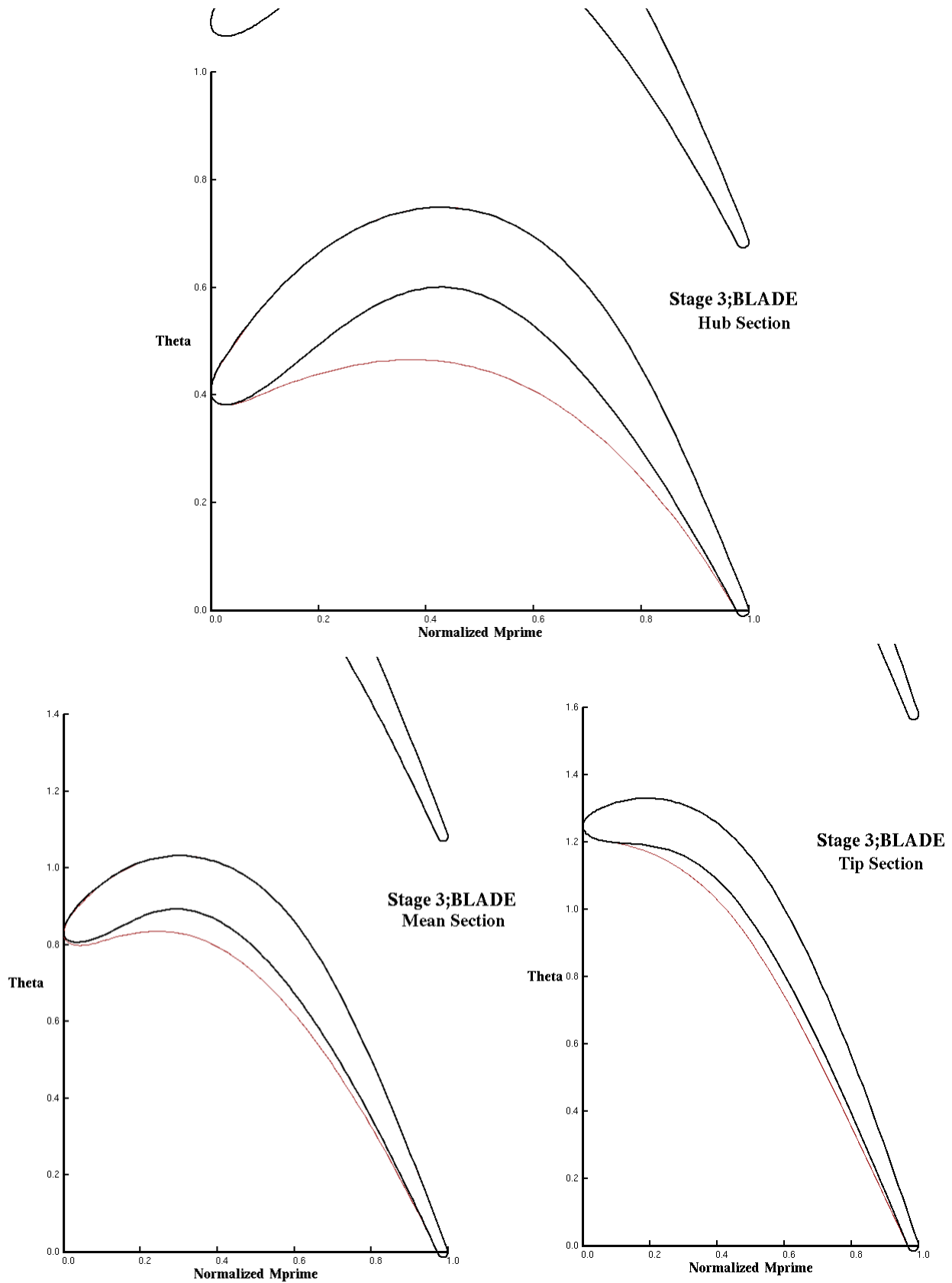


Figure 2.22.—Blade Profile Modifications

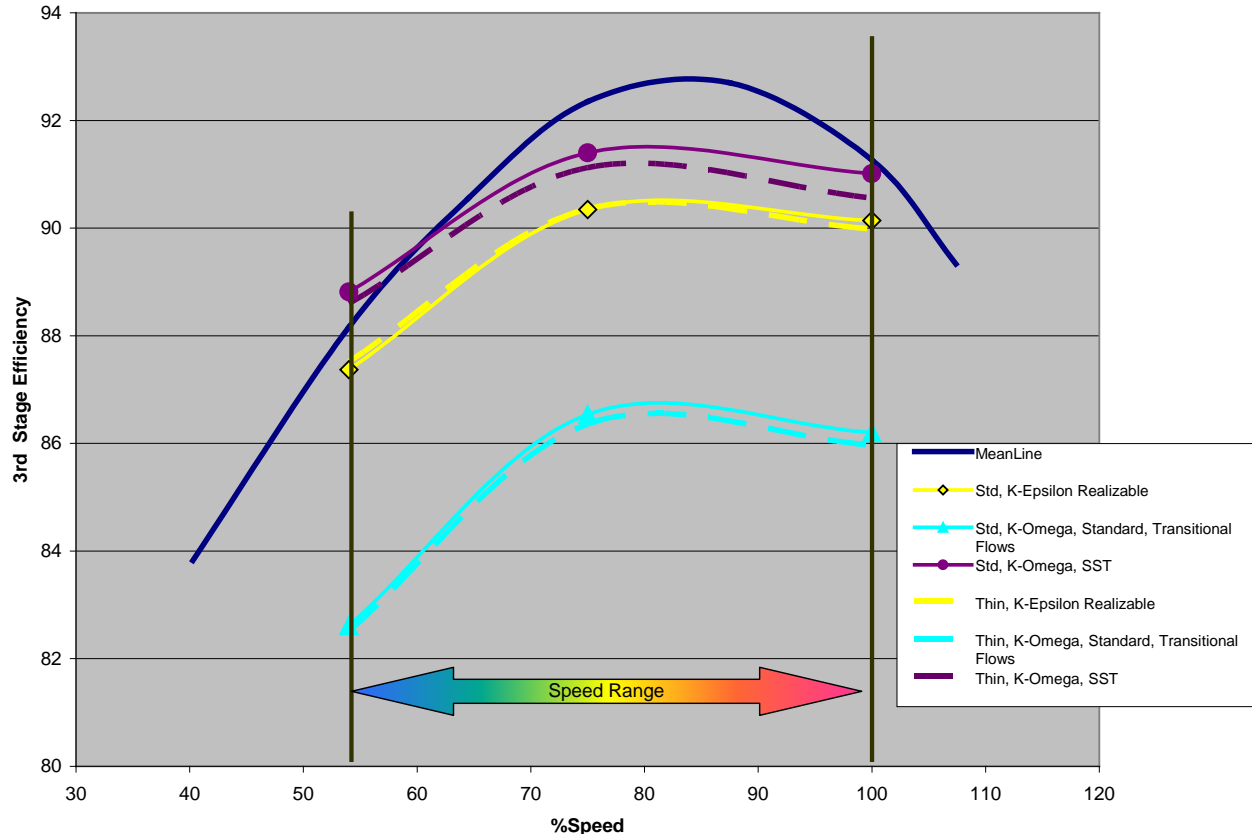


Figure 2.23.—Thin turbine blade geometry compared to nominal

The thin blade should be more susceptible to pressure side separation at high negative incidence (high speed). At positive incidence (low speed), the air impinges on the airfoil in a more favorable way for the pressure side and may not separate. We would therefore expect a thin blade to be similar or better at low speed but potentially worse at high speed. The airfoil in Figure 2.22 was run through FLUENT in a consistent manor with Figure 2.19. The results are shown in Figure 2.23. The dash lines indicate the results of the thin airfoil and are color consistent with the nominal blade run to the same turbulence model. The results are very similar with the thin blade overall slightly higher in loss. All three analyzes hint that low speed performance trends better than high speed performance. Based on this study there is no compelling evidence to depart from normal design philosophy (i.e., smooth channel convergence).

## 2.12 Third Stage Combined Incidence Study

The third Stage combined study was conducted in similar fashion as the third blade only study. The simulation was composed of the second blade, the third vane and the third blade. (Figure 2.24) The inlet conditions into the second blade were held fixed in the absolute frame of reference simulating the exit conditions of the second vane. The exit condition of the third blade was a free vortex boundary with the average static pressure iterated to match the proper exit corrected flow. In order to assess the third stage performance, the efficiency of the second blade was ignored and the third stage was calculated based on its inlet and exit conditions in the converged solution. The meanline analysis was performed in exactly the same manor so that the CFD and meanline results may be compared directly. The speed was varied in a similar way as was done in the blade only study. There was no tip clearance, leakage or cooling modeled. In this calculation both the third vane and third blade experience the incidence swing associated with the speed change, therefore the efficiency impact with speed is higher than the previous study. Figure 2.25 compares the resulting meanline efficiency to the CFD prediction. The conclusions are generally the same

as the blade only calculations. The CFD prediction is more incidence tolerant than the meanline prediction and also indicates that negative incidence (high speed) is more forgiving than positive incidence.

The third vane total pressure loss was extracted from the CFD and compared to the meanline prediction as well (Figure 2.26).

The vane exhibits a similar trend as the blade in that it is more incidence tolerant at high speed (negative incidence) rather than low speed. The vane is exceptionally tolerant at negative incidence because the pressure side separation bubble is: 1) very small (less than  $\frac{1}{2}$  the thickness of the airfoil), and 2) completely reattached at relatively low Mach number before the airfoil throat (Figure 2.27). Unlike the blade, the vane is not subject to the high centrifugal acceleration field and therefore the low momentum fluid trapped in the separation bubble is not transported radially.

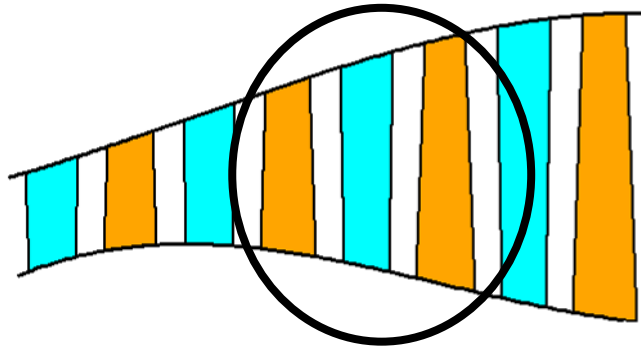


Figure 2.24.—Third Stage Speed Study composed of Three airfoils

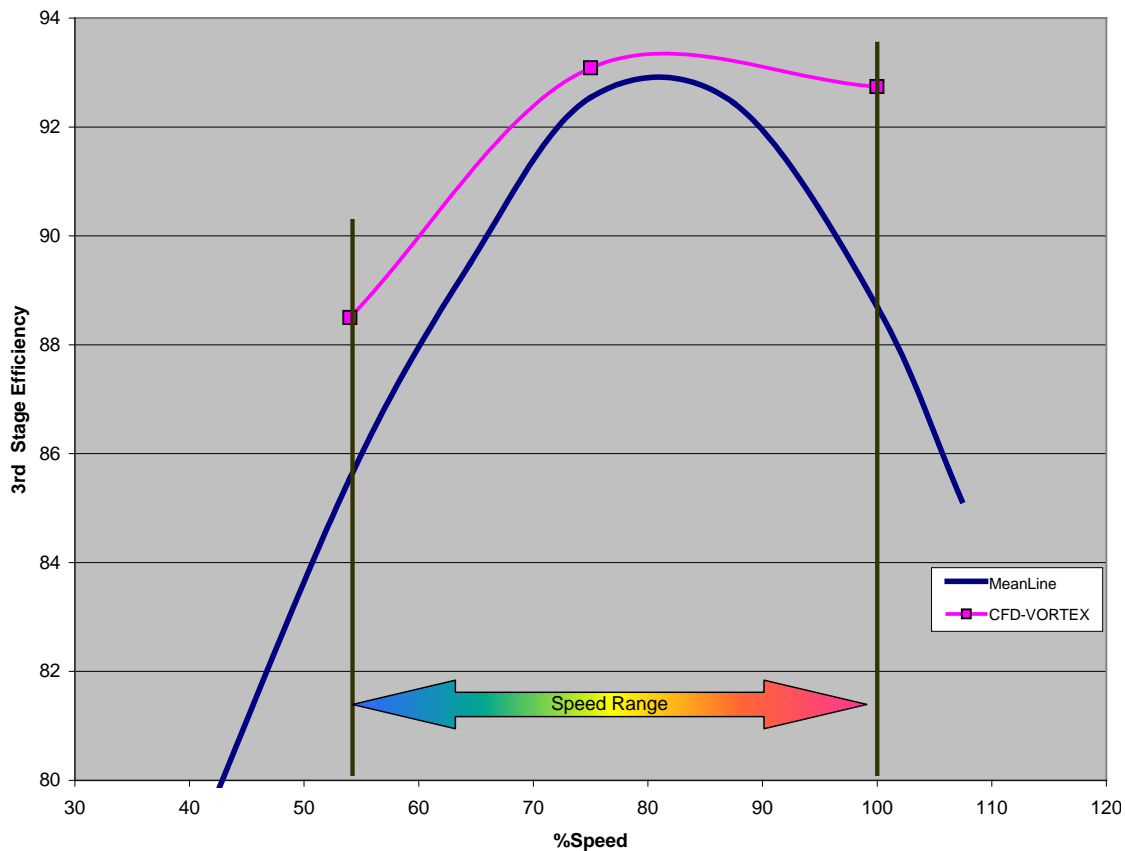


Figure 2.25.—Third Stage Performance

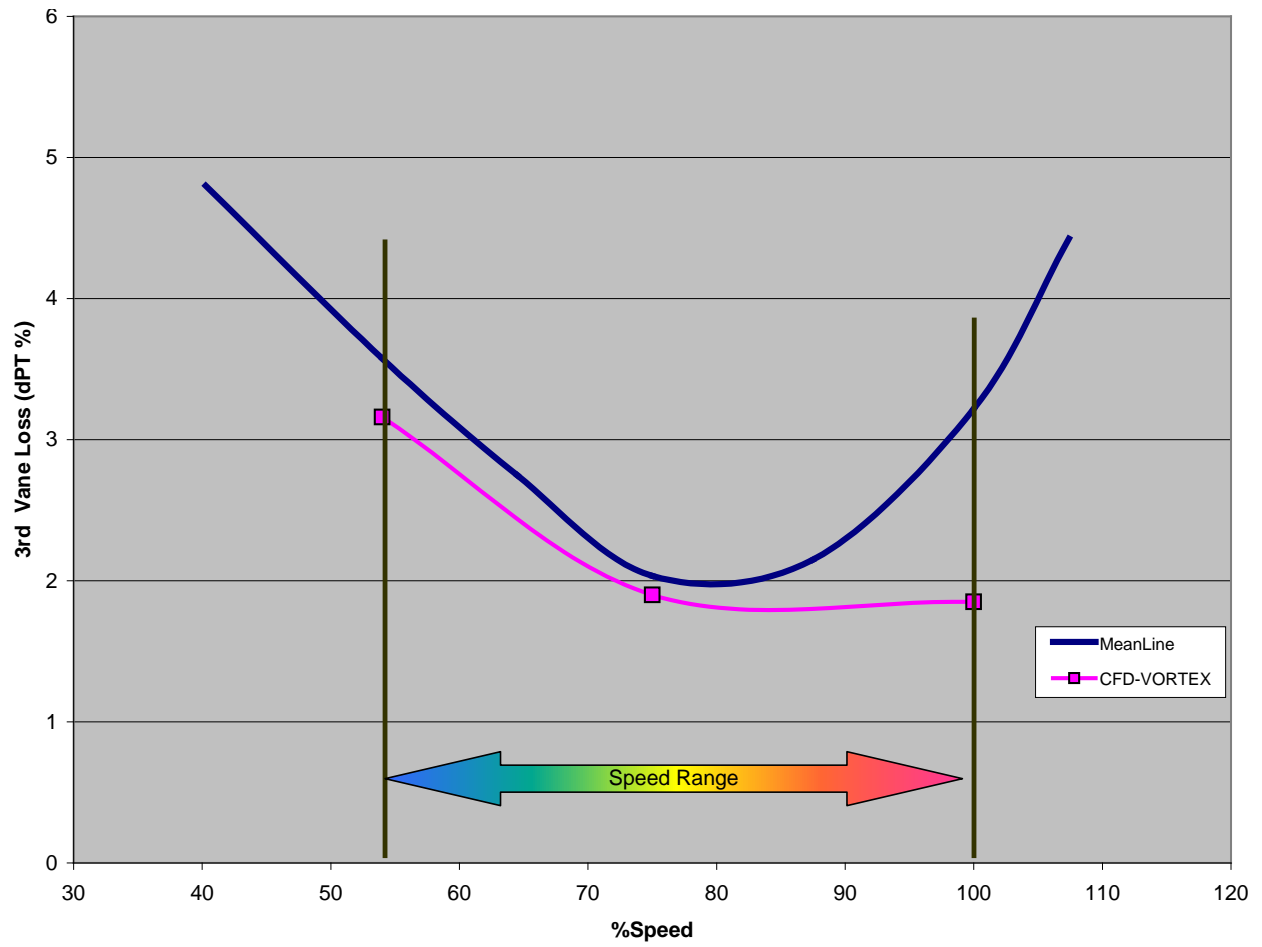


Figure 2.26.—Third Vane Pressure Loss

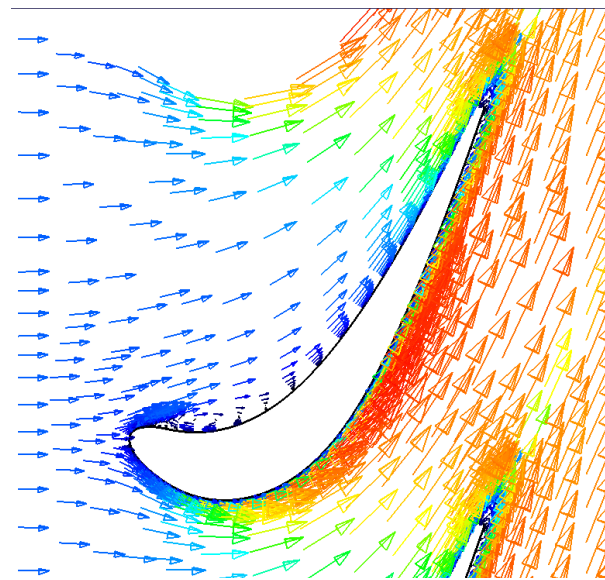


Figure 2.27.—Vane Velocity Vectors

All the CFD work performed suggests that mission fuel burn is improved by designing for relatively low corrected speed. In this present work, the design speed chosen was 75 percent speed, or approximately half way between low speed cruise (54 percent) and high speed take-off (100 percent) based on meanline predictions. The CFD suggests that the turbine is: 1) more forgiving than the meanline predictions and 2) able to tolerate higher negative incidence. A lower design speed may further improve overall mission fuel burn. Figure 2.14 would suggest a design speed of 70 percent as a logical compromise or next design iteration. Designing for lower speed also results in airfoils with higher camber. This is an added benefit because higher camber airfoils are generally stiffer and more resilient to high cycle fatigue.

### **2.13 Airfoil Leading Edge Geometry**

The aviation industry routinely designs wings for variation in loading and incidence. From the largest commercial aircraft to the private general aviation airplane, variable geometry (flaps and/or LE slats) are employed to increase loading coefficient and wing area during take-off and landing. Zenith Aircraft Company uses a fixed LE slat (Figure 2.28) to make their STOL CH 701 stall resistant to very high angles of attack. The completely passive nature of their design is very attractive from a cost and complexity standpoint. Similarly, in this VSPT design, it would be very desirable to include features that improve tolerance while being completely passive. Turbine airfoils are relatively small and made from investment castings. It would be impractical to attempt to cast them with such intricate details. It would however be very advantageous to design turbine airfoils with a LE shape that was inherently incidence tolerant. One concept investigated in this study is to attempt to smooth the LE curvature distribution as much as possible in order to allow the air to smoothly transition from the LE to the airfoil pressure and suction sides.

Turbine airfoils are typically designed with an elliptical LE connected to a curved pressure and suction side. See Figure 2.29. Although the intersection of the ellipse and airfoil curves is designed to match point and slope, it does not typically match curvature and can in fact be discontinuous. In order to assess the impact of this discontinuity, a smoothing algorithm was developed and applied to the third blade from the previous studies. The algorithm calculates the curvature as a function of surface length (S-distance) and calculates a local correction factor based on the gradient in curvature from one point to the next. Each point is moved normal to the surface in the direction to smooth the gradient by a small amount. The process was iterated 200 times until a smooth curvature distribution was obtained. See Figure 2.30. The actual change in the surface profile required to smooth the curvature distribution is well within any reasonable casting profile tolerance. As shown in Figure 2.30(b) it is nearly within the thickness of a line when plotted at a reasonable viewing size. Figure 2.30(c) clearly shows the discontinuity in curvature at the tangency points and the result of running the smoothing algorithm. Nonetheless, it is still desirable to establish the best possible design shape and apply manufacturing tolerance about that nominal shape rather than a less optimal design. In order to determine if the smooth shape is in fact better, the smoothed third blade was run through the same set of CFD calculations as in the blade incidence study.

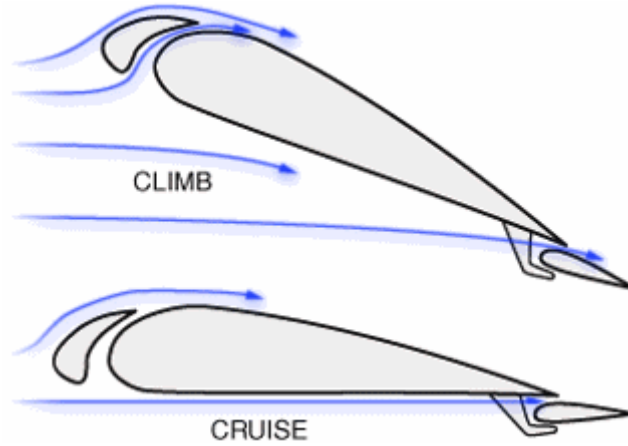


Figure 2.28.—Fixed geometry LE slats. Used with permission from Zenith Aircraft Company, Mexico, Missouri, 65265-0650.

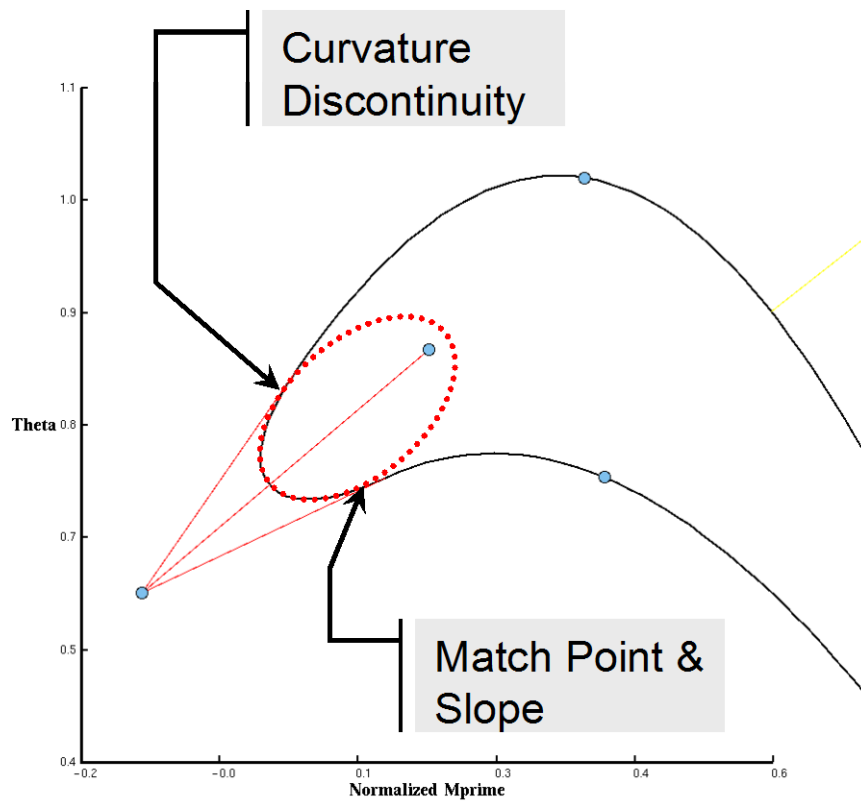


Figure 2.29.—Typical Turbine Airfoil Leading Edge Profile

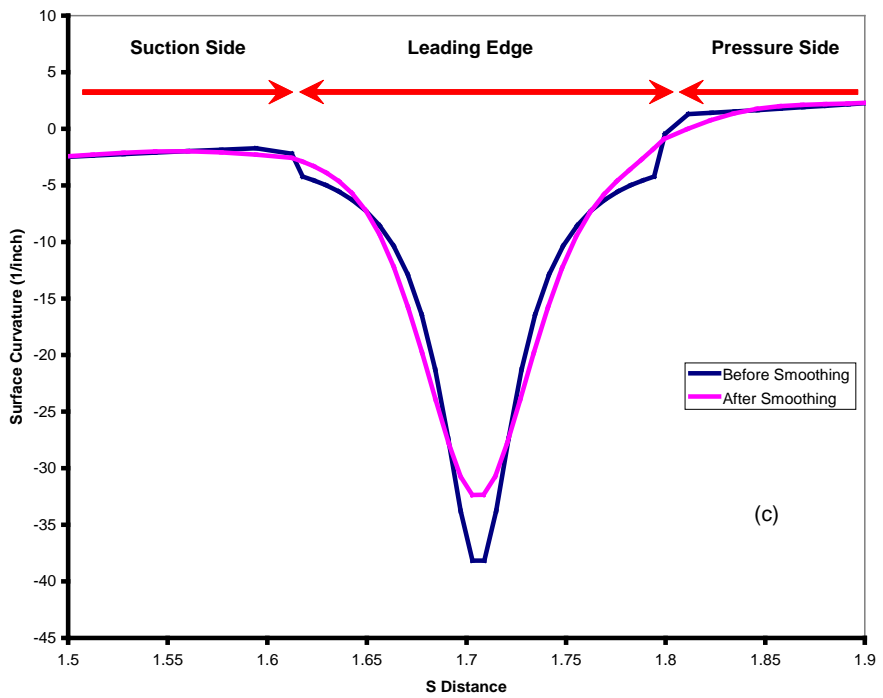
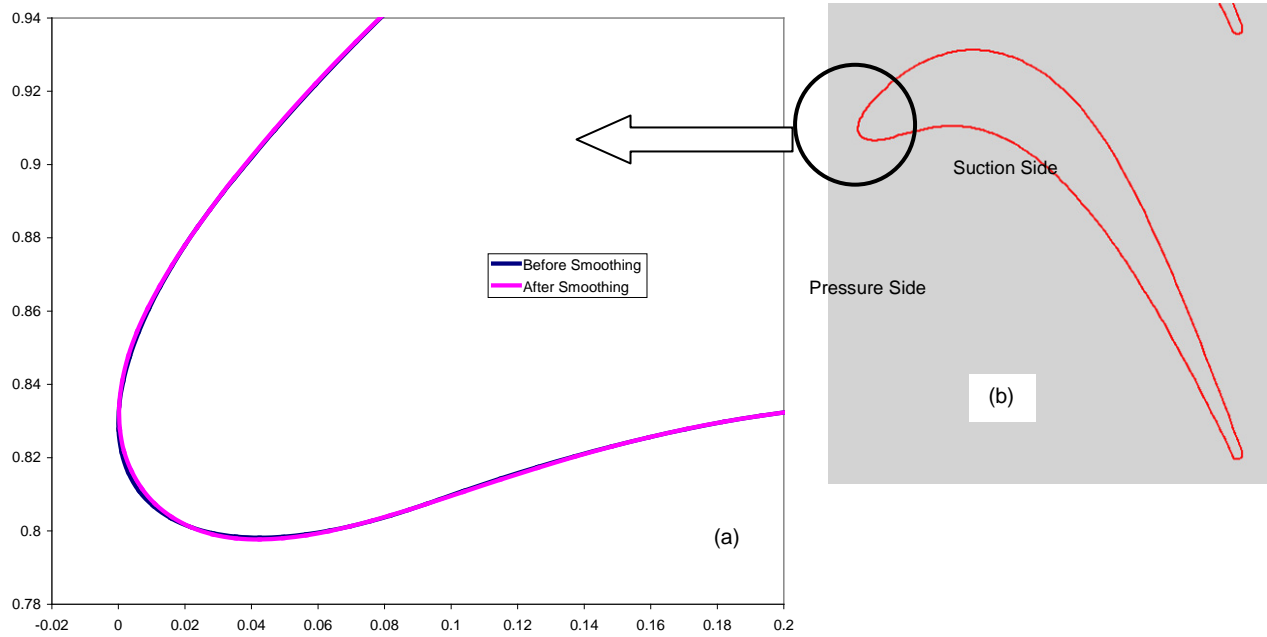
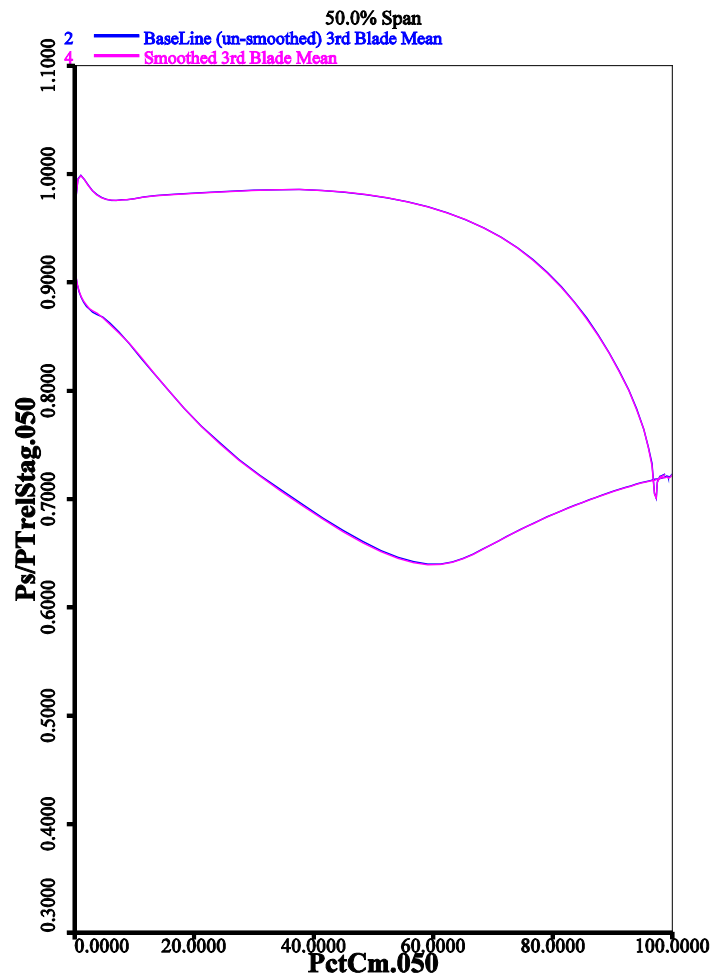


Figure 2.30.—Third Blade Mean, surface curvature smoothed

The changes to the geometry and CFD mesh were basically imperceptible to the eye. The global CFD results (i.e., efficiency and flow) for the third Blade at design speed (75 percent) were virtually unchanged relative to the non-smoothed blade. Figure 2.31 gives the mid-span surface static pressure loading also showing nearly identical results. Despite this disappointing result, the CFD was run at high and low speed to investigate off-incidence tolerance. The resulting efficiency trend with variation in speed was surprising. See Figure 2.32. Shown in green, the smoothed LE contour maintained better incidence tolerance at low speed relative the non-smoothed baseline configuration shown in pink. In order to understand this, a detailed investigation into the flow field was performed. At the design speed, no significant flow field changes were evident. This was also true at negative incidence (high speed), but at low speed, the smoothed LE resulted in an improved flow field. At approximately 80 percent span, the airfoil suction side loading is highest. As the airfoil loading is increased, this is the most likely location for the airfoil to separate.



Tue Jan 11 13:33:37 2011

Figure 2.31.—Third Blade mid span static pressure distribution

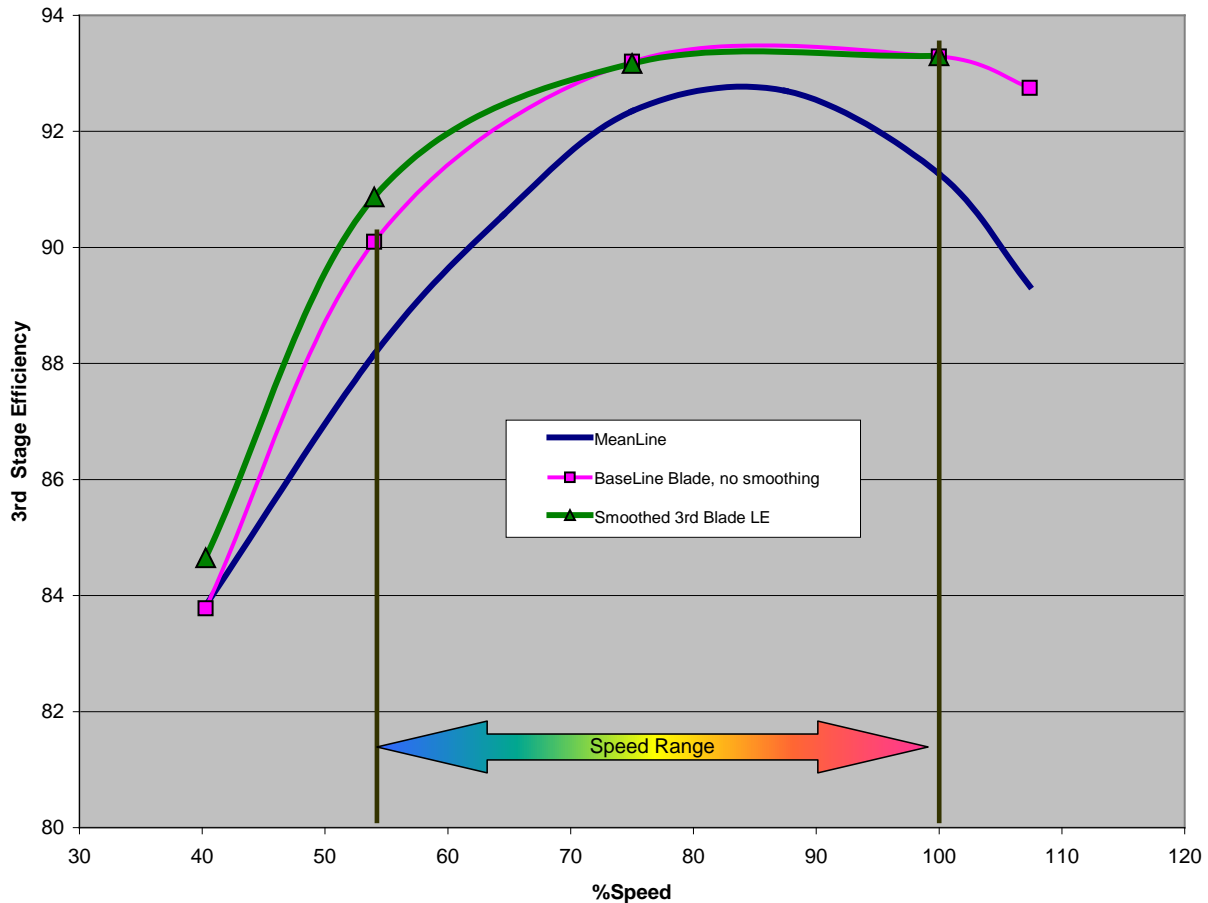


Figure 2.32.—Smoothed third Blade Efficiency Trend with Speed

Combing through the velocity vectors did reveal a separation in this location for the baseline (unsmoothed) blade. The easiest way to visualize this is to capture the separation bubble with a constant Mach number surface.

In Figure 2.33, the non-smoothed blade is compared to the smoothed blade. An iso-Mach number surface was generated for each calculation. The yellow-green surfaces shown are surfaces of Mach number equal to 0.15. Since the through-flow Mach numbers are all much higher than 0.15, all of the flow beneath the surfaces shown are boundary layers or separations. The non-smoothed blade has a separation bubble near the tip that is nearly completely removed after the blade is smoothed. The separation bubble is visually interacting with the secondary flow field near the shroud line.

This result is based on a single solver and turbulence model. No further CFD modeling was performed within this study. It is not know how transition from laminar to turbulent flow may be impacted by curvature smoothing. Likewise, the impact of the unsteady flow field is not known.

This work reinforces the importance of maintaining boundary layer health upstream of diffusing flowpaths. These results are encouraging: they suggest careful design of LE geometry can improve airfoil incidence tolerance. Additional, this completely passive design does not change the design point methodology. The design point analysis was completely unaffected by the incorporation of the smoothing algorithm. Addition research in this area may result in airfoil shapes that are inherently more incidence capable.

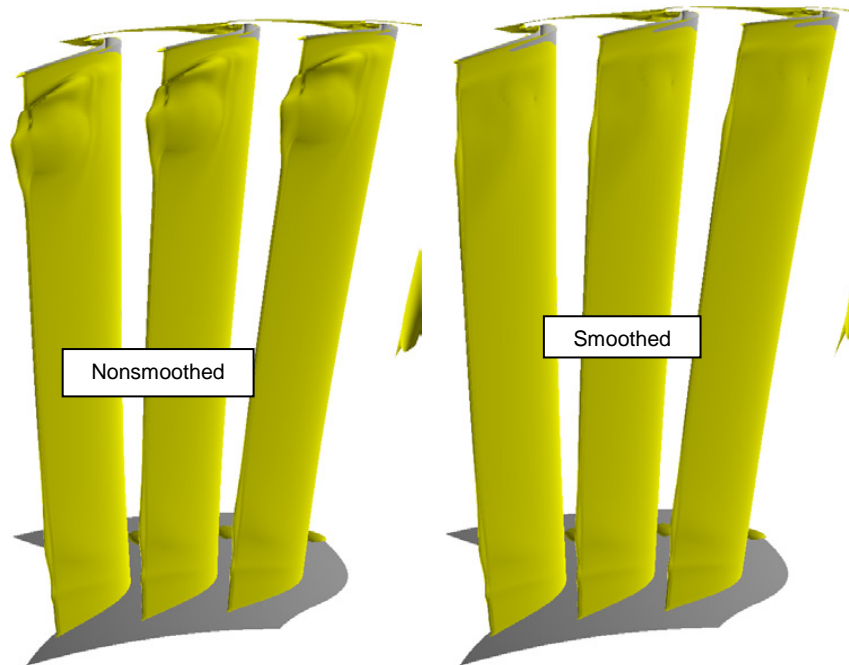


Figure 2.33.—Separation bubble visualization

### 3.0 VSPT LCTR Mission Performance Modeling

A thermodynamic cycle model was developed to study the performance impact of various power turbine designs. The basis of this study was the TS2-NPSS model provided by the NASA Glenn Research Center. The model was originally created March 5, 2010, and has description: “two-spool turboshaft about equal work for LPC/HPC, HPC is PR=1.3 axial + centrifugal - includes update for turbine cooling (best guess for number turbine stages)”. The model was updated from NPSSv1.6.5 to NPSSv2.3 and the output of the model was enhanced. A copy of the updated model was provided to NASA to assist in adopting the latest version of NPSS consistent with NASA’s overall goals. The only performance feature of the cycle model that was modified was the Power Turbine maps.

Three turbine designs were evaluated at the three critical mission points defined in the LCTR “Design” Mission Profile. These mission points define the design conditions for the overall cycle and present some challenges for the turbine design because of the wide range of shaft speeds. Table 3.1 summarizes the flight conditions and shaft speeds.

TABLE 3.1.—CRITICAL MISSION POINTS

Mission Segment	Takeoff hot	Climb	Cruise
Time, hr	0.07	1.00	3.00
Power, hp	7859	2646	2351
N3, rpm	15000	15000	8077
Ambient			
Mach Number	0	0.51	0.51
Altitude, ft	0	28000	28000
Delta T from standard conditions, F	45	0	0
VTAS, knot	0	303	303

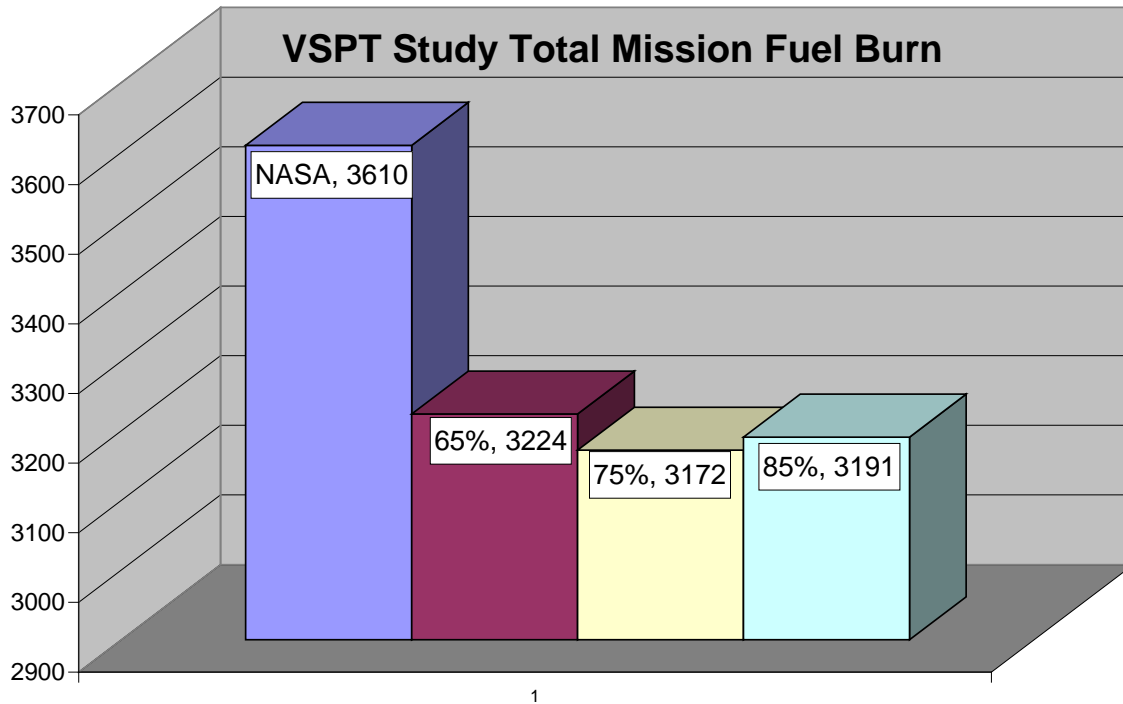


Figure 3.1.—VSPT Total Mission Fuel Burn for Three Williams International Designs

The Takeoff hot condition requires the maximum power at high rotor speed, but the amount of time at that condition is limited to 3 min for takeoff and 3 min for landing with an additional minute for taxi. The climb is represented by the top of climb condition at high rotor speed and represents 30 min to climb plus an additional 30 min to fly to an alternate destination. The cruise condition is represented by the same flight condition as the climb point, but at shaft rpm that is 54 percent of the full throttle condition and also at high power output for 3 hr.

The power turbine map provided with the NASA model was run at the three flight conditions and the power output was used as the requirement for each flight condition. Three power turbines were designed to provide performance at the cruise condition and to meet the maximum shaft speed requirement. The turbine design points were set at 65, 75 and 85 percent corrected speed and are labeled accordingly. Figure 3.1 shows the total mission fuel burn for the three designs.

The three proposed designs have significantly reduced mission fuel burn compared to the baseline power turbine design. The 75 percent design has the lowest mission fuel burn and is the best design on this basis. The 75 percent design uses 1.6 percent less fuel than the 65 percent design and 0.6 percent less fuel than the 85 percent design. The 75 percent design uses 12.1 percent less fuel than the baseline design and is the best overall design based on this preliminary design study. For each of the three turbine designs, the NPSS output for the three critical mission points is given in Appendix H.

In the cycle detailed output, there are 6 points presented for each turbine design. The takeoff point (T/O) is the cycle design point at takeoff power on a standard day at 15,000 rpm power turbine speed. The second point is takeoff on a hot day. The third point is at the climb condition, 15,000 rpm at the same power setting as the NASA design climb condition; however the power setting condition logic does not result in the same power output for different turbine designs. The fourth point is at the climb condition at the same power output as the NASA design to allow fuel flow comparisons. The fifth point is at the Cruise condition at reduced shaft speed of 8,077 rpm at the NASA power setting. The sixth point is at the Cruise condition at the NASA power level and is used for the fuel flow comparison.

## 4.0 Development of a Cost-Effective Approach to an LCTR-Relevant VSPT Component Experiment

Testing of a power turbine presents unique challenges in that it is not self-supporting. In order to test a power turbine, inlet compressed air is required that requires heating to at least several hundred degrees F to avoid ice formation on exhaust structures and instrumentation. A power sink is also required that has excellent control characteristics in order to set rpm and avoid overspeeds. Ideally, the power turbine should be tested at full scale to minimize Reynolds effects and so that key inter-stage instrumentation can be inserted without unduly affecting the flow conditions in the local area. Since the VSPT for the LCTR will be relatively large, full scale testing will require a test facility that can provide continuous flow of large volumes of heated inlet air with substantial power absorption capability. Use of an existing engine as a gas generator testbed for testing the VSPT was considered as an option, but ruled out because the engine operating line would severely limit the range of power turbine entrance conditions that could be achieved during test. The optimum approach appears to be to develop a dedicated VSPT rig to mate to the single-spool turbine test facility at NASA GRC. The capabilities and limits of the single-spool turbine facility, listed in Table 4.1, provide more than sufficient capability to produce the entrance and exit conditions needed to evaluate the LCTR VSPT design concept at full scale.

There are two basic engine configurations that can provide power to the rotor system, and both have been used successfully in large numbers of turboshaft and turboprop systems. The gas generator can be mounted with the compressor facing in the direction of flight, or opposite to the direction of flight. The aft-facing compressor configuration, similar to that used by the Pratt & Whitney PT-6 turboprop, provides a very large advantage in that the power turbine shaft can be very short and large in diameter since the power turbine module is adjacent to the reduction drive gearbox, compared to the long, thin shaft needed by the forward-compressor configuration, which needs to pass the turbine shaft through the center of the gas generator shafts. This greatly reduces or eliminates the rotordynamics and torque limitations issues associated with the long, thin shaft. The disadvantage of this configuration is that the airflow must be turned 180° prior to entering the inlet, and once again in the exhaust duct. This is necessary to avoid having the inlets face the ground during VTOL operation. An advantage is that it provides a simple method for rejecting ice, birds, or other foreign matter before it can enter the gas generator. The forward-facing compressor configuration requires an S-duct inlet and can use an axial exhaust, which have lower aerodynamic losses. The aft-facing compressor design also provides a much easier approach to an inertial separator design for ejecting ice and solid objects, another distinct advantage. Mostly because of the reduced rotordynamics concerns, the compressor-aft configuration is recommended for the LCTR application. Figure 4.1 is a schematic of this configuration for a twin-pack LCTR design. The spacing between the power turbine exhaust and the reduction drive gearbox is the minimum required to provide a low-loss turn in the exhaust duct.

TABLE 4.1.—NASA GRC SINGLE-SPOOL TURBINE TEST FACILITY CAPABILITIES

• Maximum Turbine Inlet Pressure	50 psia
• Minimum Exhaust Pressure	2 psia
• Maximum Inlet Air Temperature <small>(from in-line vitiated natural gas combustors)</small>	940°F
• Maximum Primary Air Flow Rate	27 pps
• Secondary Air (150 psig supply):	
» 2 Legs – 1.5 pps each up to 550°F	
» 4 Legs – 0.08 to 1.19 pps each up to 250°F	
» 6 Legs – at 70°F	
• Maximum Turbine Rotational Speed <small>(with maximum Gear Ratio, G.R., of 7.87)</small>	14,000 rpm
• Maximum Turbine Torque	36,217 ft·lb <sub>t</sub> /G.R.
• Minimum Gear Ratio, G.R. = 1.51 <small>(<math>N_{max} = 2,718</math> rpm; <math>Torque_{max} = 24,000</math> ft·lb<sub>t</sub>)</small>	
• Maximum Test Article Diameter	52 inch

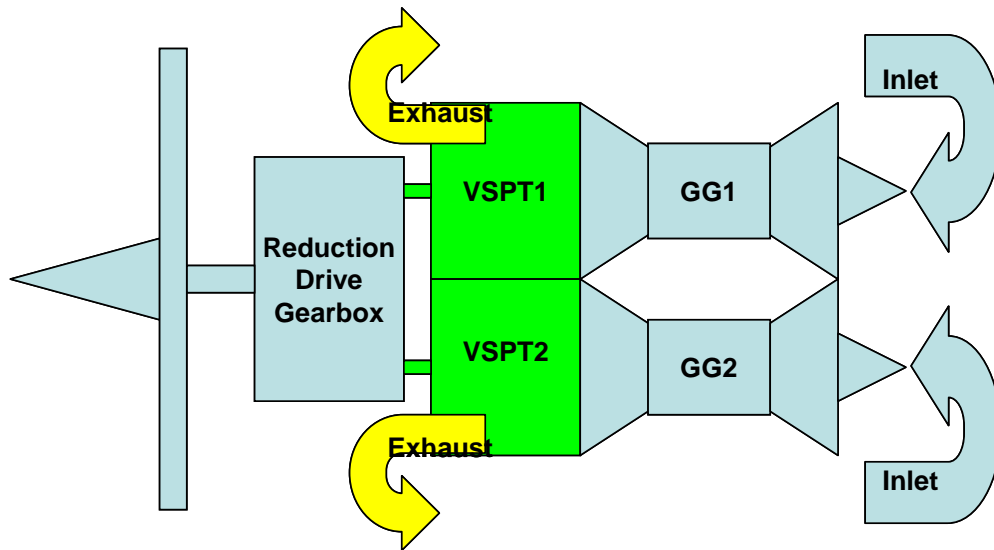


Figure 4.1.—Schematic of Recommended Engine Configuration for LCTR

Rotordynamics of turboshaft machinery such as tilt rotors are generally divided up into two categories, lateral and torsional. Each has its own set of typical challenges.

Lateral challenges typically involve long flexible drive shafts that operate above the first flexible critical mode, i.e., supercritical rotors. Inadequate damping at the bearings results in damaging vibrations when traversing the lateral critical modes of drive shaft. Controlling run-out and wall thickness variation of long hollow flexible shafts at reasonable cost is often challenging. Misalignment of drive shaft between gearbox and power-turbine adds further complexity that must be addressed. Last and perhaps most important the large overhung tilt rotor makes the system sensitive to rotating unbalance.

Torsional challenges typically involve shock from start up and elevated transient loading through the drive shaft. Unloading of gear teeth during surge events, back lash, gear run out, random vibration due to gear inaccuracies and rolling element defects, and closed loop control system instabilities have all been known to lead to torsional failure modes. All of these issues need to be addressed as part of the full engine and test article designs.

Figure 4.2 shows a layout of the proposed full scale VSPT test article mated to the NASA GRC single spool turbine test facility dynamometer drive frame. Locations are indicated for multi-element instrumentation rakes at the inlet and exit of the VSPT, and for cylindrical radially-translating flow angle sensors at each of the three interstage locations. The rig inner and outer flowpaths are a combination of formed sheet metal and machined details, with the inner flowpath and bearing support structures supported by an exit guide vane row set well behind the last stage rotor. The four-stage turbine is overhung on the front of the shaft, supported by an aft roller bearing and forward ball bearing to react thrust loads. As shown, the thrust loads are intended to be reacted through the front bearing and out into the outer frame structure through the exit guide vane row. The bearing cartridge in the SSTTF has sufficient load capacity to support the VSPT test article as an entirely overhung mass, so an alternative approach would be to eliminate the VSPT bearings altogether and hang the VSPT off the front of the drive spindle. If feasible, this arrangement would simplify the system and eliminate the bearing lubrication requirements, as well as reducing the cost of the design and hardware. It will be necessary to analyze the shaft system to ensure that critical speeds are not an issue and displacements do not drive excessive tip clearances in the test article. The preliminary aero and structural design tasks in the experimental program will determine if it will also be necessary to include one or more balance pistons to offset some of the thrust load.

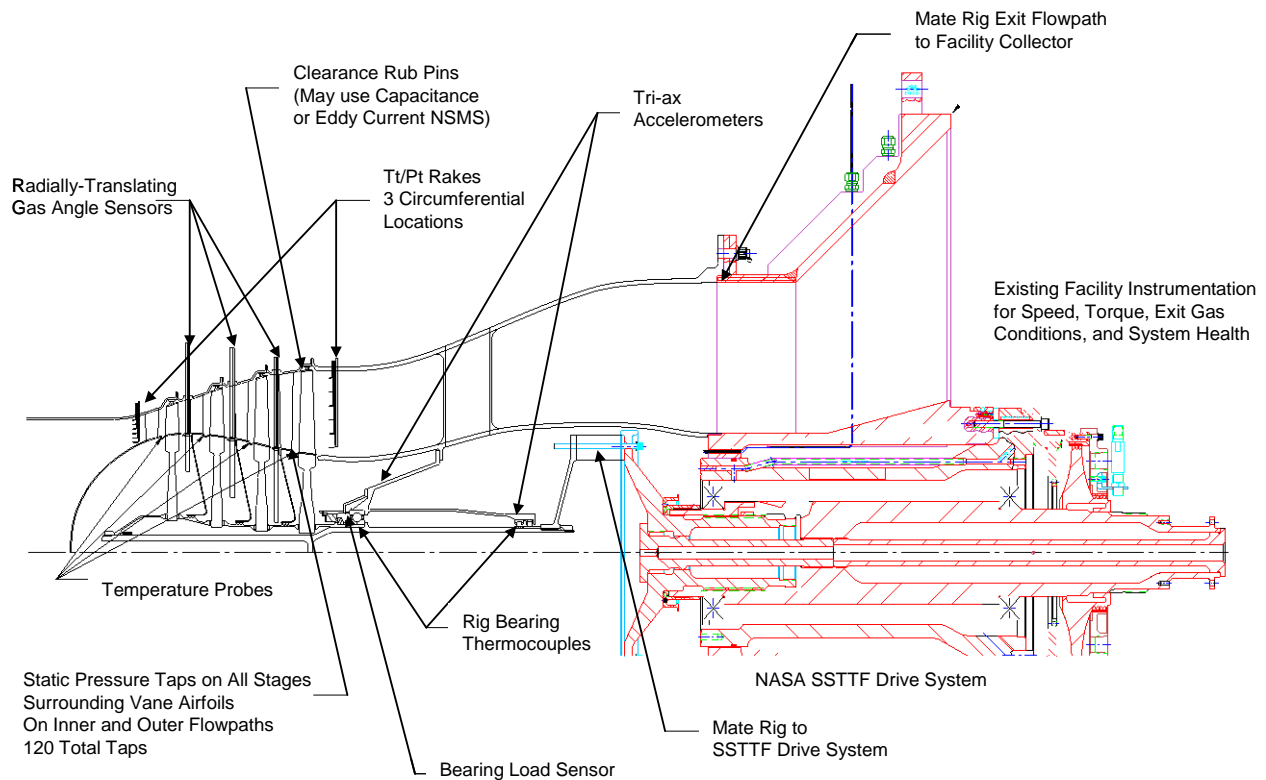


Figure 4.2.—VSPT Test Article Mated to NASA-GC Single Spool Turbine Test Facility

The four-stage rotor is shown as a clamped assembly with the clamp loads applied at the hub through curvic couplings. This was done in order to make it possible to use the cylindrical wake angle sensors. This type of sensor has performed very well in past tests and has the advantage of being much smaller in diameter than traditional cobra probe sensors because it is supported at both ends of the flowpath rather than cantilevered from the outer wall. This greatly minimizes blockage but imposes some limitations on the design of the test component. Since the sensing position on the probe has to transit the entire span from the outer to the inner wall, provisions must be made for the probe body to penetrate an equal distance beneath the inner flowpath when the inlet holes are at the innermost radial position. This makes it impossible to use with a drum rotor configuration. A detailed rotordynamic analysis of the rotor/shaft system will be a key part of the experimental program and its results will determine whether this approach is feasible or if a drum rotor configuration with conventional probes is required to achieve sufficient speed and frequency margins relative to the operating speed range. The spacing between stages and between vane and blade rows shown in the figure is notional and would be optimized during the test article design process to provide access and routing for all of the planned instrumentation.

#### 4.1 Experimental Test Plan and Instrumentation List

The proposed operating conditions of the VSPT vary from 54 to 100 percent speed. Therefore, it would be beneficial to develop a turbine map that fully describes the turbine efficiency within this range. The proposed test plan to characterize this turbine would include a pressure ratio sweep from 3.0 to 7.0 and a speed sweep of 40 to 120 percent (Table 4.2). Generally speaking, it is easier to change speed than PR in a test facility so the order of operations would be to set PR and then increment through the speed range to develop lines of constant PR.

TABLE 4.2.—PROPOSED MAP/TEST PLAN

	PR								
Speed%	3	3.5	4	4.5	5	5.5	6	6.5	7
40									
50									
60									
70									
80									
90									
100									
110									
120									

The turbine map should be developed at both high and low Reynolds number where “high” is equivalent to a SLTO condition and “low” is equivalent to the cruise condition.

Low Reynolds number cruise at highest corrected speed is most challenging condition, and requires vacuum. For similitude in Reynolds number, PR, Corrected Flow and Corrected speed, the following table defines the 100 percent speed conditions for the turbine:

	Engine	Proposed Rig
Inlet PT	31.01 psia	20.6 psia
Inlet TT	1749.1°R	1260.°R (800 °F)
Inlet Mass Flow	12.04 lbm/s	9.425 lbm/s
Power	2740 hp	1525 hp
Exit PT	5.35 psia	3.55 psia
rpm	14898	12645
First Vane Reynolds Number	178,000	172,000
Last Blade Reynolds Number	61,000	61,000

The SLTO (high Reynolds Number) condition requires the following parameters:

	Engine	Proposed Rig
Inlet PT	88.49 psia	45 psia
Inlet TT	2166.3°R	1260 °R (800 °F)
Inlet Mass Flow	9.41 lbm/s	20.6 lbm/s
Power	7500 hp	3350 hp
Exit PT	15.43 psia	7.76 psia
rpm	14898	12645
First Vane Reynolds Number	395,000	377,000
Last Blade Reynolds Number	130,000	134,000

These rig conditions are within the advertised capability of the New Single Spool Turbine Facility proposed by NASA to replace W-6A Warm Core Turbine Facility.

In order to simplify the rig as much as possible, the rig would be uncooled. The proposed warm inlet temperature of 800 °F should allow for nearly no cooling flow. This allows for simple turbine efficiency calculations based only on measured inlet and exit total pressure and total temperatures. The Turbine efficiency can be calculated as follows:

$$\eta = \frac{\Delta T}{T_{in} (1.0 - PR^{\frac{1.0-\gamma}{\gamma}})}$$

where  $\gamma$  is the ratio of specific heats calculated at the average of the inlet and exit temperatures.

The corrected speed is calculated as:

$$\text{rpm}_{\text{corr}} = \text{rpm} \sqrt{\frac{518.67}{T_{\text{in}}}}$$

where 100 percent is defined as  $\text{rpm}_{\text{corr}} = 8113$ .

Of great interest is the turbines performance at the two design conditions (54 and 100 percent) speed. At these conditions, inter stage gas swirl angle and total pressure profiles will be measured and compared back to predictions. The use of a cylindrical probe between the stages is proposed to measure gas angles behind rotors with minimal blockage. It is significantly more difficult to measure the gas angles behind stators because the circumferential variation in angle and pressure complicates the measurement and therefore it is not recommended.

Table 4.3 comprises an initial recommendation for instrumentation required to collect the desired test data.

TABLE 4.3.—PROPOSED INSTRUMENTATION LIST FOR VSPT COMPONENT EXPERIMENT

Sensor type	Objective	Location	Quantity	Required accuracy
Radially translating cylindrical gas angle sensor	Measure flow angles exiting each turbine stage	Nozzle vane Leading Edge	1 per stage, 3 total	$\pm 1^\circ$
Six-element total pressure rake	Measure total pressure at entrance and exit of VSPT	Inlet and exit	6	$\pm 0.5\%$
Static pressure taps	Determine pressure distribution around vanes	Outer and inner wall, at root of nozzle vane	20 OD, 20 ID, 3 locations, 120 total	$\pm 0.5\%$
Six-element total temperature rake	Determine stage temperature drop	Inlet and exit	6	$\pm 1^\circ\text{F}$
Bearing Thermocouple, type K	Monitor bearing health	Outer race	2 per bearing, 4 total	$\pm 10^\circ\text{F}$
NSMS or capacitance probe	Actively monitor tip clearance	At tip of each blade row	4	$\pm 0.001$ in.
Rub Pins	Verify min tip clearance	At tip of each blade row	2 per row, 8 total	$\pm 0.001$ in.
Triax accelerometer	Monitor vibes for rig health	On fwd and aft bearing housing	2	$\pm 1$ g
Real Time Spectrum Analyzer	Monitor vibes and frequencies for rig health	Accelerometer output	1	N/A
Oil sump thermocouple, type K	Monitor oil temperature	Oil sump	1	$\pm 10^\circ\text{F}$
Strain gage thrust ring	Monitor bearing thrust load	Fwd bearing	2	$\pm 10$ lbf
Facility Speed pickup	Monitor speed	facility	2	$\pm 10$ rpm

## 4.2 VSPT Component Experiment Program Plan, Schedule, and ROM Cost

A program to provide experimental validation of the proposed LCTR VSPT using the NASA GRC Single Spool Turbine Facility can be accomplished in 36 months, of which 33 months are required for the technical effort and 3 months for reporting. Figure 4.3 shows a notional program schedule to accomplish this effort. During the preliminary design task, the concept for the VSPT will be refined to the point where all key aspects of the component and rig designs have been defined in sufficient detail to ensure that no key risk items are likely to force substantive design changes during detailed design. This requires that a comprehensive layout be produced, from which a bill of materials and parts list can be generated. Preliminary aerodynamics will be defined for each blade and vane row, from which structural models will be prepared. The aerodynamic, structural, and dynamic design of the blades, vanes, and other flowpath elements needs to take into consideration the actual operating conditions the VSPT would see in operation behind the gas generator, not just the relatively cold rig operating conditions, since it would do no good to test a component design which has no chance of surviving the actual operating conditions in the real engine. Rotordynamic analyses will be required as a part of the preliminary design in order to ensure that sufficient speed and frequency margins can be obtained with the proposed configuration. For a power turbine module that interfaces with the reduction gearbox directly rather than by extending a shaft through

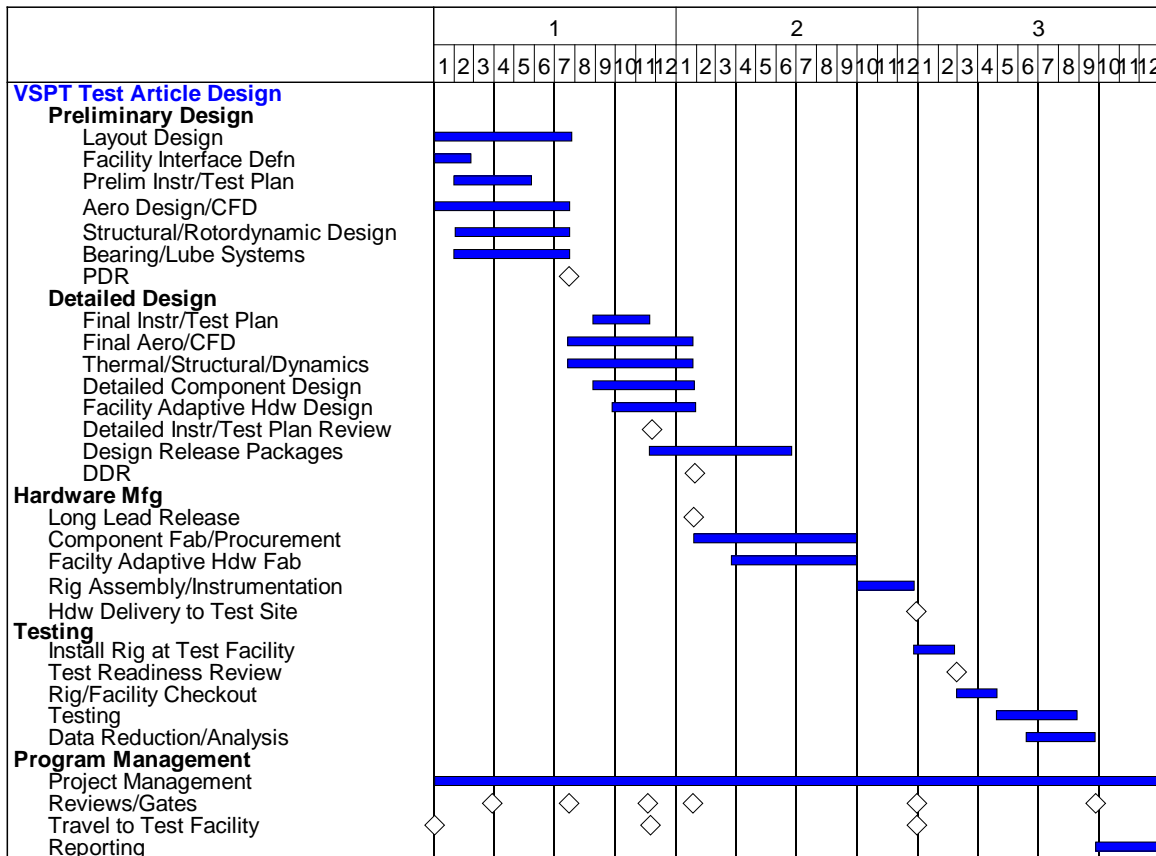


Figure 4.3.—Proposed Schedule for VSPT Experiment

the gas generator (e.g., PT-6 configuration) there is substantial freedom in the design and opportunity to vary shaft characteristics and bearing spacing to achieve sufficient margins, so the risk of not achieving acceptable margins is fairly low. To reduce risk, a Design Failure Modes and Effects Analysis (DFMEA) will be conducted during preliminary design. This will help identify any potential failure modes and define mitigation approaches early enough in the program so they can be incorporated into the design and test plan.

The rig configuration will be driven by the requirements to obtain the key data for validating the design, and by the interfaces with NASA’s single spool turbine facility. At the outset of the preliminary design task, Substantial coordination with the NASA technical team will be required to define the rig/facility interface requirements, as well as routing for instrumentation and secondary systems plumbing and rig and facility safety requirements.

The lubrication and secondary air systems will also be defined in the preliminary design. For the rig, a conventional jetted recirculating oil lubrication system will be used. Facility pumps will provide motive flow and scavenge and these will be sized according to the predicted requirements of the rig across its operating range of speed and power output. Purge air flow and pressure requirements for bearing compartments and to prevent flowpath air ingestion will also be defined. The preliminary design effort is expected to require 7 months to complete. At the conclusion of the preliminary design efforts, a preliminary design review with the NASA technical team is planned.

Since all of the key characteristics of the VSPT component and rig design will have been defined in Preliminary Design, the detailed design efforts will focus on substantiating the preliminary design configuration via detailed modeling and analysis. The instrumentation and test plan will be finalized and will be provided to NASA along with a 3-D external model of the test rig and all its secondary systems and plumbing. Component aerodynamics will be finalized via detailed CFD, structural, and dynamics

analyses, including transient analyses to define final operating and build tip clearances. If necessary due to design changes, the rotordynamics model will be updated and exercised to finalize the design of the rotary group and bearing system. Design release packages will be produced, comprising all the design and manufacturing information needed to produce or procure the component and rig hardware. At the completion of the detailed design task, a detailed design review will be held with the NASA technical team. The DDR will include a review of the updated DFMEA based on the completed state of the design.

Once the DDR is approved, long lead hardware will be ordered and hardware fabrication will begin. Since the rig and component hardware is primarily to be made of steel and aluminum, it is likely the only long lead hardware may be the bearings. As a risk reduction approach, the rig can be designed around bearings that are already in hand and available, or are known to be available on short lead. Fabrication of rig and component hardware, as well as facility adaptive hardware, can be completed in 8 months, at which time instrumentation and assembly of the rig will begin. The milestone for delivery of the completed instrumented rig to the NASA test facility occurs at month 24.

A detailed test readiness and safety review will be conducted once the rig is installed at the test facility. This review will address all aspects of rig operation and data collection, including a review of the DFMEA.

Testing will begin at month 28 and will follow the approved test plan. Ideally, two sets of hardware with slightly different aerodynamics will be tested back-to-back to bracket the design and provide data for a sensitivity analysis. At completion of the test program, the rig and component hardware will be torn down and assessed to determine if any conditions exist that may have affected the test data, such as tip rubs or damage to any of the hardware or instrumentation. The test data will be reduced and analyzed and compared to pre-test predicted maps. The maps used in the cycle model will be updated to reflect actual performance and the mission analysis will be re-run to determine the effects of the status updates on the overall mission performance.

The program schedule shows milestones for major reviews and on-site meetings at the test facility. A final report will be compiled and submitted at month 36.

A ROM cost estimate for the proposed 36-month VSPT experiment program shown in Figure 4.3 is \$4.5M, broken down as follows:

- Preliminary Design: \$800,000
- Detailed Design: \$1,400,000
- Component and rig hardware: \$1,200,000
- Testing: \$300,000
- Program management: \$800,000

This ROM represents an estimate of contractor cost to perform the design, build the hardware, conduct testing, and manage the effort. It does not include an estimate of costs for use of the test facility and support from NASA and government service contractors. If it is determined that the VSPT test components can be overhung directly from the facility bearing cartridge, eliminating the need for the dedicated component bearings and lube system, the cost to design and build the components would be reduced, and the total cost of the program could potentially be lower by as much as \$200,000.

## 5.0 Conclusions

In this study, a variable speed power turbine design was executed for a proposed Large Civil Tiltrotor. This application is unique in that it requires a turbine with far greater off-design capability than traditional propulsion related gas turbines. Airfoil incidence can change as much as 60° between the high speed and low speed rotor settings. These large changes in incidence cause airfoil separations and large loading changes resulting in reduced efficiency. In order to address these large loading swings, a study was performed in which a methodical multiple design-point process was used to arrive at a flowpath that

is fundamentally speed insensitive. This is in direct contrast to other techniques such as variable geometry or a variable gear ratio transmission. The figure of merit used in this study was to minimize the fuel burn throughout the mission by weighting various performance conditions in such a way as to mimic a typical flight. Various designs were analyzed and traded against each other with a turbine meanline code and CFD calculations were used to validate the results. CFD consistently showed better negative incidence tolerance (high speed) than the 1-D meanline loss systems. This finding would suggest moving the design point selection to lower speed than the 1-D prediction. Any further research would require testing.

A component experiment program plan was proposed that can be accomplished within a 36-month period. This program would design and fabricate a stand-alone rig to mate to the NASA GRC Single Spool Turbine Test Facility and take advantage of its capabilities to run the testing at full scale for the proposed LCTR application in an economical manner. A notional component test article design was proposed that emulates the configuration recommended for the LCTR engine, and which greatly minimizes rotordynamic issues that would be major concerns for alternative configurations.

The design methodology and technology investigated in this study can provide benefits to other systems beyond the LCTR. Any system that can benefit from improved off-design performance, whether turbofan, turboshaft, or turboprop, may be able to take advantage of the proposed approach to avoid the complexity and cost associated with traditionally variable geometry approaches. This includes not only aviation engines, but also ground power and automotive engines.





TABLE A.1.—Concluded.

----DUCTS----	dPhorm	MN	Aphy	C_LPTUncharg	El>	0.0563	1.0000	1.0000	1.6163	1248.88	173.74	294.057
Duct1	0.0000	0.4000	132.95	C_HPTCharg	El>	0.0916	1.0000	1.0000	2.4239	1661.69	282.22	294.057
ICduct	0.0020	0.4000	14.19	C_HPTUncharg	El>	0.1751	1.0000	1.0000	4.6347	1661.69	282.22	610.864
Duct6	0.0000	0.2500	5.85									
Duct43	0.0000	0.3000	19.55									
ITduct	0.0000	0.2000	89.22									
Duct12	0.0000	0.3000	292.50									
---SHAFTS----	Nmech	trq in	pwr in									
HP_Shaft	14800.0	1613.4	4546.4									
IP_Shaft	12000.0	2984.7	6819.3									
LP_Shaft	15000.0	2626.1	7500.0									
---BURNERS---	TtOut	eff	dPhorm	Wfuel	PAR	EINOx	ppm					
Burner	3660.00	1.0000	0.0200	0.71702	0.03695							
---NOZZLES---	PR	Cfg	CdTh	Cv	Atb	MNth	Vact	Pg				
Nozzle	1.050	0.9900	1.0000	0.9900	320.24	0.271	500.5	457.5				

TABLE A.2.—2,000 ALTITUDE, +45 °F DAY, HOVER (NOT AT MAXIMUM POWER) 100 PERCENT NPR

*****												
Date:08/27/10 Time:09:18:25 Model: Generic turbohaft engine - Off-design converge = 1 CASE: 114												
Version:NPSS 1.6.5 - Rev: -> Gas Package: Janaf iter/pass/Jacob/Broy= 4/ 15/ 1/ 2 Run by: csnyder PC: 35												
*****												
MN	alt	dTs	W	Fn	TSFC	Wfuel	VTAS	OPR	T4	T41	T47	Dyn P.
0.000	1999.9	45.00	21.13	338.8	5.1997	1761.60	0.12	32.845	3516.1	3199.7	2634.0	0.0
SUMMARY OUTPUT DATA												
FLOW STATION DATA												
	W	ht	FAR	Mc	Ps	Ts	Aphy	MN	gamt	gamma		
FL1 Ambient.Fl_O	21.13	13.665	556.54	2.91	0.0000	23.54	13.665	556.54	0.000	1.3997		
FL2 Inlet.Fl_O	21.13	13.665	556.54	2.91	0.0000	23.54	12.745	545.58	0.317	1.3997		
FL22 Duct1.Fl_O	21.13	13.665	556.54	2.91	0.0000	23.54	13.414	553.60	0.163	1.3997		
FL23 LPC.Fl_O	21.13	157.430	1194.47	159.84	0.0000	2.99	141.778	1161.19	0.394	1.3684		
FL24 ICduct.Fl_O	21.13	157.115	1194.47	159.84	0.0000	3.00	141.495	1161.19	0.394	1.3705		
FL25 HPC axi.Fl_O	21.13	178.300	1240.86	171.69	0.0000	2.69	168.045	1221.32	0.296	1.3655		
FL26 Hld25.Fl_O	19.49	178.300	1240.86	171.69	0.0000	2.48	160.616	1206.58	0.394	1.3655		
FL27 HPC centri.Fl_O	19.49	448.807	1636.08	275.35	0.0000	1.13	421.830	1610.32	0.305	1.3435		
FL28 Hld3.Fl_O	14.29	448.807	1636.08	275.35	0.0000	0.83	429.876	1618.15	0.254	1.3435		
FL3 Duct6.Fl_O	14.29	448.807	1636.08	275.35	0.0000	0.83	436.588	1624.58	0.203	1.3435		
FL4 Burner.Fl_O	14.78	439.831	3516.12	227.00	0.0342	1.29	399.216	3444.48	0.399	1.2602		
FL42 HPT.Fl_O	19.98	211.768	2708.62	125.92	0.0251	3.17	200.056	2674.04	0.300	1.2873		
FL43 Duct43.Fl_O	19.98	211.768	2708.62	125.92	0.0251	3.17	191.472	2647.68	0.400	1.2873		
FL44 LPT.Fl_O	21.62	66.179	2092.41	-23.97	0.0232	9.64	64.601	2080.51	0.193	1.3085		
FL45 ITduct.Fl_O	21.62	66.179	2092.46	-23.97	0.0232	9.64	60.194	2046.08	0.383	1.3081		
FL6 PowerT.Fl_O	21.62	14.348	1558.00	-175.66	0.0232	38.38	13.835	1543.95	0.234	1.3313		
FL7 Duct12.Fl_O	21.62	14.348	1558.06	-175.66	0.0232	38.38	13.835	1544.01	0.234	1.3313		
FL9 Nozzle.Fl_O	21.62	14.348	1558.12	-175.66	0.0232	38.38	13.665	1539.29	0.271	1.3313		
TURBOMACHINERY PERFORMANCE DATA												
	Mc	PR	eff	TR	efPoly	pwr	SMN	SMW	W	Tt	ht	Pt
LPC	23.54	11.521	0.8564	11309.372	2.1462	0.8953	-4691.4	21.06	21.55			
HPC_axi	3.00	1.135	0.8893	9597.988	1.0388	0.8912	-354.2	19.71	11.97			
HPC_cen>	2.48	2.517	0.8579	9416.842	1.3185	0.8736	-2858.1	22.75	21.37			
HPT	1.29	2.077	0.8502	245.635	1.1376	0.8209	3212.4					
LPT	3.17	3.200	0.8516	225.094	1.2476	0.8285	4691.4					
PowerT	9.64	4.612	0.8266	327.916	1.3431	0.7964	4639.6					
TURBOMACHINERY MAP DATA												
	PRmap	McMap	effMap	R/Parm	s_Prdes	s_effDes	s_Ncdes					
LPC	24.61	7.278	0.8637	1.8331	1.6759	0.9916	0.8333					
HPC_axi	29.63	1.200	0.8542	1.9397	0.100682	0.6728	0.0001					
HPC_cen>	29.62	3.086	0.8515	2.0262	0.083407	0.7273	0.0001					
HPT	30.15	5.998	0.9290	100.408	0.042649	4.6409	0.0179					
LPT	149.98	5.735	0.9294	99.582	0.021123	2.1523	0.0194					
PowerT	172.96	1.763	0.8861	101.749	0.055750	0.2112	0.0136					
---INLETS----												
Inlet	eRam	Afs	Fram	BLEEDS - output	Wb/Win	hscale	Pscale	W	Tt	ht	Pt	
	1.0000	-----	0.1	C_LPTCharg B1>	0.0214	1.0000	1.0000	0.4525	1240.86	171.69	66.179	

TABLE A.2.—Concluded.

---DUCTS----	dPnorm	MN	Aphy	C_LPTUncharg	B1>	0.0563	1.0000	1.6163	1248.88	173.74	294.057
Duct1	0.0000	0.4000	132.95	C_HPTUncharg	B1>	0.0916	1.0000	2.4239	1661.69	282.22	294.057
ICduct	0.0020	0.4000	14.19	C_HPTUncharg	B1>	0.1751	1.0000	4.6347	1661.69	282.22	610.864
Duct6	0.0000	0.2500	5.85								
Duct43	0.0000	0.3000	19.55								
ITduct	0.0000	0.2000	89.22								
Duct12	0.0000	0.3000	292.50								
---SHAFTS----	Nmech	trq in	pwr in								
HP_Shaft	14800.0	1613.4	4546.4								
IP_Shaft	12000.0	2984.7	6819.3								
LP_Shaft	15000.0	2626.1	7500.0								
---BURNERS----	TtOut	eff	dPnorm	Wfuel	FAR	EINOx	PPm				
Burner	3660.00	1.0000	0.0200	0.71702	0.03695						
---NOZZLES----	PR	Cfg	CdTh	Cv	Ath	MNth	Vact	Pg			
Nozzle	1.050	0.9900	1.0000	0.9900	320.24	0.271	500.5	457.5			

TABLE A.3.—CRUISE MISSION 1, 303.4 kn, 28,000 ALTITUDE, +0 °F DAY, INITIAL CRUISE POWER LEVEL, 100 PERCENT NPR rpm/650 ROTOR TIP SPEED  
 (this is just before shift, power turbine at 100% mechanical, 110% corrected speed from engine, power is a touch higher to match  
 rotor efficiency loss @ 650 fps (75k) vs. 350 fps (84.8k) at cruise speed)

\*\*\*\*\*  
 Date:08/30/10 Time:11:24:01 Model: Generic turbohaft engine - Off-design converge = 1 CASE: 115  
 Version:NPSS\_1.6.5 - Rev: -> Gas Package: Janaf iter/pass/Jacob/Broy- 4/ 15/1/1/ 2 Run by: csnyder PC: 47

MN	alt	dTs	W	Fn	TSPC	MFuel	VTAS	OPR	T4	T41	T47	Dyn P.
0.510	28000.0	-0.00	11.74	-20.3	----	836.01	511.85	40.872	3105.0	2816.5	2302.6	125.3

FLOW STATION DATA												
	W	Pt	Tt	ht	FAR	Mc	Ps	Aphy	Ts	MN	gamt	gams
FL1 Ambient.F1_O	11.74	5.705	440.66	-24.88	0.0000	27.88	4.776	107.32	418.82	0.510	1.4010	1.4011
FL2 Inlet.F1_O	11.74	5.705	440.66	-24.88	0.0000	27.88	5.147	132.95	427.87	0.386	1.4010	1.4010
FL22 Duct1.F1_O	11.74	5.705	440.66	-24.88	0.0000	27.88	5.557	247.79	437.36	0.194	1.4010	1.4010
FL23 LPC.F1_O	11.74	80.217	1019.82	115.84	0.0000	3.02	72.108	990.31	14.19	0.396	1.3795	1.3813
FL24 ICduct.F1_O	11.74	80.057	1019.82	115.84	0.0000	3.02	71.963	990.31	14.22	0.396	1.3795	1.3813
FL25 HPC.axi.F1_O	11.74	90.864	1060.53	126.01	0.0000	2.72	85.549	1043.16	16.37	0.297	1.3770	1.3780
FL26 Hld25.F1_O	10.83	90.864	1060.53	126.01	0.0000	2.50	81.693	1030.03	11.79	0.396	1.3770	1.3789
FL27 HPC.centri.F1_O	10.83	233.165	1416.67	217.21	0.0000	1.13	219.298	1394.07	6.75	0.302	1.3550	1.3563
FL28 Hld3.F1_O	7.94	233.165	1416.67	217.21	0.0000	0.83	223.430	1400.93	5.85	0.252	1.3550	1.3559
FL3 Duct6.F1_O	7.94	233.165	1416.67	217.21	0.0000	0.83	226.879	1406.57	7.22	0.201	1.3550	1.3556
FL4 Burner.F1_O	8.17	228.501	3105.04	178.28	0.0292	1.29	207.187	3039.09	6.24	0.397	1.2738	1.2756
FL42 HPT.F1_O	11.06	109.688	2369.82	88.37	0.0214	3.17	103.594	2338.53	19.55	0.298	1.2998	1.3008
FL43 Duct43.F1_O	11.06	109.688	2369.82	88.37	0.0214	3.17	99.130	2314.75	15.24	0.398	1.2998	1.3016
FL44 LPT.F1_O	11.97	32.595	1799.98	-46.75	0.0198	10.06	31.745	1788.36	89.22	0.200	1.3219	1.3224
FL45 ITduct.F1_O	11.97	32.595	1799.98	-46.75	0.0198	10.06	29.350	1754.45	47.72	0.401	1.3219	1.3239
FL6 PowerT.F1_O	11.97	5.015	1225.94	-203.25	0.0198	53.94	4.645	1201.58	292.50	0.338	1.3530	1.3545
FL7 Duct12.F1_O	11.97	5.015	1225.94	-203.25	0.0198	53.95	4.645	1201.64	292.50	0.338	1.3530	1.3545
FL9 Nozzle.F1_O	11.97	5.015	1226.01	-203.25	0.0198	53.95	4.776	1210.48	358.41	0.269	1.3530	1.3539

TURBOMACHINERY PERFORMANCE DATA												
	Mc	PR	eff	Nc	TR	effPoly	Pwr	SMN	SMW	Wb/Min	hscale	Pscale
LPC	27.88	14.061	0.8467	11891.743	2.3143	0.8913	-2337.9	19.31	19.32			
HPC axi	3.02	1.135	0.8860	9688.471	1.0399	0.8879	-169.0	19.85	12.38			
HPC cen>	2.50	2.566	0.8558	9500.707	1.3358	0.8724	-1397.3	21.32	19.72			
HPT	1.29	2.083	0.8494	243.803	1.1438	0.8269	1566.3					
LPT	3.17	3.365	0.8484	225.162	1.2676	0.8263	2337.9					
PowerT	10.06	6.499	0.8485	353.555	1.4685	0.8139	2651.5					

TURBOMACHINERY MAP DATA												
	McMap	PRmap	effMap	NcMap	R/Parm	McDes	s PRdes	s effDes	s McDes	W	Tt	Pt
LPC	29.15	8.793	0.8539	99.098	1.9377	0.956433	1.6759	0.9916	0.8333			
HPC axi	29.90	1.201	0.8521	0.997	1.9792	0.100682	0.6728	1.0354	0.0001			
HPC cen>	29.90	3.153	0.8503	0.996	2.0213	0.083407	0.7273	1.0019	0.0001			
HPT	30.16	6.027	0.9281	99.659	6.0270	0.042649	4.6409	0.9152	0.0179			
LPT	149.97	6.091	0.9259	99.611	6.0905	0.021123	2.1523	0.9163	0.0194			
PowerT	180.41	2.162	0.9096	109.705	2.1615	0.055750	0.2112	0.9328	0.0136			

---INLETS----												
	cRam	Afs	Fram	BLEEDS - output	Wb/Min	hscale	Pscale	W	Tt	ht	Pt	
Inlet	1.0000	107.32	186.8									

TABLE A.3.—Concluded.

----DUCTS----	dPnorm	MN	Aphy	C_LPTCharg	Bl>	0.0214	1.0000	1.0000	0.2515	1060.53	126.01	32.595
Duct1	0.0000	0.3862	132.95	C_LPTUncharg	Bl>	0.0563	1.0000	1.0000	0.6614	1060.53	126.01	109.688
ICduct	0.0020	0.3957	14.19	C_HPTCharg	Bl>	0.0916	1.0000	1.0000	0.9920	1416.67	217.21	109.688
Duct6	0.0000	0.2515	5.85	C_HPTUncharg	Bl>	0.1751	1.0000	1.0000	1.8967	1416.67	217.21	228.501
Duct43	0.0000	0.2982	19.55									
ITduct	0.0000	0.2002	89.22									
Duct12	0.0000	0.3380	292.50									
----SHAFTS----	Nmech	trq in	pwr in									
HP Shaft	13585.4	605.5	1566.3									
IP Shaft	10961.0	1120.2	2337.9									
LP Shaft	15000.0	928.4	2651.5									
----BURNERS----	TtOut	eff	dPnorm	Wfuel	FAR	EINOx	Fpm					
Burner	3105.04	1.0000	0.0200	0.23223	0.02924							
----NOZZLES----	PR	CEg	CdTh	Cv	Ath	MNth	Vact	Fg				
Nozzle	1.050	0.9900	1.0000	0.9900	320.24	0.269	447.3	166.5				

TABLE A.4.—CRUISE MISSION 1, 303.4 kn, 28,000 ALTITUDE, +0 °F DAY, INITIAL CRUISE POWER LEVEL,  
54 PERCENT NPR\_rpm/350 ROTOR TIP SPEED—NO MULTISPEED GEARBOX

(reduction in speed from engine to rotor is achieved totally through speed reduction in the power turbine)  
 \*\*\*\*\*  
 Date:08/27/10 Time:09:18:48 Model: Generic turbohaft engine - Off-design converge = 1 CASE: 146  
 Version:NPS5\_1.6.5 - Rev: -> Gas Package: Jansaf iter/pass/Jacb/Broy= 1/ 1/ 0/ 0 Run by: csnyder PC: 48

MN	alt	dTs	W	Fa	TSPC	Wfuel	VIAS	OPR	T4	T41	T47	Dyn P.
0.510	28000.0	-0.00	11.81	-19.4	-----	805.23	511.85	40.644	3039.9	2760.7	2259.4	125.3
SUMMARY OUTPUT DATA												
FLOW STATION DATA												
	W	Pt	Tt	ht	FAR	Wc	Ps	Ts	Apby	MN	gamt	gams
FL1 Ambient.F1.O	11.81	5.705	440.66	-24.88	0.0000	28.05	4.776	418.82	107.98	0.510	1.4010	1.4011
FL2 Inlet.F1.O	11.81	5.705	440.66	-24.88	0.0000	28.05	5.139	427.68	132.95	0.389	1.4010	1.4010
FL22 Duct1.F1.O	11.81	5.705	440.66	-24.88	0.0000	28.05	5.555	437.32	247.79	0.195	1.4010	1.4010
FL23 LPC.F1.O	11.81	81.953	1026.41	117.49	0.0000	2.98	73.893	997.56	14.19	0.390	1.3791	1.3809
FL24 ICduct.F1.O	11.81	81.789	1026.41	117.49	0.0000	2.99	73.746	997.56	14.22	0.390	1.3791	1.3809
FL25 HPC axi.F1.O	11.81	92.859	1067.28	127.71	0.0000	2.68	87.570	1050.28	16.37	0.293	1.3765	1.3776
FL26 Bld25.F1.O	10.90	92.859	1067.28	127.71	0.0000	2.47	83.748	1037.50	11.79	0.390	1.3765	1.3784
FL27 HPC centri.F1.O	10.90	231.865	1413.31	216.33	0.0000	1.14	217.760	1390.22	6.75	0.305	1.3552	1.3565
FL28 Bld3.F1.O	7.99	231.865	1413.31	216.33	0.0000	0.84	221.969	1397.23	5.85	0.254	1.3552	1.3561
FL3 Duct6.F1.O	7.99	231.865	1413.31	216.33	0.0000	0.84	225.477	1403.01	7.22	0.203	1.3552	1.3558
FL4 Burner.F1.O	8.21	227.228	3039.88	179.09	0.0280	1.29	206.009	2874.87	6.24	0.397	1.2763	1.2781
FL42 HPT.F1.O	11.12	109.465	2324.19	91.12	0.0205	3.16	103.413	2293.55	19.55	0.297	1.3018	1.3028
FL43 Duct43.F1.O	11.12	109.465	2324.24	91.12	0.0205	3.16	98.983	2270.27	15.24	0.396	1.3018	1.3036
FL44 LPT.F1.O	12.04	31.006	1749.03	-45.80	0.0189	10.48	30.126	1736.72	89.22	0.209	1.3247	1.3253
FL45 Iduct.F1.O	12.04	31.006	1749.08	-45.80	0.0189	10.48	27.613	1699.96	47.72	0.421	1.3247	1.3270
FL6 PowerT.F1.O	12.04	5.016	1242.37	-183.50	0.0189	54.59	4.636	1217.10	292.50	0.343	1.3525	1.3541
FL7 Duct12.F1.O	12.04	5.016	1242.44	-183.50	0.0189	54.59	4.636	1217.16	292.50	0.343	1.3525	1.3541
FL9 Nozzle.F1.O	12.04	5.016	1242.50	-183.50	0.0189	54.59	4.776	1226.77	362.53	0.270	1.3525	1.3535

TURBOMACHINERY PERFORMANCE DATA												
	Wc	PR	eff	Nc	TR	efPoly	SMN	SMW	W	hscale	Pscale	Pt
LPC	28.05	14.366	0.8466	11919.382	2.3293	0.8915	-2379.7	17.62	17.54			
HPC axi	2.99	1.135	0.8894	9571.222	1.0398	0.8913	-170.8	19.52	11.74			
HPC_cen>	2.47	2.497	0.8572	9386.157	1.3242	0.8732	-1366.3	23.43	22.14			
HPT	1.29	2.076	0.8499	244.205	1.1442	0.8283	1537.1					
LPT	3.16	3.530	0.8473	227.887	1.2805	0.8240	2379.6					
PowerT	10.48	6.182	0.7859	193.128	1.4080	0.7428	2345.4					
TURBOMACHINERY MAP DATA												
	WcMap	PRmap	effMap	NcMap	R/Parm	s WcDes	s PRDes	s effDes	s NcDes	W	Tt	Pt
LPC	29.33	8.975	0.8538	99.328	1.8890	0.956433	1.6759	0.9916	0.8333			
HPC axi	29.53	1.201	0.8552	0.985	1.9200	0.100682	0.6728	1.0354	0.0001			
HPC_cen>	29.52	3.058	0.8516	0.984	2.0308	0.083407	0.7273	1.0019	0.0001			
HPT	30.15	5.993	0.9286	99.824	5.9528	0.042649	4.6409	0.9152	0.0179			
LPT	149.61	6.446	0.9246	100.817	6.4463	0.021123	2.1523	0.9163	0.0194			
PowerT	187.94	2.094	0.8424	59.926	2.0945	0.055750	0.2112	0.9328	0.0136			
---INLETS----	eRam	Afs	Fram									
Inlet	1.0000	107.98	188.0		BLEEDS - output	Wb/Win	hscale	Pscale	W	Tt <td>ht</td> <td>Pt</td>	ht	Pt
					C_LPTCharg B1>	0.0214	1.0000	1.0000	0.2530	1067.28	127.71	31.006

TABLE A.4.—Concluded.

----DUCTS----	dPnorm	MN	Aphy	C_LPTUncharg	B1>	0.0563	1.0000	1.0000	0.6655	1067.28	127.71	109.465
Duct1	0.0000	0.3890	132.95	C_HPTCharg	B1>	0.0916	1.0000	1.0000	0.9980	1413.31	216.33	109.465
ICduct	0.0020	0.3900	14.19	C_HPTUncharg	B1>	0.1751	1.0000	1.0000	1.9084	1413.31	216.33	227.228
Duct6	0.0000	0.2544	5.85									
Duct43	0.0000	0.2972	19.55									
ITduct	0.0000	0.2088	89.22									
Duct12	0.0000	0.3428	292.50									
---SHAFTS---	Nmech	trq in	pwr in									
HP Shaft	13464.3	599.6	1537.1									
IP Shaft	10986.5	1137.6	2379.6									
LP Shaft	8077.0	1525.1	2345.4									
---BURNERS---	TtOut	eff	dPnorm	WFuel	FAR	EINOx	PPm					
Burner	3039.88	1.0000	0.0200	0.22367	0.02800							
---NOZZLES---	PR	Cfg	CdTh	Cv	Ath	MNth	Vact	Fg				
Nozzle	1.050	0.9900	1.0000	0.9900	320.24	0.270	450.5	168.6				

## Appendix B.—Definitions

$AN^2$  is an indicator of blade pull stress. This stems from the fact that the pull stress of a spinning radial cylinder is proportional to  $AN^2$ . A good rule of thumb is that blade stress will be proportional to  $AN^2$  at the rate of 10 ksi per  $10E9 AN^2$ . For example, a well designed turbine blade with nickel based alloys operating at  $50E9 AN^2$  will have an average pull stress of about 50 ksi.

$$AN^2 \equiv (\text{Flowpath Annulus area in.}^2) \times (\text{rpm}^2)$$

Rim speed combined with  $AN^2$  is an indicator of disk loading. Rim speed is calculated using the TE hub radius.

$$\text{Rim Speed(ft/s)} = \text{Radius}_{\text{Hub}} (\text{in.}) / 12. * \text{rpm} * \pi / 30.$$

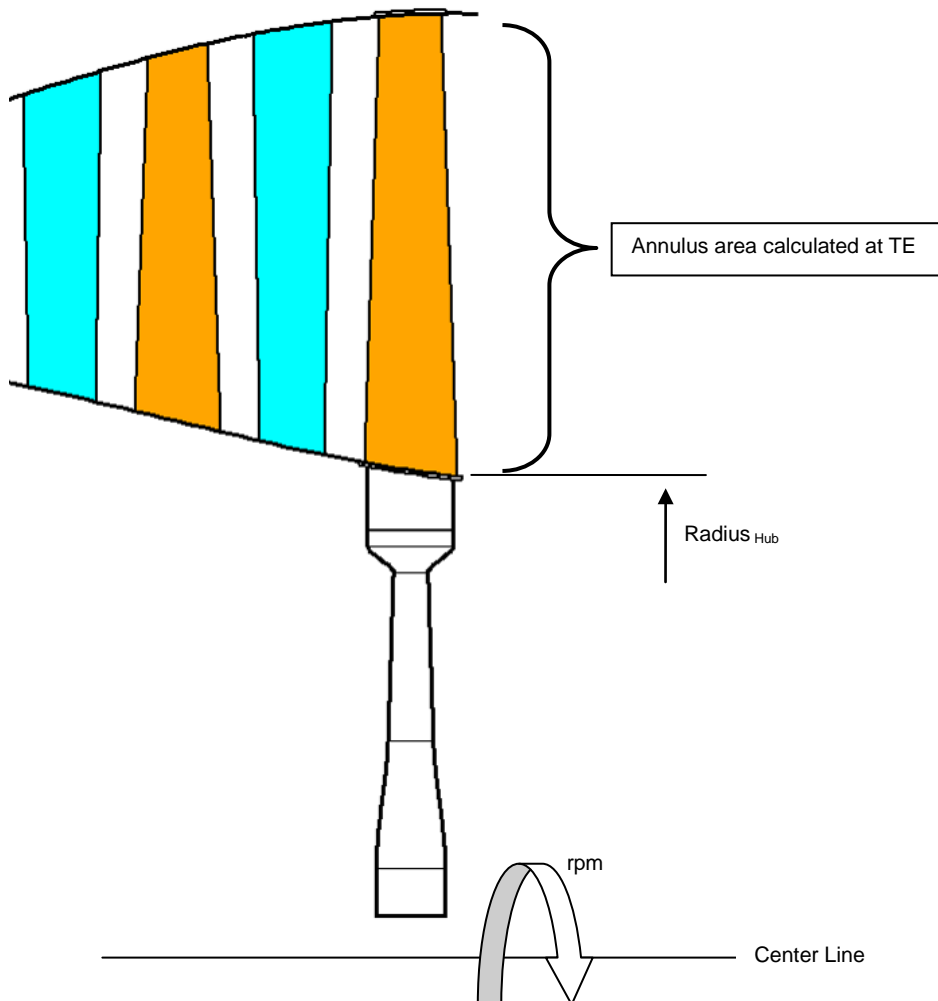
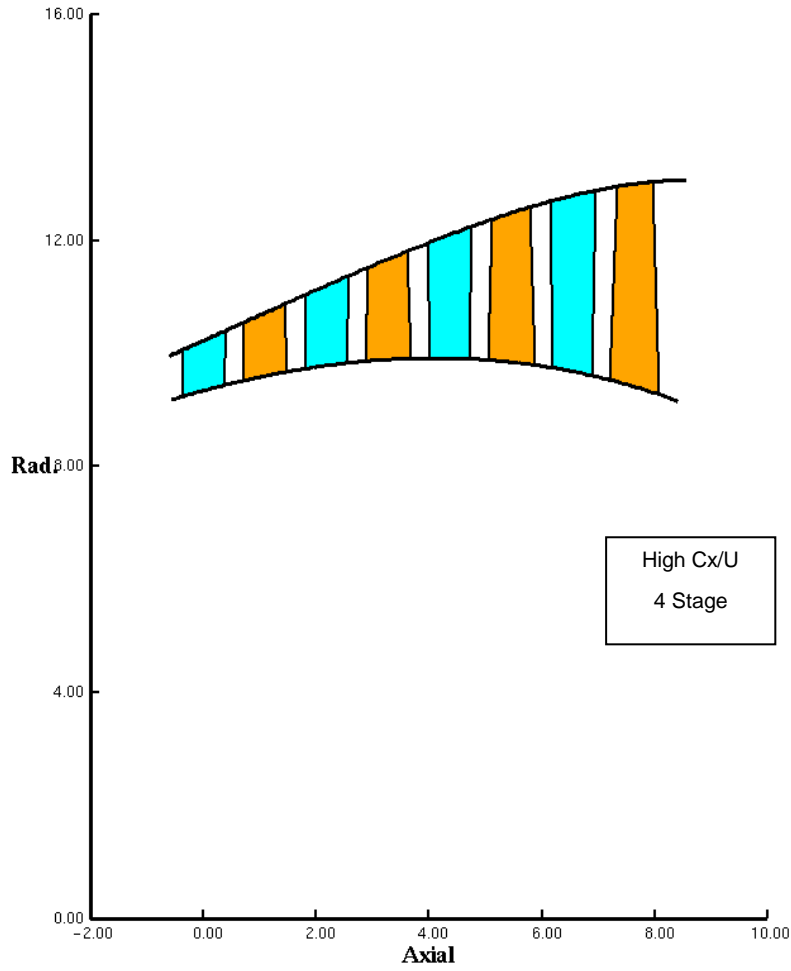


Figure B.1.—Turbine  $AN^2$  and Rim Speed Definitions



## Appendix C.—FlowPath Details

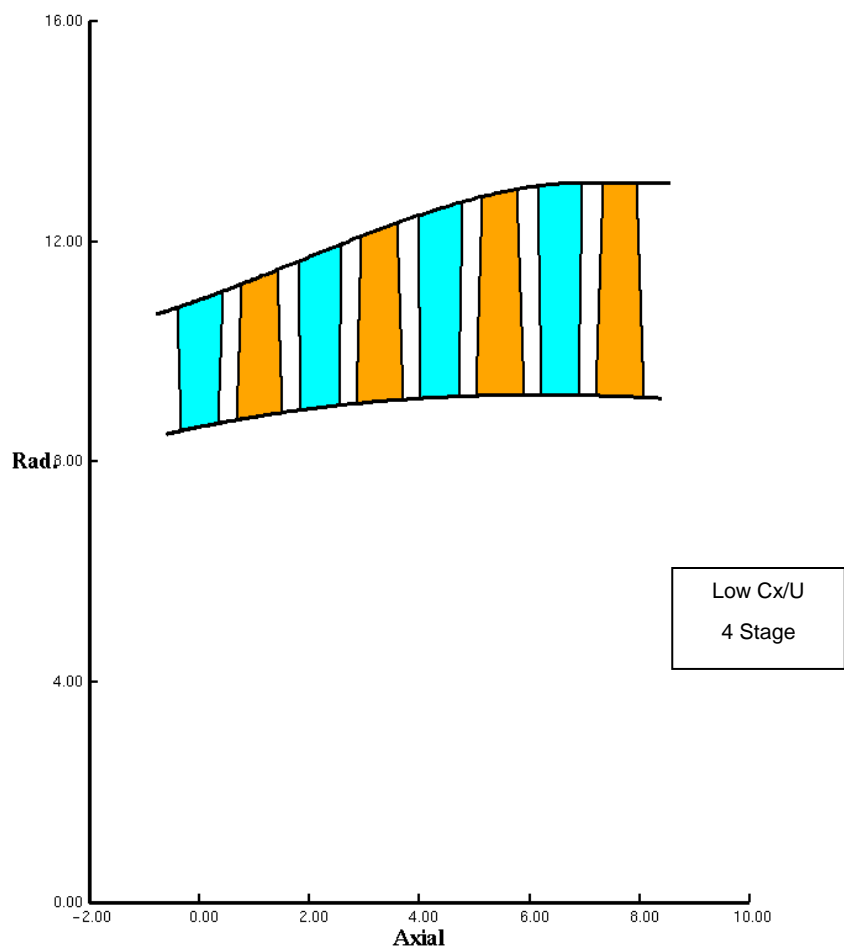


### High CX/U

% Speed	Design RPM	Fuel Burn%	ETA 1	ETA 2	ETA 3	ETA 4
53.8	8045	-3.29	73.34	68.62	69.34	91.39
69.2	10343	-7.88	88.33	84.71	84.12	88.62
84.6	12642	1.41	92.95	90.84	90.63	74.87
100.0	14941	23.20	91.25	91.58	92.80	57.42

%Speed	Work Coeff.	Flow Coeff.
54	1.68	0.813
100	0.5	0.448

Figure C.1.—High Cx/U Four Stage

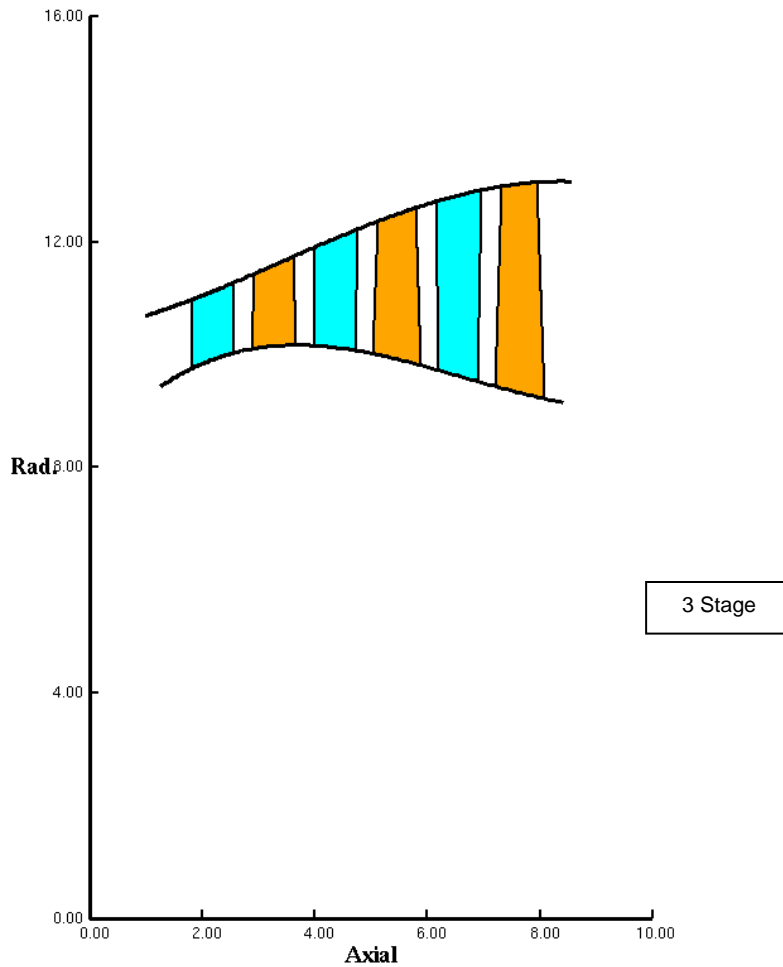


### Low CX/U

% Speed	Design RPM	Fuel Burn%	ETA 1	ETA 2	ETA 3	ETA 4
53.8	8045	-2.22	69.98	66.62	69.30	90.20
69.2	10343	-7.80	87.58	83.60	82.85	89.14
84.6	12642	-1.84	92.00	89.60	89.44	78.75
100.0	14941	24.30	89.29	89.78	91.43	57.00

%Speed	Work Coeff.	Flow Coeff.
<b>54</b>	<b>1.66</b>	<b>0.532</b>
<b>100</b>	<b>0.49</b>	<b>0.3</b>

Figure C.2.—Low Cx/U Four Stage

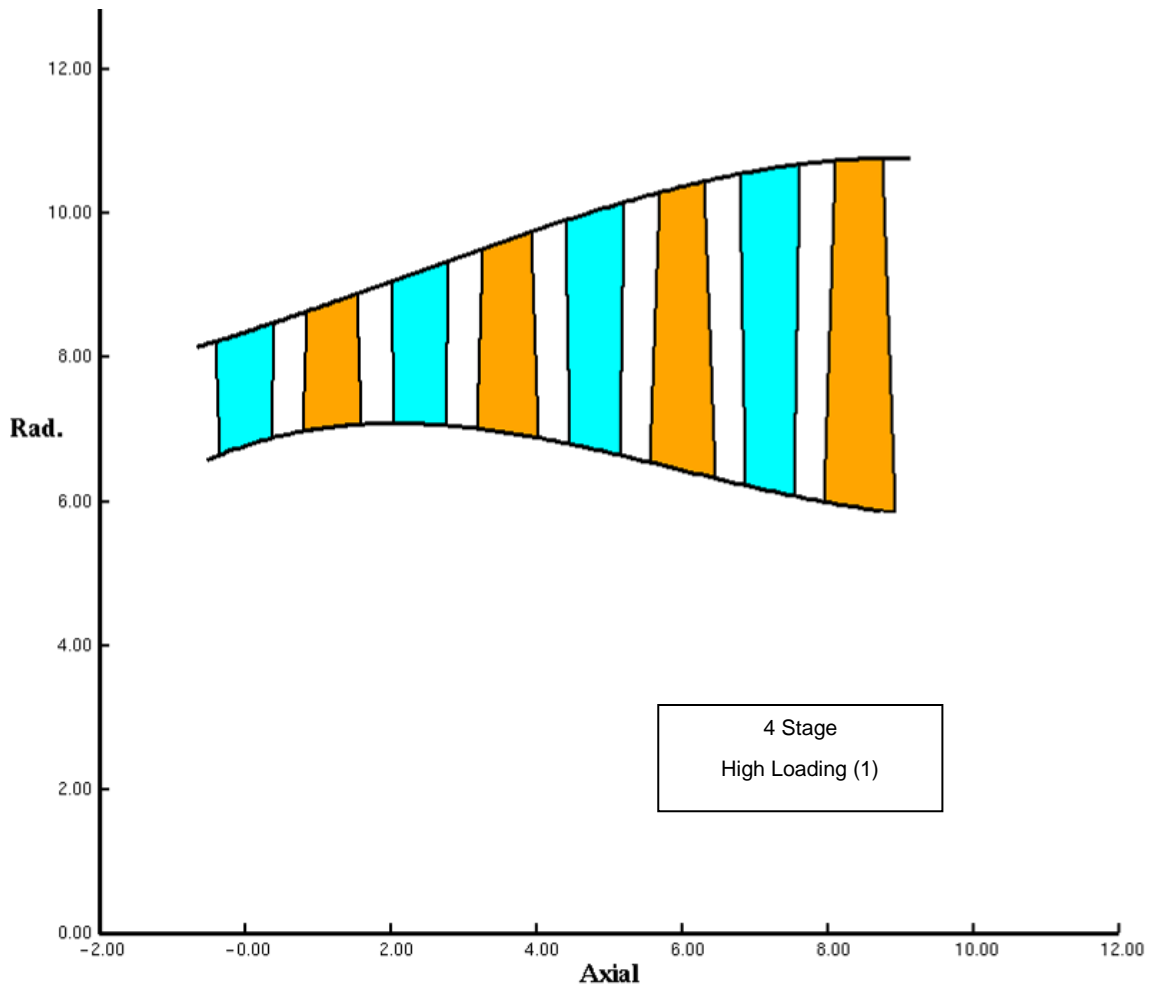


### 3 Stg

% Speed	Design RPM	Fuel Burn%	ETA 1	ETA 2	ETA 3	ETA 4
53.8	8045	-1.11	70.57	66.14	67.52	89.72
69.2	10343	-4.51	78.24	74.89	74.04	89.63
84.6	12642	-7.19	93.53	91.76	91.60	84.44
100.0	14941	-6.36	92.35	92.49	93.53	66.26

%Speed	Work Coeff.	Flow Coeff.
<b>54</b>	<b>2.11</b>	<b>0.722</b>
<b>100</b>	<b>0.63</b>	<b>0.368</b>

Figure C.3.—Three Stage

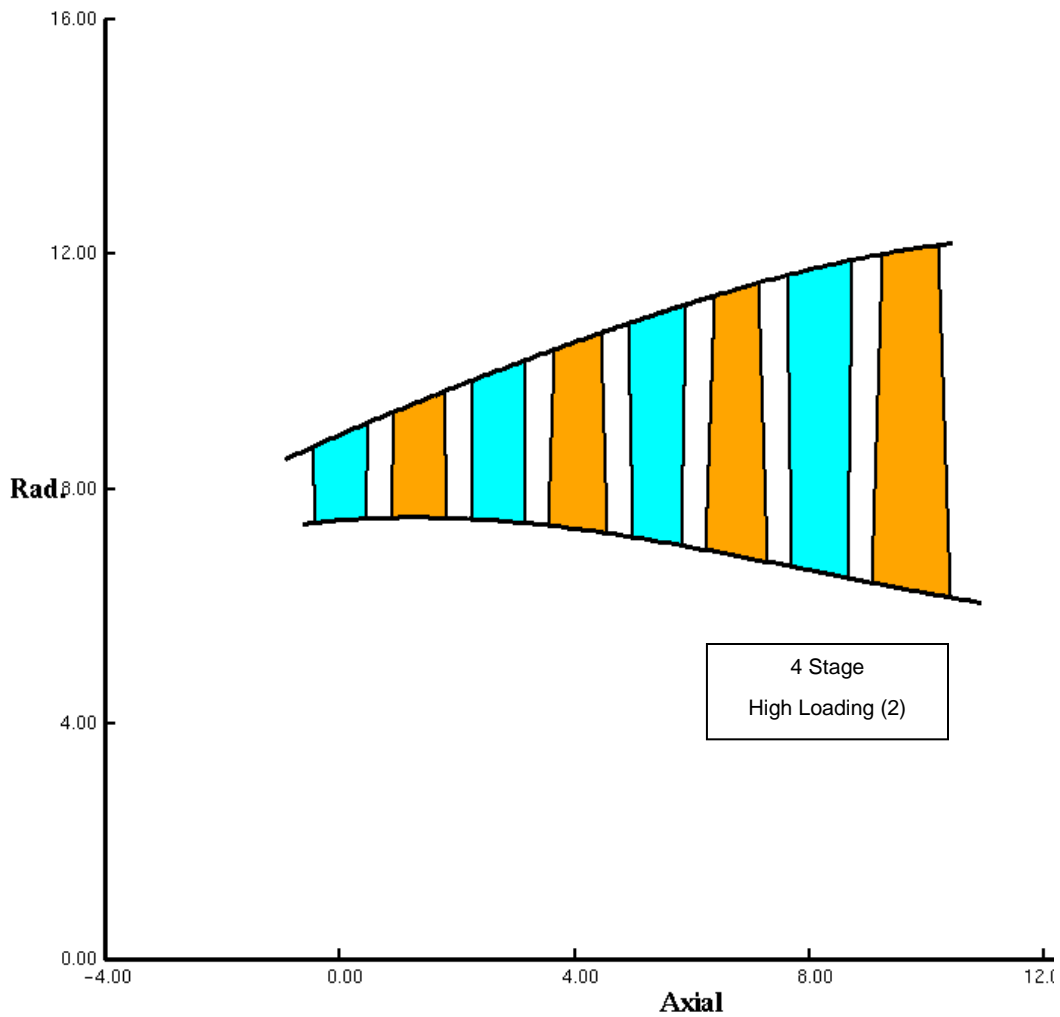


### 4 Stg Hi Loading (1)

% Speed	Design RPM	Fuel Burn%	ETA 1	ETA 2	ETA 3	ETA 4
53.8	8045	-0.84	78.77	71.42	69.10	87.45
69.2	10343	-7.98	90.15	87.28	87.13	87.37
84.6	12642	-8.31	93.67	92.32	92.37	85.64
100.0	14941	-3.68	93.96	93.59	94.26	79.31

%Speed	Work Coeff.	Flow Coeff.
54	2.826	1.008
100	0.828	0.467

Figure C.4.—Four Stage High Loading (1)

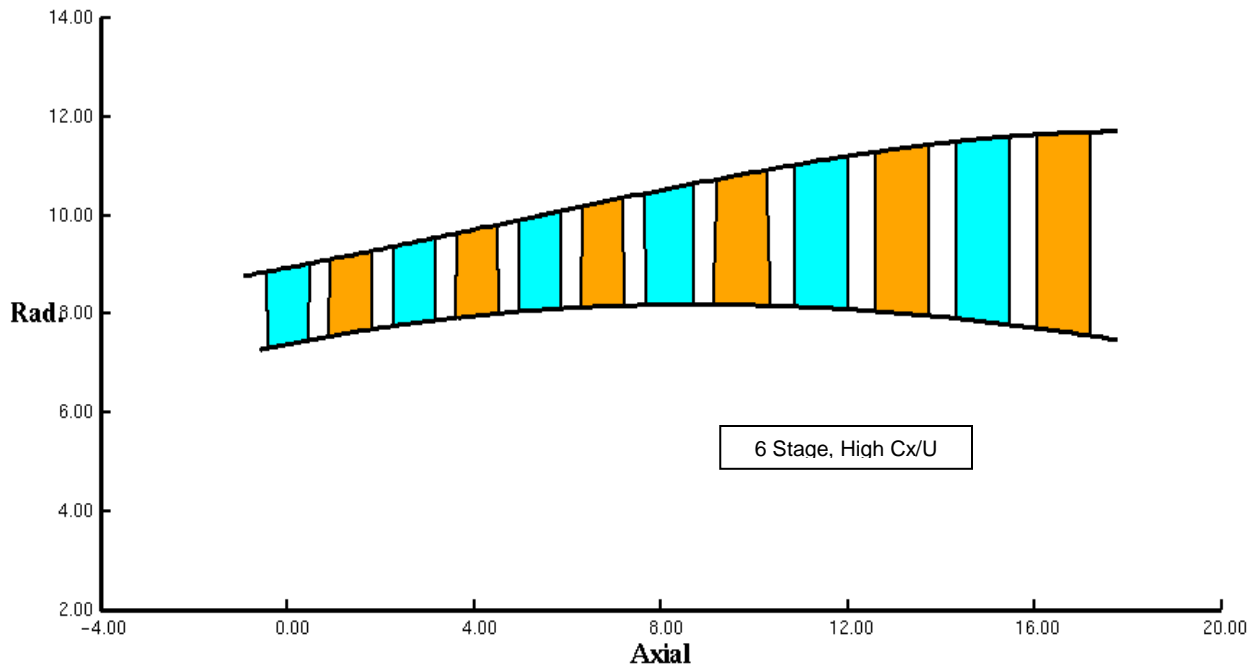


### 4 Stg Hi Loading (2)

% Speed	Design RPM	Fuel Burn%	ETA 1	ETA 2	ETA 3	ETA 4
54.0	7000	3.62	76.30	65.58	63.81	85.34
69.3	8988	-6.27	89.07	85.79	86.38	85.44
84.7	10975	-8.11	92.90	91.62	92.32	85.12
100.0	12963	-7.29	93.67	93.29	94.31	83.67

%Speed	Work Coeff.	Flow Coeff.
54	3.116	0.832
100	0.919	0.377

Figure C.5.—Four Stage High Loading (2)

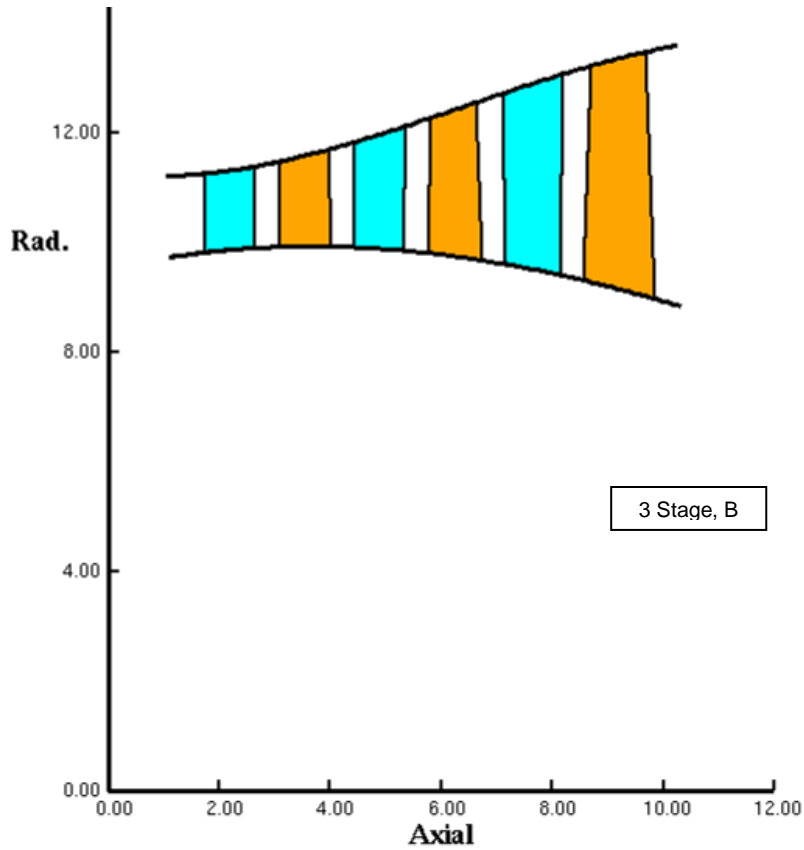


### 6 Stage A

% Speed	Design RPM	Fuel Burn%	ETA 1	ETA 2	ETA 3	ETA 4
54.0	7000	1.01	69.66	63.25	64.03	89.39
69.3	8988	-6.27	87.12	83.61	82.71	87.05
84.7	10975	0.50	92.74	90.47	90.61	75.84
100.0	12963	20.42	92.19	92.22	93.34	59.02

%Speed	Work Coeff.	Flow Coeff.
<b>54</b>	<b>2.031</b>	<b>1.037</b>
<b>100</b>	<b>0.611</b>	<b>0.541</b>

Figure C.6.—SixStage High Cx/U

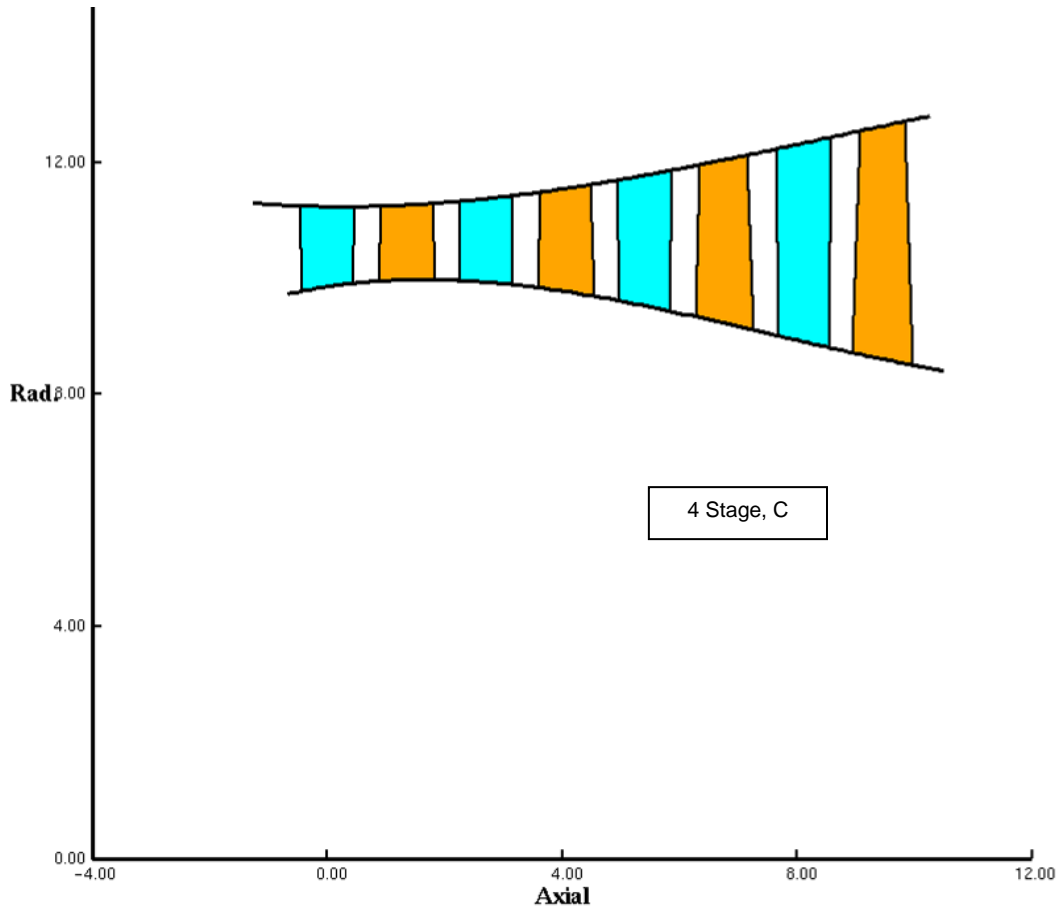


### 3 Stage B

% Speed	Design RPM	Fuel Burn%	ETA 1	ETA 2	ETA 3	ETA 4
54.0	6790	4.91	65.66	61.47	62.07	85.80
69.3	8718	-5.68	87.75	83.89	83.69	85.81
84.7	10646	-8.02	92.48	91.06	91.67	85.58
100.0	12574	-7.45	93.23	92.82	93.98	84.00

%Speed	Work Coeff.	Flow Coeff.
54	2.991	0.8423
100	0.966	0.4147

Figure C.7.—Three Stage B



### 4 Stage C

% Speed	Design RPM	Fuel Burn%	ETA 1	ETA 2	ETA 3	ETA 4
54.0	6200	4.41	68.91	60.48	62.16	86.31
69.3	7960	-5.84	87.29	83.39	83.22	86.26
84.7	9721	-6.21	92.48	90.80	91.14	83.40
100.0	11482	0.60	93.00	92.65	93.82	74.85

%Speed	Work Coeff.	Flow Coeff.
54	2.925	1.09025
100	0.864	0.507

Figure C.8.—Four Stage C

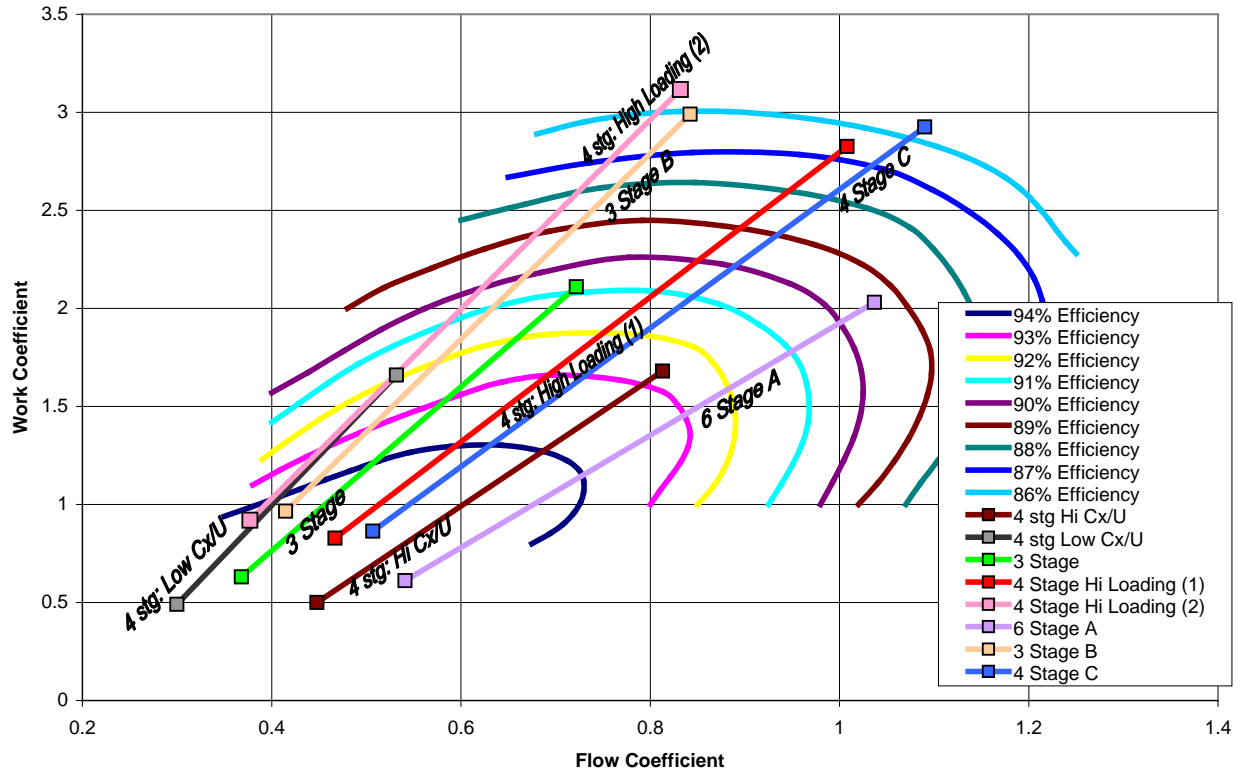


Figure C.9.—Smith Curve of All Turbines

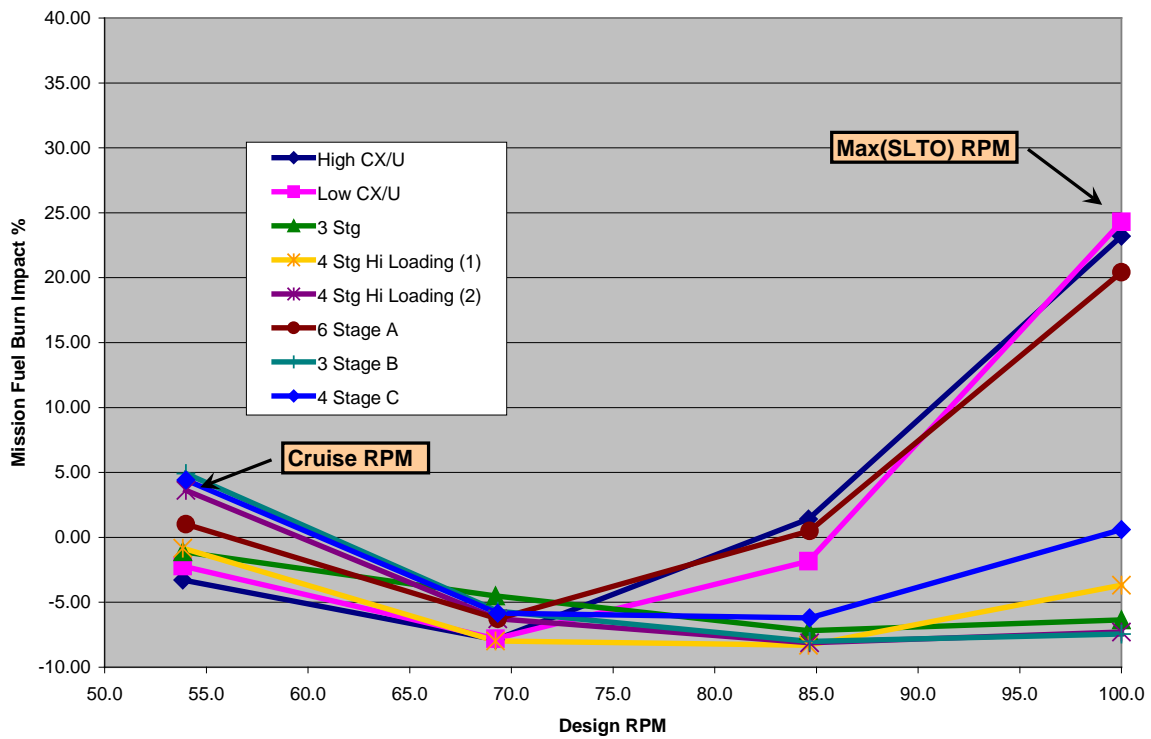


Figure C.10.—Design Speed Comparison: All Turbines



## Appendix D.—Four Stage CFD Analysis

The Four Stage power turbine presented in this study was analyzed using a Williams International proprietary CFD code called VORTEX. VORTEX is a 3–D, finite volume, explicit time marching flow solver. The solution assumes steady-state, time averaged flow. Each blade row is analyzed in the relative frame using mixing planes to jump from rotating to stationary blade rows. The mixing planes assure conservation of mass, momentum and energy. The performance used to analyze the turbine was based on the mission point 4 (see Table 2.1 and Table A.4) with small modifications. Point 4 corresponds to a 54 percent speed cruise condition. The CFD uses a fictitious design point. To execute the design, point 4 is used for the thermodynamics, but the speed is increased to 75 percent. The pressure ratio was also modified. The NPSS model had an efficiency at point 4 of 78.6 percent and an efficiency at point 3 (100 percent speed) of 84.9 percent. The predicted efficiency of this four stage is 86.54 and 90.74 percent respectively which requires less PR in order to meet the power requirement. This would be a significant rematch to the engine and would require additional cycle work, possible including a reduction in engine core size. Below is a summary of the parameters used in the CFD as well as the cycle targets. The inlet temperature and pressures shown are mass averaged values taken from the converged solution and differ slightly from the targets. Typically the inlet profiles can be adjusted as the simulation/design matures to hone in on the target values. The inlet mass flow is approximately 2.7 percent high which would require closing airfoil throat areas to assure proper engine matching.

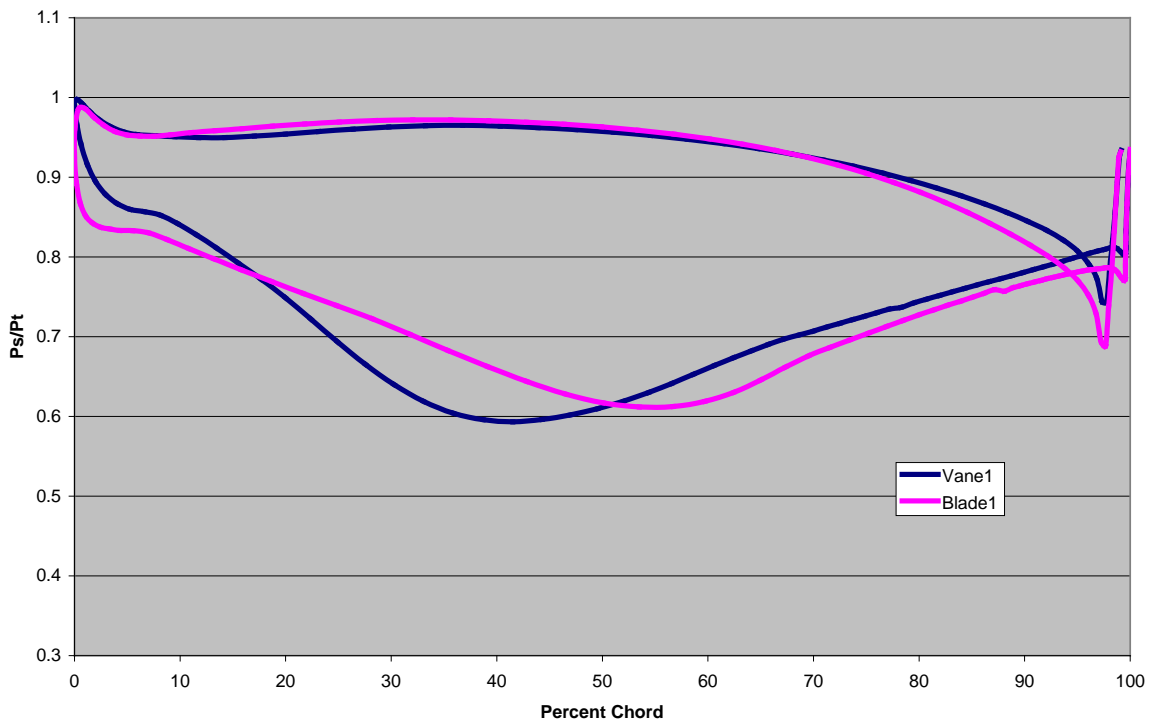
	<u>Cycle</u>	<u>CFD</u>
• PT	31.0 psia	30.93 psia
• TT	1749 °R	1696 °R
• Mdot	12.04 lbm/s	12.37 lbm/s
• rpm		11174 (75 percent speed)
• PR	6.18	5.6
• ETA	78.6 - 84.9 percent	92.9 percent <sup>1</sup>

<sup>1</sup> No leakage, cooling or tip clearance: MeanLine prediction = 93.55 percent @ PR = 5.78

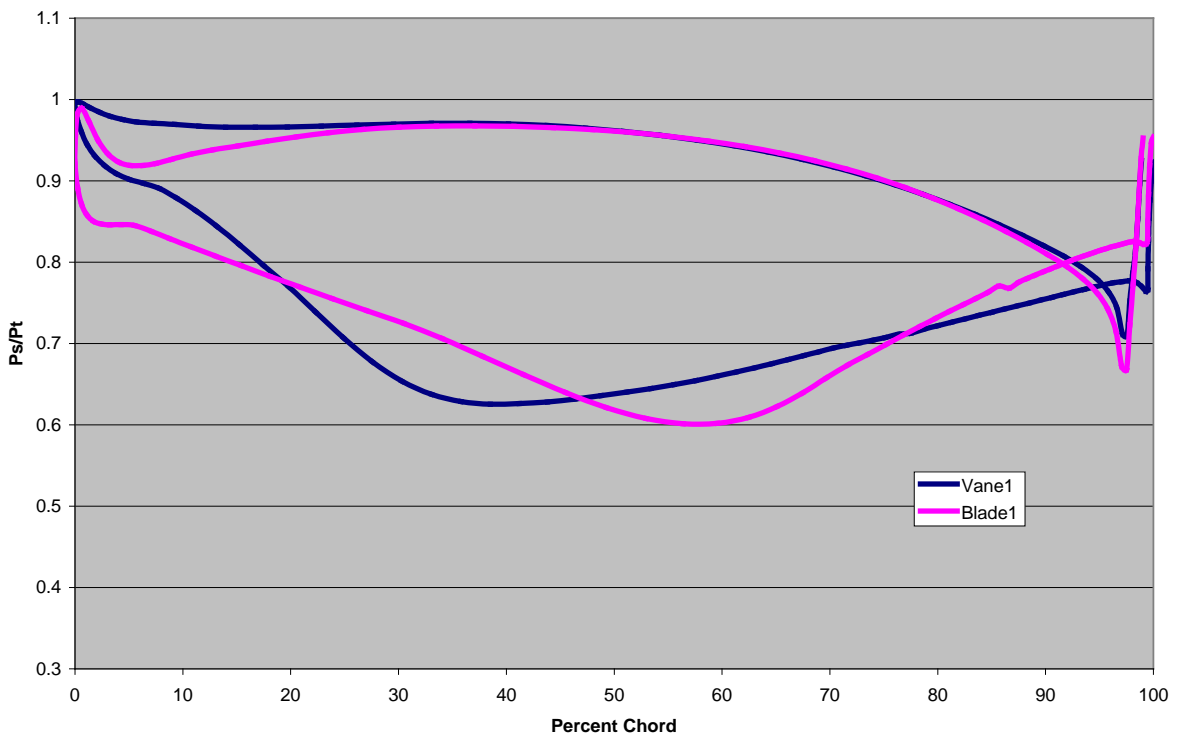
The geometry used in the CFD did not have fillets between the airfoil and endwall intersection. The following are surface static pressure loading plots of each stage. The vane and blade are plotted together: Hub, Mean and Tip.

## D.1 Stage 1

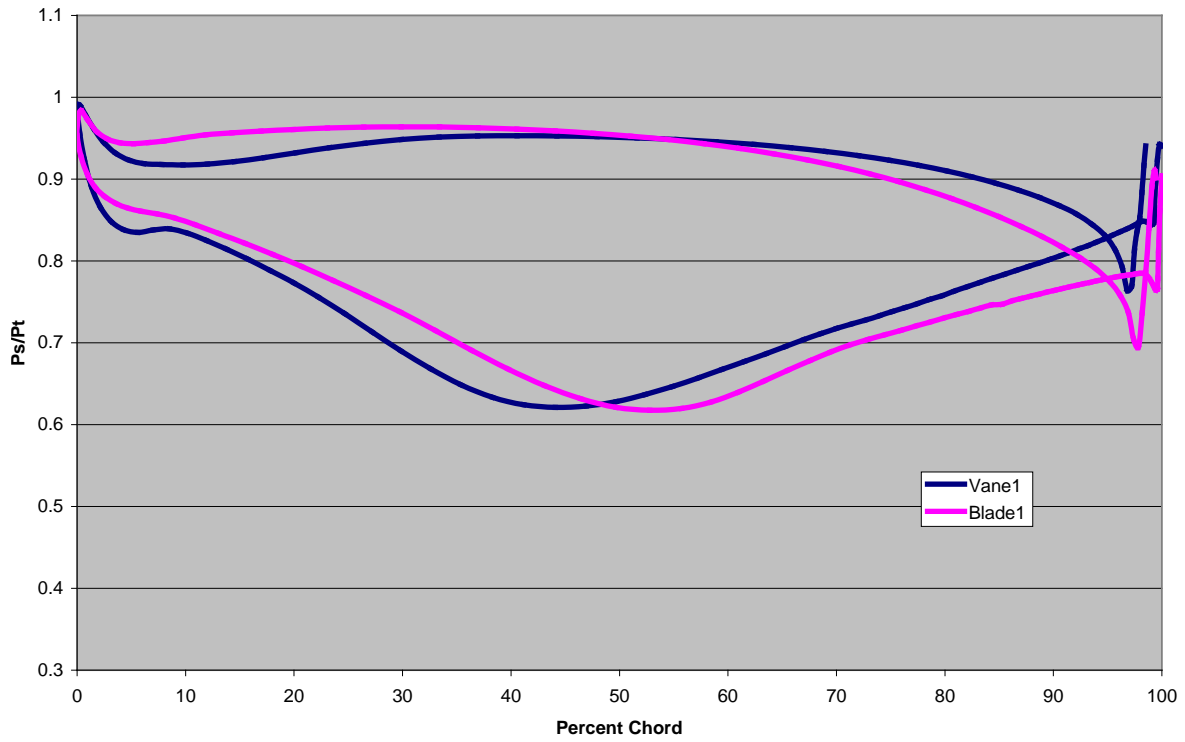
50% Span



10% Span

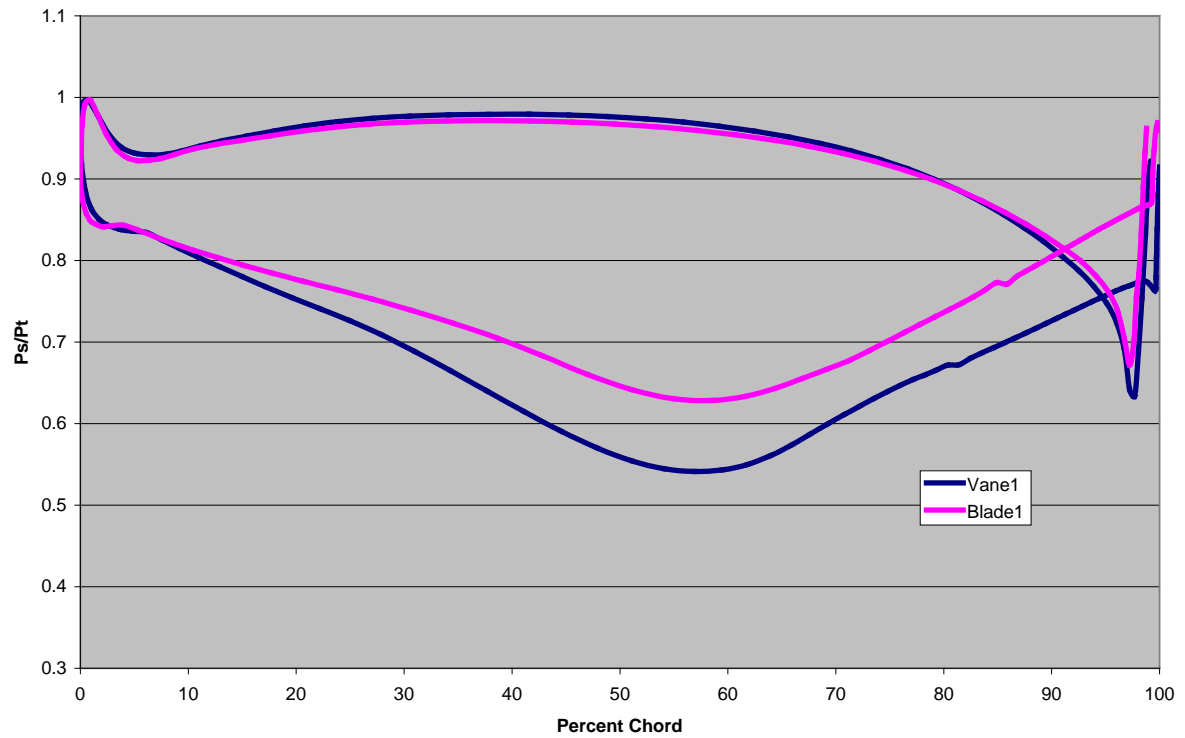


### 90% Span

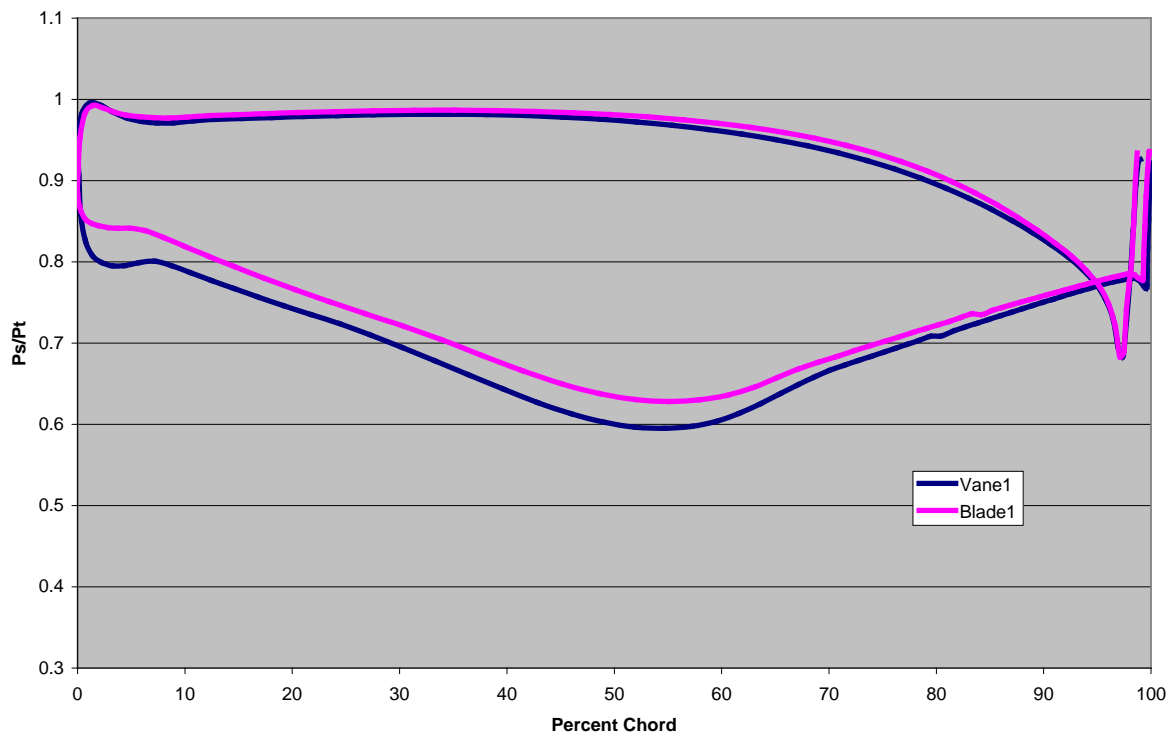


## D.2 Stage 2

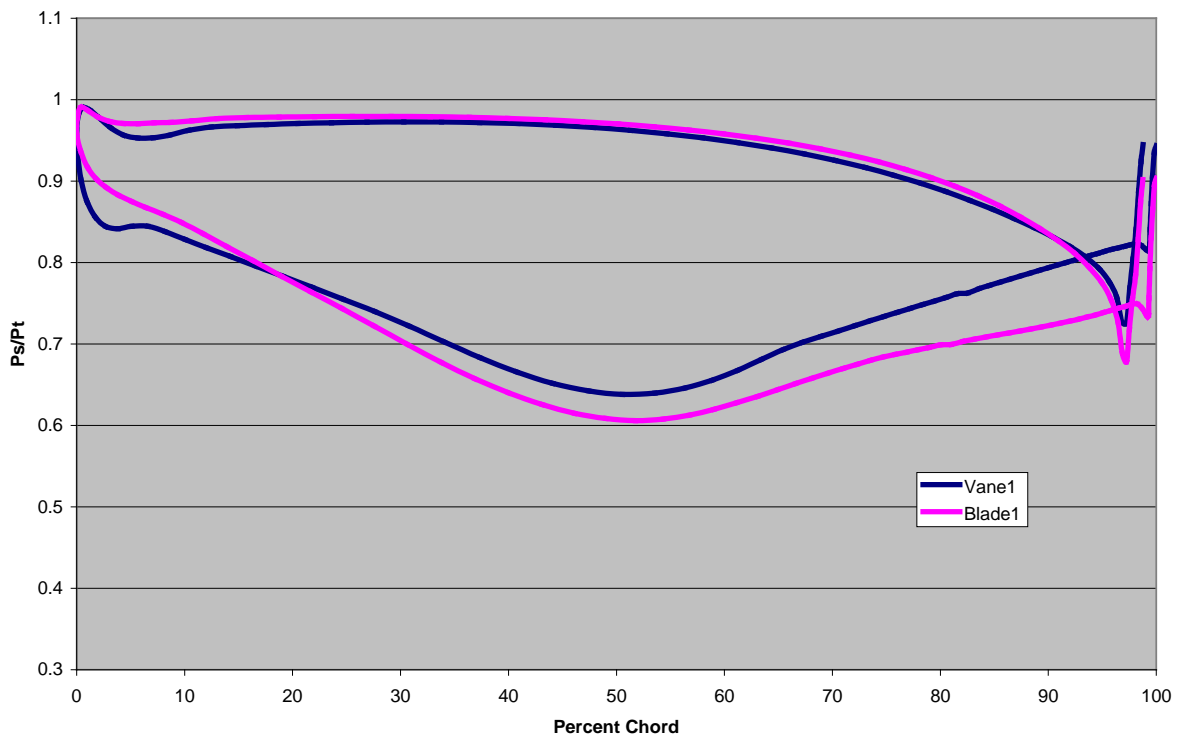
### 10% Span



### 50% Span

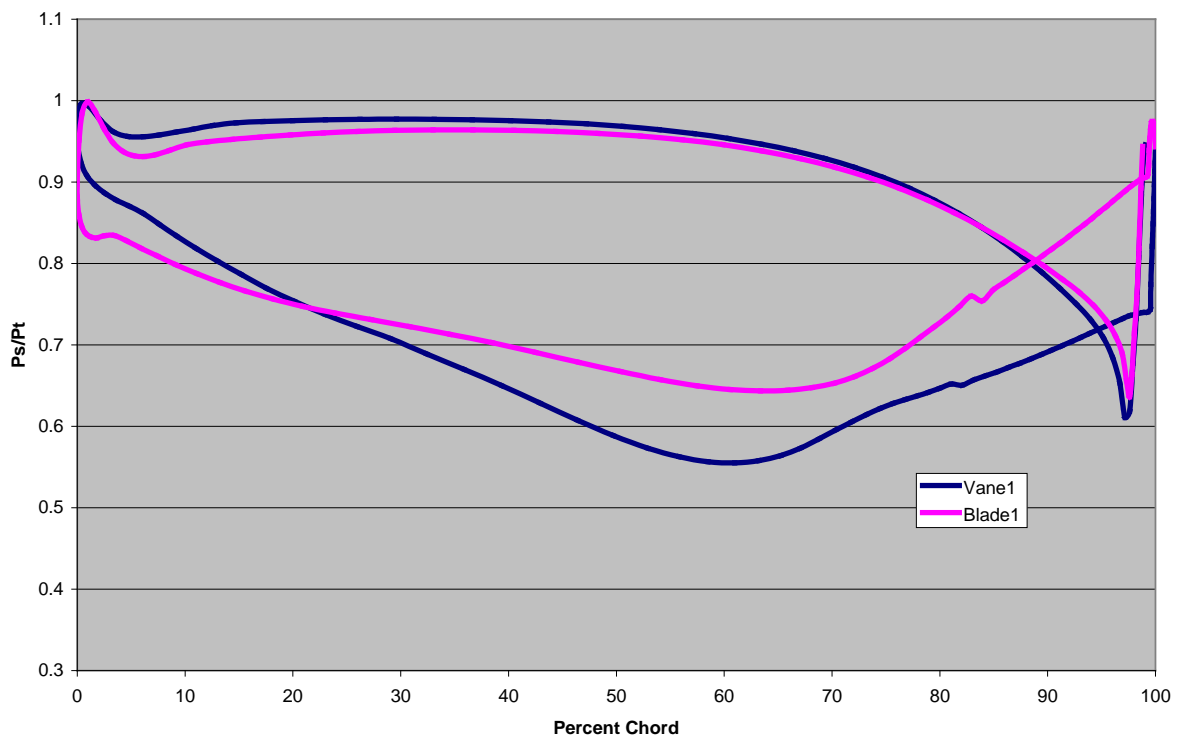


### 90% Span

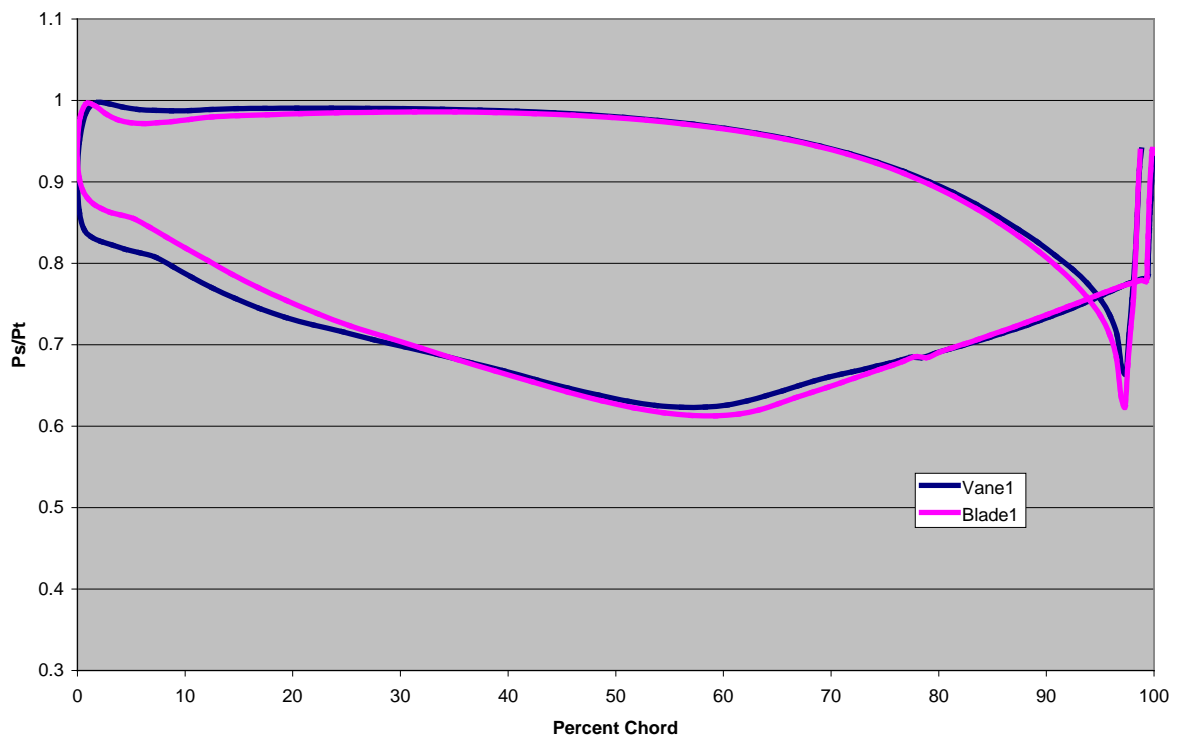


### D.3 Stage 3

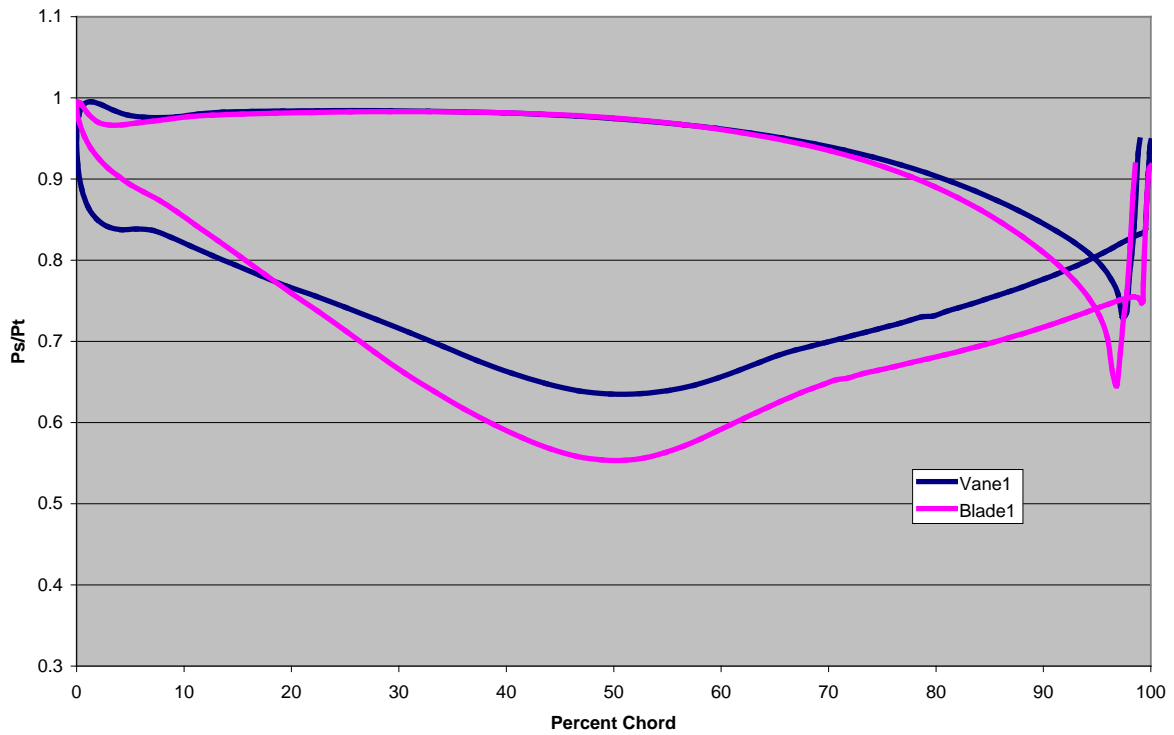
10% Span



50% Span

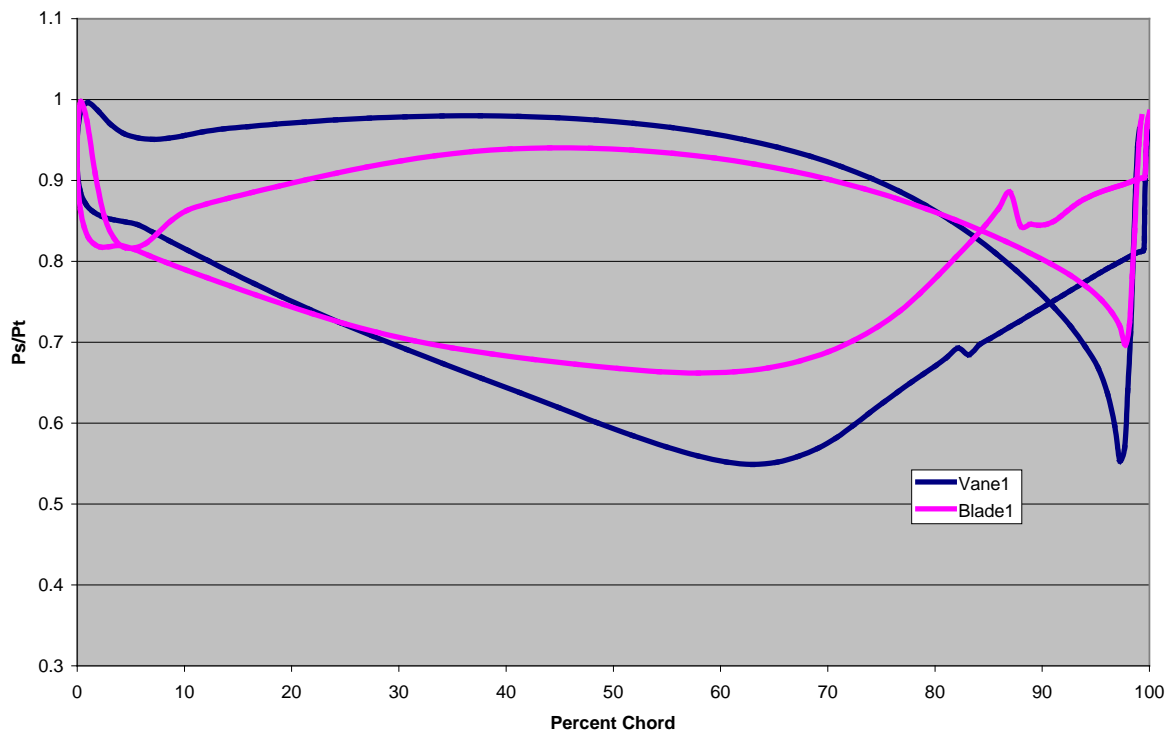


### 90% Span

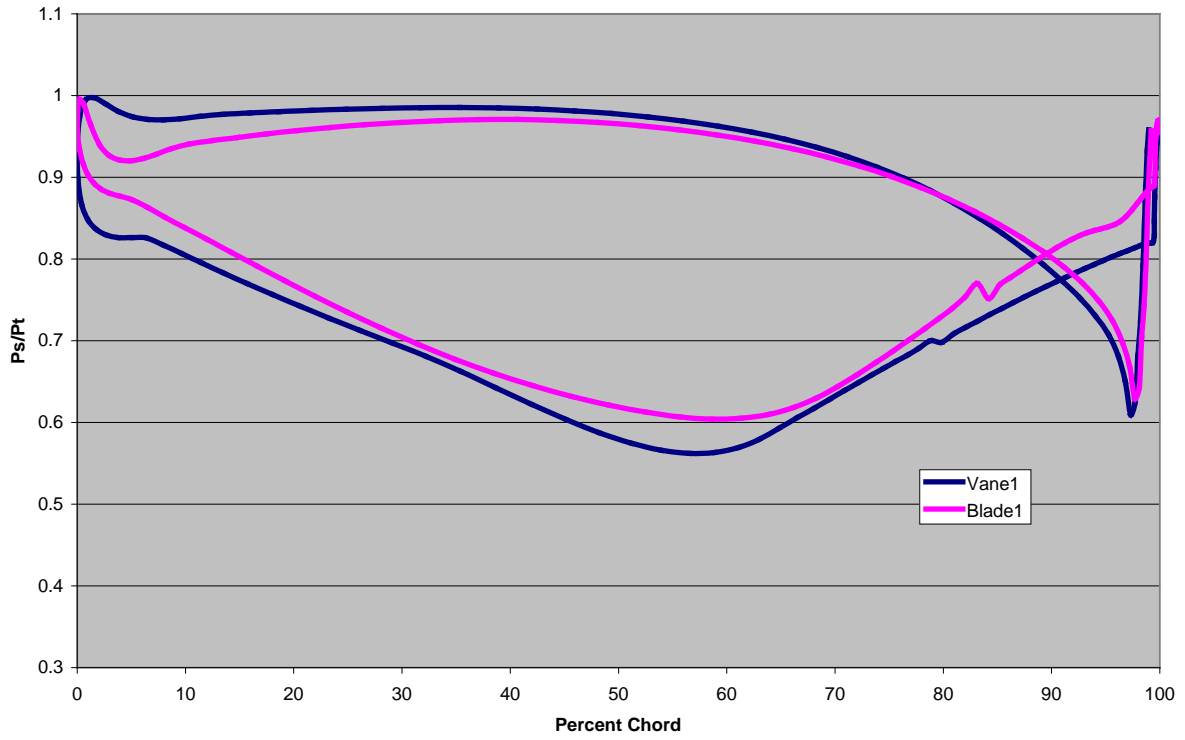


## D.4 Stage 4

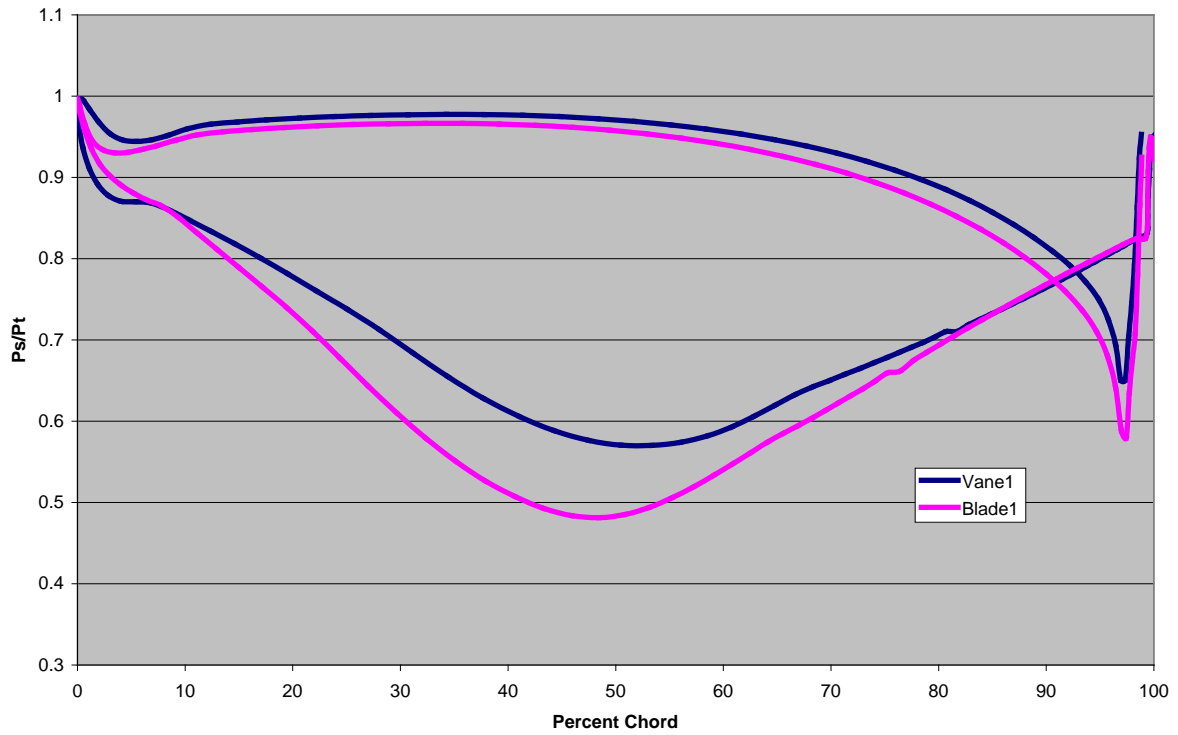
### 10% Span



### 50% Span



### 90% Span



**Meanline Analysis of Design Point  
75% Speed (11174 rpm)**

Flow Parm. (Inlet) : 16.240  
 Mass Flow : 12.040  
 Efficiency : 92.8662%  
 Flow Parm. (Exit) : 76.472  
 Power(hp) : 2684.958  
 Pressure Ratio (Total/Total) : 5.769  
 Pressure Ratio (Total/Static) : 6.330  
 Inlet Temp. (degrees R / F) : 1749.080 / 1289.410  
 TRIT (degrees R / F) : 1749.080 / 1289.410  
 Exit TT (degrees R / F) : 1165.389 / 705.719  
 Enthalpy Drop (BTU/lbm) : 39.608  
 Ratio Specific Heats (Gamma) : 1.340  
 Gas Constant (ft-lbf/degR/lbm): 53.374  
 Avg. Work Coefficient : 1.459  
 Core Flow (lbm/s) : 12.040  
 Nozzle Cooling : 0.000%  
 Rotor Cooling : 0.000%

**Rotor Summary:**

Title	Reaction	WorkCoef	Cm/U	AN^2	RimSpeed
ROTOR: STAGE 1	48.000%	1.470	0.726	11.390	689.720
ROTOR: STAGE 2	47.000%	1.490	0.563	18.720	671.266
ROTOR: STAGE 3	45.000%	1.496	0.551	27.121	617.638
ROTOR: STAGE 4	40.000%	1.384	0.702	32.240	567.395

Corrected Speed (rpm) : 6085.02  
 (based on TRIT & 1st rpm found)

=====

	Vane	Blade
Turning	58.1564 85.9121 92.4592 88.4801	78.4812 90.6473 93.8363 81.7638
RVR	2.0792 2.0969 2.4743 2.4598	1.9532 2.2366 2.4077 2.0300
Convergence Ratio	1.8046 1.7790 2.0383 1.9660	1.6902 1.8930 1.9791 1.6718
Reynolds #, SS/1000.	179.2235 145.1666 118.1032 80.7626	152.0635 126.1129 93.2357 59.2618
LE Mach # (relative)	0.2733 0.2872 0.2553 0.2783	0.2985 0.2673 0.2647 0.3262
TE Mach # (relative)	0.5824 0.6181 0.6509 0.7092	0.5983 0.6148 0.6579 0.6836
LE Swirl (relative)	0.0000 -22.1197 -25.4011 -24.2202	17.9747 24.7990 27.7528 23.9420
TE Swirl (relative)	58.1564 63.7159	-60.3947 -65.7272

	66.9995	-65.9808
	64.2247	-57.7576
Total Loss %	1.4064	1.9212
	2.0358	2.1632
	2.1774	2.3416
	2.1681	2.2357
Zweifel	1.0569	1.0284
	1.0437	1.0370
	1.0391	1.0437
	1.0225	1.0499
Throat Area	37.6309	-42.5160
	49.0312	-59.0217
	69.3542	-85.1203
	102.2492	-131.8714
Number of Airfoils	52	65
	62	62
	59	65
	67	76
Exit Mach/Swirl (Absolute)	0.3718	-9.3783



## Appendix E.—Meanline Results for Four Stage: High Loading 1

Rotor Summary at Design Speed of 54 percent:

Title	Reaction	WorkCoef	Cm/U	AN <sup>2</sup>	RimSpeed
ROTOR: STAGE 1	48.000%	2.826	1.072	5.902	496.707
ROTOR: STAGE 2	45.000%	2.840	0.857	9.700	483.381
ROTOR: STAGE 3	45.000%	2.863	0.880	14.081	444.190
ROTOR: STAGE 4	39.992%	2.774	1.224	16.650	410.626
Overall Efficiency = 87.5%					

Rotor Summary @ Design Speed 100%:

Title	Reaction	WorkCoef	Cm/U	AN <sup>2</sup>	RimSpeed
ROTOR: STAGE 1	48.000%	0.834	0.539	20.240	919.819
ROTOR: STAGE 2	45.000%	0.848	0.416	33.265	895.143
ROTOR: STAGE 3	45.000%	0.851	0.402	48.287	822.569
ROTOR: STAGE 4	40.000%	0.778	0.512	57.098	760.413
Overall Efficiency = 94%					

### Airfoil Summary

	54% Speed		100% Speed	
	<u>Vane</u>	<u>Blade</u>	<u>Vane</u>	<u>Blade</u>
<b>Turning</b>	59.3261	101.7896	57.7106	51.4604
	110.8252	114.7838	58.0856	58.7734
	115.4375	116.0826	53.8484	56.6190
	110.8802	100.6000	52.2701	50.9701
<b>Vexit/Vinlet</b>	2.2231	1.7296	2.0611	2.0179
	1.6517	1.6362	2.2851	2.4019
	1.8324	1.7477	2.6784	2.6977
	1.7983	1.5571	2.6875	2.2304
<b>Reynolds #, SS/1000.</b>	192.2316	162.2900	176.8202	166.8413
	147.8500	121.7398	160.8162	137.0289
	112.3183	87.5698	136.1440	106.9008
	73.1437	53.5719	94.8810	66.7247
<b>LE Mach # (relative)</b>	0.2730	0.3809	0.2730	0.2876
	0.4105	0.4037	0.2644	0.2426
	0.3843	0.4147	0.2332	0.2325
	0.4390	0.5105	0.2532	0.2931
	54% Speed		100% Speed	

	<u>Vane</u>	<u>Blade</u>	<u>Vane</u>	<u>Blade</u>
<b>TE Mach # (relative)</b>	0.6244	0.6770	0.5764	0.5956
	0.6956	0.6769	0.6213	0.5993
	0.7258	0.7479	0.6439	0.6480
	0.8204	0.8226	0.7056	0.6759
<b>LE Swirl (relative)</b>	0.0000	39.4746	0.0000	-9.0460
	-46.1872	48.9328	5.9468	-6.6781
	-48.6347	50.4989	13.3548	-9.6122
	-47.9455	44.9543	12.4835	-7.2519
<b>TE Swirl (relative)</b>	59.3261	-62.1228	57.7106	-60.5652
	64.5339	-65.7028	64.0554	-65.4882
	66.7344	-65.4703	67.2378	-66.2728
	62.8947	-55.5671	64.7740	-58.2441
<b>Total Loss %</b>	1.6196	3.4411	1.3734	1.4617
	3.8016	3.8811	1.5134	1.5536
	3.8187	4.4511	1.6540	1.6506
	4.1192	5.0666	1.6129	1.5247
<b>Zweifel</b>	1.0550	1.0259	1.0649	1.0237
	1.0657	1.0499	1.0140	1.0355
	1.0641	1.0576	1.0127	1.0284
	1.0377	1.0356	1.0124	1.0190
<b>Number of Airfoils</b>	51	76	52	50
	74	77	50	49
	72	82	45	49
	88	105	49	56
<b>Exit Mach/Swirl (Absolute)</b>	0.5549	-32.7647	0.3768	18.4055

## Appendix F.—Disk Sizing

A 2-D disk sizing tool was used to approximate disk mass and structural feasibility. Below is a screen shot of disks that were designed based on achieving 25 percent over speed capability with typical disk alloys. The resulting weight and mass moment of inertia of each disk plus the blades is shown.

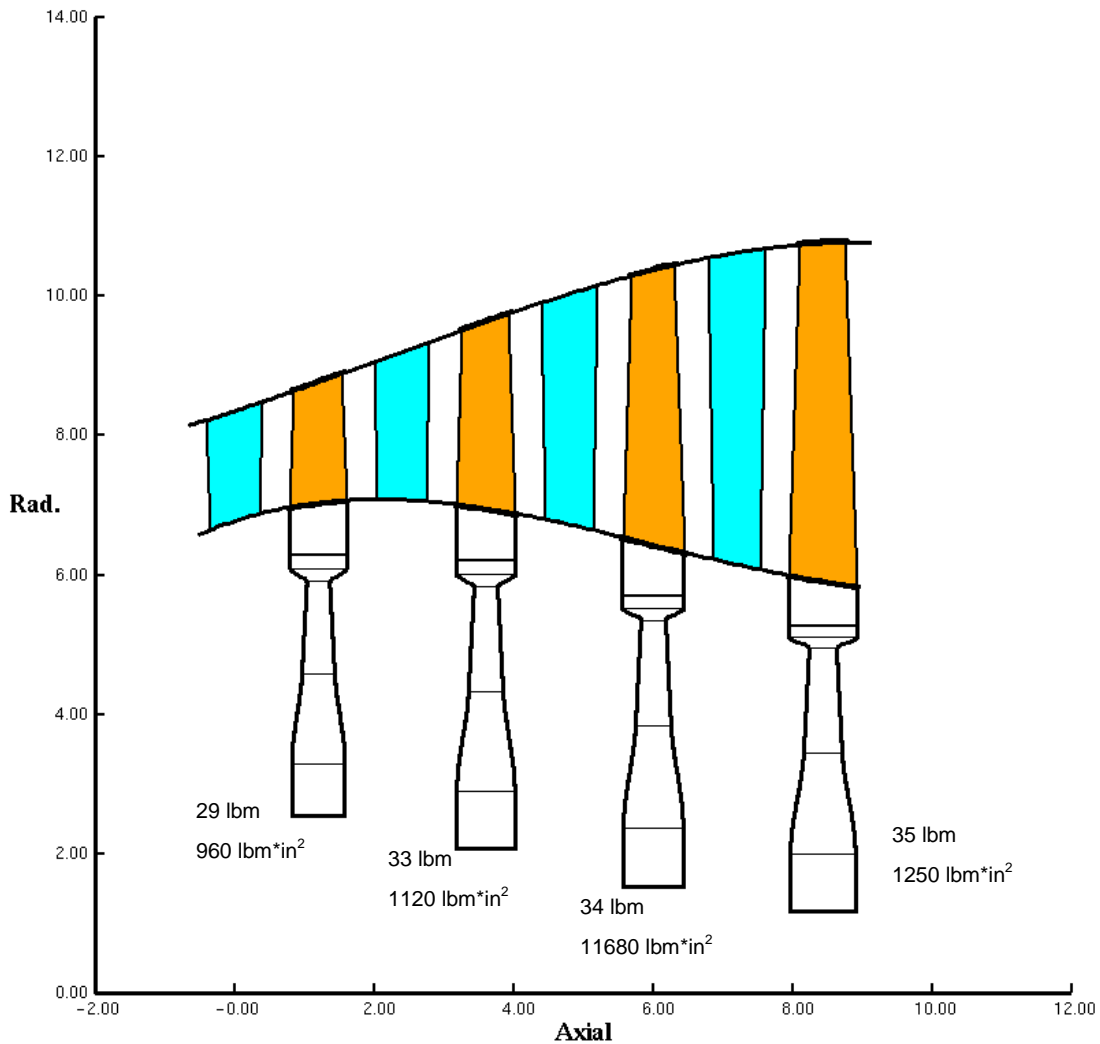


Figure F.1.—Approximate Disk Size



## Appendix G.—Efficiency and Reaction Definitions

The scope of this work is concentrated on understanding speed variations and the impact to turbine efficiency. In order to simplify this understanding, the analysis presented in this report does not consider cooling flows. This simplifies the efficiency definition. The efficiency numbers presented in this report are calculated assuming ideal gas as follows.

$$\eta \equiv \frac{\text{ActualPower}}{\text{IdealPower}} = \frac{\Delta T_t}{T_{in} * \left( 1 - Pr^{\frac{1-\gamma}{\gamma}} \right)}$$

where:

Pr = Total Pressure at inlet / Total Pressure at outlet

$\Delta T_t$  = Total Temperature at inlet – Total Temperature at outlet

$T_{in}$  = Total temperature at inlet

$\gamma$  is the ratio of specific heats taken at the average of the inlet and exit Total Temperatures.

In this work, stage reaction refers to pressure reaction defined as the static pressure drop across the rotor normalized by the static pressure drop across the whole stage.

$$\text{Reaction} \equiv \left( \frac{P_{S_{RotorLE}} - P_{S_{RotorTE}}}{P_{S_{NozzleLE}} - P_{S_{RotorTE}}} \right)$$



## **Appendix H.—NPSS Output for Critical Mission Point**

TABLE H.1.—65 PERCENT DESIGN SPEED TAKE OFF

\*\*\*\*\*  
Date:05/24/11 Time:13:01:28 Model: AHS 2010 Govt turboshaft engine - 65% speed turbine - Takeoff converge = 1 CASE: 100  
Version: NPSS\_2.3 Gas Package: Janaf iter/pass/Jacob/Broy7 = 7/ 18/ 1/ 5 Run by: tmi862  
\*\*\*\*\*

MN	alt	dT5	W	Power	BSFC	Wfuel	VTAS	OPR	T4	T41	T47	Dyn P.
0.000	0.0	45.00	28.17	464.6	0.3305	2668.99	0.00	42.231	3769.2	3471.0	2884.2	0.0
SUMMARY OUTPUT DATA												
FLOW STATION DATA												
FL1	InletStart.F1_O	W	Et	Tt	fc	FAR	Wc	Ps	Ts	Aphy	MN	grams
FL2	Inlet.F1_O	28.17	14.696	563.67	4.62	0.0000	29.36	14.696	563.67	---	0.000	1.3995
FL3	Duct1.F1_O	28.17	14.696	563.67	4.62	0.0000	29.36	13.162	546.20	136.07	0.400	1.3995
FL4	LPC.F1_O	28.17	213.118	1302.21	187.46	0.0000	29.36	14.292	559.20	253.60	0.200	1.3996
FL5	ICduct.F1_O	28.17	212.682	1302.21	187.46	0.0000	3.08	191.446	1465.56	14.45	0.399	1.3617
FL6	HPC_axi.F1_O	28.17	239.929	1349.79	199.78	0.0000	2.78	125.836	1265.56	14.48	0.399	1.3617
FL7	HPC_axi.F1_O	28.17	239.929	1349.79	199.78	0.0000	2.59	125.836	1265.56	16.76	0.300	1.3589
FL8	HPC_centri.F1_O	26.23	620.620	1786.31	315.94	0.0000	1.15	584.548	1759.54	12.18	0.300	1.3589
FL9	Duct6.F1_O	19.87	620.620	1786.31	315.94	0.0000	0.87	595.290	1767.95	6.98	0.250	1.3367
FL10	Burner.F1_O	20.61	608.208	3769.16	260.95	0.0373	1.34	52.163	3694.08	7.70	0.200	1.3372
FL11	Duct43.F1_O	26.97	291.135	2956.47	148.09	0.0283	3.25	275.130	2819.73	20.07	0.400	1.2786
FL12	LPT.F1_O	28.91	84.443	2274.77	-26.60	0.0263	10.54	82.257	2260.99	15.65	0.300	1.2786
FL13	ITduct.F1_O	28.91	84.443	2274.77	-26.60	0.0263	10.54	76.075	2260.99	15.65	0.202	1.2998
FL14	PowerT.F1_O	28.91	15.430	1605.82	-219.51	0.0263	48.45	14.537	1582.36	293.77	0.301	1.3269
FL15	Duct12.F1_O	28.91	15.430	1605.82	-219.51	0.0263	48.45	14.537	1582.36	293.77	0.301	1.3269
FL16	Nozzle.F1_O	28.91	15.430	1605.88	-219.51	0.0263	48.45	14.636	1586.69	323.12	0.272	1.3269
TURBOMACHINERY PERFORMANCE DATA												
LPC	WC	PR	NC	TR	efPoly	FWR	SMN	SMW				
LPC	29.36	14.502	12000.000	2.3102	0.8889	-7286.8	19.91	19.50				
HPC_axi	3.08	1.128	9681.203	1.0365	0.8892	-490.9	19.92	12.44				
HPC_cen	1.59	2.587	9509.053	1.3234	0.8748	-4311.1	20.24	18.65				
HPT	3.25	0.889	249.863	1.1353	0.8159	4802.0						
LPT	3.25	3.448	8504.0	1.2582	0.8239	7286.7						
PowerT	10.54	5.472	314.498	1.4168	0.8587	7890.5						
TURBOMACHINERY MAP DATA												
LPC	WCMap	PRmap	NCMap	R/Param	S_McDes	S_PRDes	S_effDes	S_NcDes				
LPC	30.00	9.006	100.000	1.9970	0.978660	1.6865	0.9916	0.8333				
HPC_axi	29.90	1.200	0.997	1.9839	0.103125	0.6398	1.0418	0.0001				
HPC_cen	29.89	3.182	0.997	1.9961	0.086701	0.7273	1.0086	0.0001				
HPT	30.15	5.972	100.188	5.9722	0.044531	4.5654	0.9152	0.0176				
LPT	149.72	6.032	100.511	6.0322	0.021712	2.0559	0.9163	0.0192				
PowerT	10.03	5.473	7162.562	5.4727	1.050286	1.0001	1.0001	1.0000				
===INLETS===												
Inlet	eRam	Afs	Fram	BLEEDS - output	Wb/Win	hscale	Pscale	Tt	hL	Pt		
Inlet	1.0000	----	0.0	C_LPTCharg Bl>	0.0182	1.0000	1.0000	1349.79	199.78	239.929		
===DUCTS===												
Duct1	dProrm	MN	Aphy	C_LPTUncharg Bl>	0.0506	1.0000	1.0000	1349.79	199.78	239.929		
ICduct	0.0020	0.3994	14.45	C_HPTUncharg Bl>	0.0823	1.0000	1.0000	1786.31	315.94	620.620		
Duct6	0.0000	0.2503	6.24									
Duct43	0.0000	0.3004	20.07									
ITduct	0.0000	0.2016	93.61									
Duct12	0.0000	0.3009	293.77									
===SHAFTS===												
HP_Shaft	Nmech	trq_in	Fwr_in									
IP_Shaft	15340.0	1644.1	4802.0									
LP_Shaft	12509.7	3059.3	7286.7									
LP_Shaft	15000.0	2762.8	7890.5									
===BURNERS===												
Burner	TtOut	eff	dProrm	Wfuel	FAR	ETINOx	ppm					
Burner	3769.16	1.0000	0.0200	0.74138	0.03731							
===NOZZLES===												
Nozzle	PR	Cfg	CaTh	Cv	Ath	MNth	Vact	Fg				
Nozzle	1.050	1.0000	1.0000	1.0000	321.89	0.272	517.0	464.6				

TABLE H.2.—65 PERCENT DESIGN SPEED CLIMB

\*\*\*\*\*  
Date:05/24/11 Time:13:01:28 Model: AHS 2010 Govt turboshaft engine - 65% speed turbine - Climb converge = 1 CASE: 100  
Version: NPSS\_2.3 Gas Package: Janaf iter/pass/Jacb/Broy= 20/ 31/ 1/18 Run By: tml1862 PC: 50

SUMMARY OUTPUT DATA  
MN 0.000 alt 0.0 dts 0.00 W 19.98 W 19.98 Wfuel 1259.82 VTAS 0.00 OPR 25.976 T4 2903.4 T41 2674.3 T47 2203.1 Dyn P. 0.0

FLOW STATION DATA  
FL1 InletStart.F1\_O W 14.696 Et 518.67 Tt 6.18 hC 0.0000 FAR 0.0000 Wc 19.98 Ps 14.696 gramt 1.4002  
FL2 Inlet.F1\_O W 14.696 Et 518.67 Tt 6.18 hC 0.0000 FAR 0.0000 Wc 19.98 Ps 14.033 gramt 1.4002  
FL22 Duc1.F1\_O W 14.696 Et 518.67 Tt 6.18 hC 0.0000 FAR 0.0000 Wc 19.98 Ps 14.512 gramt 1.4002  
FL23 Lpc.F1\_O W 139.757 Et 1062.08 Tt 126.40 hC 0.0000 FAR 0.0000 Wc 3.01 Ps 146.302 gramt 1.3769  
FL24 ICduct.F1\_O W 139.478 Et 1062.08 Tt 126.40 hC 0.0000 FAR 0.0000 Wc 3.01 Ps 126.049 gramt 1.3787  
FL25 HPC\_axi.F1\_O W 157.365 Et 1101.89 Tt 136.40 hC 0.0000 FAR 0.0000 Wc 2.72 Ps 148.577 gramt 1.3743  
FL26 Bid25.F1\_O W 18.61 Et 1444.24 Tt 224.44 hC 0.0000 FAR 0.0000 Wc 1.20 Ps 142.244 gramt 1.3762  
FL27 HPC\_centri.F1\_O W 14.09 Et 1444.24 Tt 224.44 hC 0.0000 FAR 0.0000 Wc 0.91 Ps 357.780 gramt 1.3548  
FL28 Bid3.F1\_O W 14.44 Et 1444.24 Tt 224.44 hC 0.0000 FAR 0.0000 Wc 0.91 Ps 364.944 gramt 1.3544  
FL3 Duc6.F1\_O W 178.118 Et 2903.39 Tt 191.13 hC 0.0248 FAR 0.0188 Wc 3.26 Ps 370.907 gramt 1.3541  
FL4 Burner.F1\_O W 178.418 Et 2256.84 Tt 102.11 hC 0.0188 FAR 0.0188 Wc 3.26 Ps 166.479 gramt 1.2838  
FL42 Duc43.F1\_O W 18.96 Et 1727.95 Tt 25.88 hC 0.0175 FAR 0.0175 Wc 10.01 Ps 53.204 gramt 1.3271  
FL44 Lpt.F1\_O W 20.33 Et 1391.47 Tt 117.88 hC 0.0175 FAR 0.0175 Wc 31.71 Ps 15.063 gramt 1.3284  
FL45 ITduct.F1\_O W 20.33 Et 1391.47 Tt 117.88 hC 0.0175 FAR 0.0175 Wc 31.71 Ps 15.063 gramt 1.3443  
FL6 PowerT.F1\_O W 20.33 Et 1391.47 Tt 117.88 hC 0.0175 FAR 0.0175 Wc 31.71 Ps 15.063 gramt 1.3443  
FL7 Duc12.F1\_O W 20.33 Et 1391.47 Tt 117.88 hC 0.0175 FAR 0.0175 Wc 31.71 Ps 15.063 gramt 1.3443  
FL9 Nozzle.F1\_O W 20.33 Et 1391.47 Tt 117.88 hC 0.0175 FAR 0.0175 Wc 31.71 Ps 14.696 gramt 1.3443

TURBOMACHINERY PERFORMANCE DATA  
LPC 19.98 PR 0.8460 eff 10818.559 NC 2.0477 TR 0.8853 eFPoly -3747.7 FWR 17.84 SMW 19.09  
HPC\_axi 3.01 1.128 0.8936 9456.518 1.0375 0.8953 -282.6 19.37 11.28  
HPC\_cen> 2.53 2.426 0.8588 9284.124 1.3107 0.8741 -2317.5 26.03 25.07  
HPT 1.34 2.097 0.8502 251.138 1.1488 0.8303 2599.9  
LPT 3.26 3.275 0.8520 227.727 1.2662 0.8307 3748.0  
PowerT 10.01 3.531 0.7181 360.849 1.2420 0.6839 2646.2

TURBOMACHINERY MAP DATA  
LPC WcMap PRmap effMap 90.155 R/Parm 0.978860 s\_Ncdes s\_effdes s\_Ncdes  
20.41 6.046 0.8532 1.6865 1.6865 0.9916 0.8333  
HPC\_axi 29.21 1.200 0.8577 0.974 1.8760 0.103125 0.6398 1.0418 0.0001  
HPC\_cen> 29.21 2.961 0.8514 0.973 2.0487 0.086701 0.7273 1.0086 0.0001  
HPT 30.14 6.007 0.9290 100.699 6.0075 0.044531 4.5654 0.9152 0.0176  
LPT 149.99 5.677 0.9298 99.487 5.6772 0.021712 2.0559 0.9163 0.0176  
PowerT 9.531 3.531 0.7181 8218.192 3.5307 1.050286 1.0001 1.0001 0.0000

===INLETS=== eRam 1.0000 Afs -----  
Inlet 1.0000  
===DUCTS=== dProrm MN  
Duct1 0.0000 0.2576  
ICduct 0.0020 0.3859  
Duct6 0.0000 0.2586  
Duct43 0.0000 0.2980  
ITduct 0.0000 0.1891  
Duct12 0.0000 0.1897  
===SHAFTS=== Nmsch trg\_in  
HP\_Shaft 13532.1 1009.9  
IP\_Shaft 10818.6 1819.0  
LP\_Shaft 15000.0 926.5

===BURNERS=== TtOut eff dProrm Wfuel FAR ETINOX ppm  
Burner 2903.39 1.0000 0.0200 0.34995 0.02483

===NOZZLES=== PR Cfg Cdth Cv Ath MNth Vact Fg  
Nozzle 1.050 1.0000 1.0000 1.0000 321.89 0.270 481.3 304.1

W 1101.89 Tt 136.40 hC 136.40 Pt 157.365  
1.0101 136.40 157.365  
1.444.24 224.44 381.746  
1.444.24 224.44 381.746

TABLE H.3—65 PERCENT DESIGN SPEED CRUISE

\*\*\*\*\*  
Date:05/24/11 Time:13:01:29 Model: AHS 2010 Govt turbohaft engine - 65% speed turbine - Cruise converge = 1 CASE: 101  
Version: NPSS\_2.3 Gas Package: Janaf iter/pass/Jacob/Broy= 28/ 50/ 2/25 Run by: tml1862 PC: 50

SUMMARY OUTPUT DATA

MN	alt	dts	W	BSFC	Wfuel	VTAS	OPR	T4	T41	T47	Dyn_P
0.510	28000.0	0.00	11.80	0.3141	735.13	511.85	39.130	2847.0	2619.0	2155.0	0.0

FLOW STATION DATA

	W	Et	tt	FAR	WC	Ps	Ts	Aphy	MN	gramt	grams
FL1 InletStart.FI_O	11.80	5.705	440.86	0.0000	28.03	4.776	418.82	107.88	0.510	1.4010	1.4011
FL2 Inlet.FI_O	11.80	5.705	440.86	0.0000	28.03	5.169	428.40	136.07	0.378	1.4010	1.4010
FL22 Duct1.FI_O	11.80	5.705	440.86	0.0000	28.03	5.562	437.48	253.60	0.190	1.4010	1.4010
FL23 LPC.FI_O	11.80	80.640	1019.99	0.0000	3.02	72.819	991.72	14.45	0.387	1.3795	1.3812
FL24 ICduct.FI_O	11.80	80.479	1019.99	0.0000	3.02	72.819	991.72	14.48	0.387	1.3795	1.3812
FL25 HPC_axi.FI_O	11.80	90.847	1058.62	0.0000	2.73	85.741	1041.97	16.76	0.291	1.3771	1.3789
FL26 Bid25.FI_O	10.99	90.847	1058.62	0.0000	2.54	82.059	1029.49	12.18	0.387	1.3771	1.3789
FL27 HPC_centri.FI_O	10.99	223.217	1394.60	0.0000	1.19	209.421	1378.44	6.98	0.308	1.3563	1.3576
FL28 Bid3.FI_O	8.33	223.217	1394.60	0.0000	0.90	216.973	1384.23	7.70	0.205	1.3563	1.3572
FL3 Duct6.FI_O	8.33	218.753	2847.03	0.0000	1.78.94	188.185	2784.66	6.50	0.397	1.2837	1.2855
FL4 Burner.FI_O	8.33	104.659	2208.49	0.0186	3.24	98.870	2179.03	20.07	0.286	1.3070	1.3080
FL42 HPT.FI_O	11.20	104.659	2208.49	0.0186	3.24	94.637	2156.67	15.65	0.395	1.3070	1.3087
FL43 Duct43.FI_O	12.01	28.056	1648.48	0.0173	11.21	27.227	1636.16	93.61	0.213	1.3306	1.3312
FL44 LPT.FI_O	12.01	28.056	1648.48	0.0173	11.21	24.842	1599.24	50.08	0.431	1.3306	1.3320
FL45 ITduct.FI_O	12.01	5.015	1131.47	0.0173	51.97	4.677	1110.97	293.77	0.321	1.3606	1.3620
FL6 PowerT.FI_O	12.01	5.015	1131.47	0.0173	51.97	4.677	1110.97	293.77	0.321	1.3606	1.3620
FL7 Duct12.FI_O	12.01	5.015	1131.47	0.0173	51.97	4.677	1110.97	293.77	0.321	1.3606	1.3620
FL9 Nozzle.FI_O	12.01	5.015	1131.47	0.0173	51.97	4.776	1117.01	345.52	0.268	1.3606	1.3616

TURBOMACHINERY PERFORMANCE DATA

LPC	PR	NC	TR	efPolY	EMR	SMN	SMW
28.03	14.136	11830.394	2.3147	0.8929	-2350.7	17.22	17.26
HPC_axi	3.02	0.8930	1.0379	0.8947	-161.2	19.31	17.36
HPC_cen	2.457	9318.289	1.3174	0.8753	-1336.0	24.66	23.60
HPT	1.34	249.497	1.1488	0.8311	1497.1		
LPT	3.24	232.035	1.2862	0.8226	2350.7		
PowerT	11.21	198.934	1.4572	0.8513	2350.9		

TURBOMACHINERY MAP DATA

LPC	WcMap	PrMap	NcMap	effMap	R/Parm	S_McDes	s_effDes	s_NcDes
28.63	8.789	98.587	1.8497	0.978660	1.6865	0.9916	0.8333	
HPC_axi	29.31	1.201	0.8571	1.8849	0.103125	1.0418	0.0001	
HPC_cen	29.30	3.003	0.8525	2.0338	0.086701	1.0086	0.0001	
HPT	30.15	5.977	0.9290	5.9770	0.044531	0.7273	0.0176	
LPT	149.41	6.613	0.9240	101.369	4.5654	0.9152	0.0176	
PowerT	10.68	5.595	0.8783	4530.633	2.0559	0.9163	0.0000	

===INLETS===

Inlet	eRam	Afs	Fram	BLEEDS - output	Wb/Win	hscale	Pscale	Tt	h	Pt
1.0000	107.88	187.8	187.8	C_LPTCharg Bl>	0.0182	1.0000	1.0000	1058.62	125.54	90.847
===DUCTS===	dProrm	MN	Aphy	C_LPTUncharg Bl>	0.0506	1.0000	1.0000	1058.62	125.54	90.847
0.0000	0.3779	136.07	136.07	C_HPTUncharg Bl>	0.0823	1.0000	1.0000	1394.60	211.44	223.217
ICduct	0.0020	0.3871	14.45	C_HPTUncharg Bl>	0.1602	1.0000	1.0000	1394.60	211.44	223.217
Duct6	0.0000	0.2563	6.24							
Duct43	0.0000	0.2965	20.07							
ITduct	0.0000	0.2127	93.61							
Duct12	0.0000	0.3214	293.77							

===SHAFTS===

HP_Shaft	Nmech	trg_in	Pwr_in
13312.5	590.7	1497.1	1497.1
LP_Shaft	10904.5	2350.7	2350.7
LP_Shaft	8077.0	1528.2	2350.9

===BURNERS===

Burner	TtOut	eff	dProrm	Wfuel	FAR	ETINOX	ppm
2847.03	1.0000	0.20420	0.02453				

===NOZZLES===

Nozzle	PR	Cfg	CaTh	Cv	Ath	MNth	Vact	Fg
1.050	1.0000	1.0000	1.0000	321.89	0.268	433.7	161.8	



TABLE H.5.—75 PERCENT DESIGN SPEED CLIMB

\*\*\*\*\*  
Date:05/24/11 Time:12:57:33 Model: AHS 2010 Govt turbohaft engine - 75% speed turbine - Climb  
Version: NPSS\_2.3 Gas Package: Janaf iter/pass/Jacob/Broy= 18/ 29/ 1716 Run by: tm1862 = 1 PC: 100  
\*\*\*\*\*

\*\*\*\*\* SUMMARY OUTPUT DATA \*\*\*\*\*  
MN 0.000 alt 0.0 dts 0.00 W 18.92 Wfuel 1150.64 VTAS 0.00 OPR 25.419 T4 2849.1 T41 2627.8 T47 2165.6 Dyn P. 0.0

\*\*\*\*\* FLOW STATION DATA \*\*\*\*\*

Station	W	Et	tt	FR	Power	BSFC	Wfuel	VTAS	OPR	T4	T41	T47	Dyn P.
FL1 InletStart.F1_O	18.92	14.696	518.67	0.0000	-6.18	0.0000	18.92	14.696	518.67	0.000	1.4002	1.4002	1.4002
FL2 Inlet.F1_O	18.92	14.696	518.67	0.0000	-6.18	0.0000	18.92	14.696	518.67	0.000	1.4002	1.4002	1.4002
FL22 Duct1.F1_O	18.92	14.696	518.67	0.0000	-6.18	0.0000	18.92	14.696	518.67	0.000	1.4002	1.4002	1.4002
FL23 LPC.F1_O	18.92	138.843	1081.32	0.0000	126.21	0.0000	2.86	125.656	1032.67	13.85	1.3769	1.3769	1.3787
FL24 ICduct.F1_O	18.92	138.843	1081.32	0.0000	126.21	0.0000	2.87	125.404	1032.67	13.85	1.3769	1.3769	1.3787
FL25 HPC_axi.F1_O	18.92	156.159	1100.69	0.0000	136.09	0.0000	2.59	147.546	1083.79	16.07	1.3744	1.3744	1.3755
FL26 BID25.F1_O	17.63	156.159	1100.69	0.0000	136.09	0.0000	2.42	141.350	1071.15	11.69	0.383	0.383	0.3763
FL27 HPC_centri.F1_O	17.63	156.159	1100.69	0.0000	136.09	0.0000	2.42	141.350	1071.15	11.69	0.383	0.383	0.3763
FL28 BID3.F1_O	13.37	373.511	1437.05	0.0000	222.55	0.0000	1.15	346.894	1412.53	6.00	0.313	0.313	0.3552
FL3 Duct6.F1_O	13.37	373.511	1437.05	0.0000	222.55	0.0000	0.88	362.894	1412.53	6.00	0.260	0.260	0.3539
FL4 Burner.F1_O	13.69	366.080	2849.07	0.0000	190.55	0.0000	1.29	321.678	2786.12	7.41	0.386	0.386	0.3545
FL42 Duct43.F1_O	17.95	174.554	2217.33	0.0000	102.80	0.0181	3.12	164.832	2164.48	19.27	0.298	0.298	0.2859
FL44 LPT.F1_O	19.24	52.057	1689.35	0.0169	-25.16	0.0169	9.80	47.276	1679.04	90.09	0.192	0.192	0.3289
FL45 ITduct.F1_O	19.24	52.057	1689.35	0.0169	-25.16	0.0169	9.80	47.276	1679.04	90.09	0.192	0.192	0.3289
FL6 PowerT.F1_O	19.24	15.430	1331.35	0.0169	-122.38	0.0169	29.35	15.080	1323.39	278.42	0.185	0.185	0.3487
FL7 Duct12.F1_O	19.24	15.430	1331.35	0.0169	-122.38	0.0169	29.35	15.080	1323.39	278.42	0.185	0.185	0.3487
FL9 Nozzle.F1_O	19.24	15.430	1331.41	0.0169	-122.38	0.0169	29.36	14.696	1314.71	195.08	0.270	0.270	0.3493

\*\*\*\*\* TURBOMACHINERY PERFORMANCE DATA \*\*\*\*\*

Component	WC	PR	NC	TR	eFPoly	SMN	SMW
LPC	18.92	9.448	10789.426	2.0462	0.8837	16.97	18.19
HPC_axi	2.87	1.127	9399.682	1.0371	0.8963	264.5	19.28
HPC_cen	1.42	2.392	9230.074	1.3056	0.8733	-2156.3	11.03
HPT	2.29	0.8504	251.907	1.1497	0.8311	2420.8	
LPT	3.12	3.353	229.131	1.2734	0.8304	3543.8	
PowerT	9.80	3.374	364.949	1.2691	0.7748	2646.4	

\*\*\*\*\* TURBOMACHINERY MAP DATA \*\*\*\*\*

Component	WCMap	PRmap	NCMap	R/Param	S_NcDes	s_Prdes	s_effDes	s_NcDes
LPC	20.15	6.004	89.912	1.6735	0.938796	1.6881	0.9911	0.8333
HPC_axi	29.04	1.200	0.968	1.8534	0.098842	0.6347	1.0414	0.0001
HPC_cen	30.14	2.914	0.968	2.0536	0.083218	0.7273	1.0077	0.0001
HPT	30.14	5.997	100.892	5.9971	0.042746	4.5543	0.9152	0.0176
LPT	149.89	5.814	100.014	5.8144	0.020843	2.0460	0.9163	0.0192
PowerT	9.99	3.374	8311.469	3.3737	0.980704	1.0000	1.0000	1.0000

==== INLETS==== eRam 1.0000 Afs -----  
Inlet -----  
==== DUCTS==== dProrm MN  
Duct1 0.0000  
ICduct 0.0020  
Duct6 0.0000  
Duct43 0.0000  
ITduct 0.0000  
Duct12 0.0000  
==== SHAFTS==== Nmech  
HP\_Shaft 13445.9  
LP\_Shaft 10789.4  
LP\_Shaft 15000.0  
==== BURNERS==== TtOut 2849.06 efi 1.0000  
Burner  
==== NOZZLES==== PR 1.050 Cfg 1.0000 Cdth 1.0000 Wfuel 0.31962 FAR 0.02390 ETINOX ppm  
Nozzle  
==== INLETS==== eRam 1.0000 Afs -----  
Inlet -----  
==== DUCTS==== dProrm MN  
Duct1 0.0000  
ICduct 0.0020  
Duct6 0.0000  
Duct43 0.0000  
ITduct 0.0000  
Duct12 0.0000  
==== SHAFTS==== Nmech  
HP\_Shaft 13445.9  
LP\_Shaft 10789.4  
LP\_Shaft 15000.0  
==== BURNERS==== TtOut 2849.06 efi 1.0000  
Burner  
==== NOZZLES==== PR 1.050 Cfg 1.0000 Cdth 1.0000 Wfuel 0.31962 FAR 0.02390 ETINOX ppm  
Nozzle

==== INLETS==== eRam 1.0000 Afs -----  
Inlet -----  
==== DUCTS==== dProrm MN  
Duct1 0.0000  
ICduct 0.0020  
Duct6 0.0000  
Duct43 0.0000  
ITduct 0.0000  
Duct12 0.0000  
==== SHAFTS==== Nmech  
HP\_Shaft 13445.9  
LP\_Shaft 10789.4  
LP\_Shaft 15000.0  
==== BURNERS==== TtOut 2849.06 efi 1.0000  
Burner  
==== NOZZLES==== PR 1.050 Cfg 1.0000 Cdth 1.0000 Wfuel 0.31962 FAR 0.02390 ETINOX ppm  
Nozzle

==== INLETS==== eRam 1.0000 Afs -----  
Inlet -----  
==== DUCTS==== dProrm MN  
Duct1 0.0000  
ICduct 0.0020  
Duct6 0.0000  
Duct43 0.0000  
ITduct 0.0000  
Duct12 0.0000  
==== SHAFTS==== Nmech  
HP\_Shaft 13445.9  
LP\_Shaft 10789.4  
LP\_Shaft 15000.0  
==== BURNERS==== TtOut 2849.06 efi 1.0000  
Burner  
==== NOZZLES==== PR 1.050 Cfg 1.0000 Cdth 1.0000 Wfuel 0.31962 FAR 0.02390 ETINOX ppm  
Nozzle

==== INLETS==== eRam 1.0000 Afs -----  
Inlet -----  
==== DUCTS==== dProrm MN  
Duct1 0.0000  
ICduct 0.0020  
Duct6 0.0000  
Duct43 0.0000  
ITduct 0.0000  
Duct12 0.0000  
==== SHAFTS==== Nmech  
HP\_Shaft 13445.9  
LP\_Shaft 10789.4  
LP\_Shaft 15000.0  
==== BURNERS==== TtOut 2849.06 efi 1.0000  
Burner  
==== NOZZLES==== PR 1.050 Cfg 1.0000 Cdth 1.0000 Wfuel 0.31962 FAR 0.02390 ETINOX ppm  
Nozzle

==== INLETS==== eRam 1.0000 Afs -----  
Inlet -----  
==== DUCTS==== dProrm MN  
Duct1 0.0000  
ICduct 0.0020  
Duct6 0.0000  
Duct43 0.0000  
ITduct 0.0000  
Duct12 0.0000  
==== SHAFTS==== Nmech  
HP\_Shaft 13445.9  
LP\_Shaft 10789.4  
LP\_Shaft 15000.0  
==== BURNERS==== TtOut 2849.06 efi 1.0000  
Burner  
==== NOZZLES==== PR 1.050 Cfg 1.0000 Cdth 1.0000 Wfuel 0.31962 FAR 0.02390 ETINOX ppm  
Nozzle

==== INLETS==== eRam 1.0000 Afs -----  
Inlet -----  
==== DUCTS==== dProrm MN  
Duct1 0.0000  
ICduct 0.0020  
Duct6 0.0000  
Duct43 0.0000  
ITduct 0.0000  
Duct12 0.0000  
==== SHAFTS==== Nmech  
HP\_Shaft 13445.9  
LP\_Shaft 10789.4  
LP\_Shaft 15000.0  
==== BURNERS==== TtOut 2849.06 efi 1.0000  
Burner  
==== NOZZLES==== PR 1.050 Cfg 1.0000 Cdth 1.0000 Wfuel 0.31962 FAR 0.02390 ETINOX ppm  
Nozzle

==== INLETS==== eRam 1.0000 Afs -----  
Inlet -----  
==== DUCTS==== dProrm MN  
Duct1 0.0000  
ICduct 0.0020  
Duct6 0.0000  
Duct43 0.0000  
ITduct 0.0000  
Duct12 0.0000  
==== SHAFTS==== Nmech  
HP\_Shaft 13445.9  
LP\_Shaft 10789.4  
LP\_Shaft 15000.0  
==== BURNERS==== TtOut 2849.06 efi 1.0000  
Burner  
==== NOZZLES==== PR 1.050 Cfg 1.0000 Cdth 1.0000 Wfuel 0.31962 FAR 0.02390 ETINOX ppm  
Nozzle

==== INLETS==== eRam 1.0000 Afs -----  
Inlet -----  
==== DUCTS==== dProrm MN  
Duct1 0.0000  
ICduct 0.0020  
Duct6 0.0000  
Duct43 0.0000  
ITduct 0.0000  
Duct12 0.0000  
==== SHAFTS==== Nmech  
HP\_Shaft 13445.9  
LP\_Shaft 10789.4  
LP\_Shaft 15000.0  
==== BURNERS==== TtOut 2849.06 efi 1.0000  
Burner  
==== NOZZLES==== PR 1.050 Cfg 1.0000 Cdth 1.0000 Wfuel 0.31962 FAR 0.02390 ETINOX ppm  
Nozzle

==== INLETS==== eRam 1.0000 Afs -----  
Inlet -----  
==== DUCTS==== dProrm MN  
Duct1 0.0000  
ICduct 0.0020  
Duct6 0.0000  
Duct43 0.0000  
ITduct 0.0000  
Duct12 0.0000  
==== SHAFTS==== Nmech  
HP\_Shaft 13445.9  
LP\_Shaft 10789.4  
LP\_Shaft 15000.0  
==== BURNERS==== TtOut 2849.06 efi 1.0000  
Burner  
==== NOZZLES==== PR 1.050 Cfg 1.0000 Cdth 1.0000 Wfuel 0.31962 FAR 0.02390 ETINOX ppm  
Nozzle

==== INLETS==== eRam 1.0000 Afs -----  
Inlet -----  
==== DUCTS==== dProrm MN  
Duct1 0.0000  
ICduct 0.0020  
Duct6 0.0000  
Duct43 0.0000  
ITduct 0.0000  
Duct12 0.0000  
==== SHAFTS==== Nmech  
HP\_Shaft 13445.9  
LP\_Shaft 10789.4  
LP\_Shaft 15000.0  
==== BURNERS==== TtOut 2849.06 efi 1.0000  
Burner  
==== NOZZLES==== PR 1.050 Cfg 1.0000 Cdth 1.0000 Wfuel 0.31962 FAR 0.02390 ETINOX ppm  
Nozzle

==== INLETS==== eRam 1.0000 Afs -----  
Inlet -----  
==== DUCTS==== dProrm MN  
Duct1 0.0000  
ICduct 0.0020  
Duct6 0.0000  
Duct43 0.0000  
ITduct 0.0000  
Duct12 0.0000  
==== SHAFTS==== Nmech  
HP\_Shaft 13445.9  
LP\_Shaft 10789.4  
LP\_Shaft 15000.0  
==== BURNERS==== TtOut 2849.06 efi 1.0000  
Burner  
==== NOZZLES==== PR 1.050 Cfg 1.0000 Cdth 1.0000 Wfuel 0.31962 FAR 0.02390 ETINOX ppm  
Nozzle

==== INLETS==== eRam 1.0000 Afs -----  
Inlet -----  
==== DUCTS==== dProrm MN  
Duct1 0.0000  
ICduct 0.0020  
Duct6 0.0000  
Duct43 0.0000  
ITduct 0.0000  
Duct12 0.0000  
==== SHAFTS==== Nmech  
HP\_Shaft 13445.9  
LP\_Shaft 10789.4  
LP\_Shaft 15000.0  
==== BURNERS==== TtOut 2849.06 efi 1.0000  
Burner  
==== NOZZLES==== PR 1.050 Cfg 1.0000 Cdth 1.0000 Wfuel 0.31962 FAR 0.02390 ETINOX ppm  
Nozzle

==== INLETS==== eRam 1.0000 Afs -----  
Inlet -----  
==== DUCTS==== dProrm MN  
Duct1 0.0000  
ICduct 0.0020  
Duct6 0.0000  
Duct43 0.0000  
ITduct 0.0000  
Duct12 0.0000  
==== SHAFTS==== Nmech  
HP\_Shaft 13445.9  
LP\_Shaft 10789.4  
LP\_Shaft 15000.0  
==== BURNERS==== TtOut 2849.06 efi 1.0000  
Burner  
==== NOZZLES==== PR 1.050 Cfg 1.0000 Cdth 1.0000 Wfuel 0.31962 FAR 0.02390 ETINOX ppm  
Nozzle

==== INLETS==== eRam 1.0000 Afs -----  
Inlet -----  
==== DUCTS==== dProrm MN  
Duct1 0.0000  
ICduct 0.0020  
Duct6 0.0000  
Duct43 0.0000  
ITduct 0.0000  
Duct12 0.0000  
==== SHAFTS==== Nmech  
HP\_Shaft 13445.9  
LP\_Shaft 10789.4  
LP\_Shaft 15000.0  
==== BURNERS==== TtOut 2849.06 efi 1.0000  
Burner  
==== NOZZLES==== PR 1.050 Cfg 1.0000 Cdth 1.0000 Wfuel 0.31962 FAR 0.02390 ETINOX ppm  
Nozzle

==== INLETS==== eRam 1.0000 Afs -----  
Inlet -----  
==== DUCTS==== dProrm MN  
Duct1 0.0000  
ICduct 0.0020  
Duct6 0.0000  
Duct43 0.0000  
ITduct 0.0000  
Duct12 0.0000  
==== SHAFTS==== Nmech  
HP\_Shaft 13445.9  
LP\_Shaft 10789.4  
LP\_Shaft 15000.0  
==== BURNERS==== TtOut 2849.06 efi 1.0000  
Burner  
==== NOZZLES==== PR 1.050 Cfg 1.0000 Cdth 1.0000 Wfuel 0.31962 FAR 0.02390 ETINOX ppm  
Nozzle

==== INLETS==== eRam 1.0000 Afs -----  
Inlet -----  
==== DUCTS==== dProrm MN  
Duct1 0.0000  
ICduct 0.0020  
Duct6 0.0000  
Duct43 0.0000  
ITduct 0.0000  
Duct12 0.0000  
==== SHAFTS==== Nmech  
HP\_Shaft 13445.9  
LP\_Shaft 10789.4  
LP\_Shaft 15000.0  
==== BURNERS==== TtOut 2849.06 efi 1.0000  
Burner  
==== NOZZLES==== PR 1.050 Cfg 1.0000 Cdth 1.0000 Wfuel 0.31962 FAR 0.02390 ETINOX ppm  
Nozzle

==== INLETS==== eRam 1.0000 Afs -----  
Inlet -----  
==== DUCTS==== dProrm MN  
Duct1 0.0000  
ICduct 0.0020  
Duct6 0.0000  
Duct43 0.0000  
ITduct 0.0000  
Duct12 0.0000  
==== SHAFTS==== Nmech  
HP\_Shaft 13445.9  
LP\_Shaft 10789.4  
LP\_Shaft 15000.0  
==== BURNERS==== TtOut 2849.06 efi 1.0000  
Burner  
==== NOZZLES==== PR 1.050 Cfg 1.0000 Cdth 1.0000 Wfuel 0.31962 FAR 0.02390 ETINOX ppm  
Nozzle

==== INLETS==== eRam 1.0000 Afs -----  
Inlet -----  
==== DUCTS==== dProrm MN  
Duct1 0.0000  
ICduct 0.0020  
Duct6 0.0000  
Duct43 0.0000  
ITduct 0.0000  
Duct12 0.0000  
==== SHAFTS==== Nmech  
HP\_Shaft 13445.9  
LP\_Shaft 10789.4  
LP\_Shaft 15000.0  
==== BURNERS==== TtOut 2849.06 efi 1.0000  
Burner  
==== NOZZLES==== PR 1.050 Cfg 1.0000 Cdth 1.0000 Wfuel 0.31962 FAR 0.02390 ETINOX ppm  
Nozzle

==== INLETS==== eRam 1.0000 Afs -----  
Inlet -----  
==== DUCTS==== dProrm MN  
Duct1 0.0000  
ICduct 0.0020  
Duct6 0.0000  
Duct43 0.0000  
ITduct 0.0000  
Duct12 0.0000  
==== SHAFTS==== Nmech  
HP\_Shaft 13445.9  
LP\_Shaft 10789.4  
LP\_Shaft 15000.0  
==== BURNERS==== TtOut 2849.06 efi 1.0000  
Burner  
==== NOZZLES==== PR 1.050 Cfg 1.0000 Cdth 1.0000 Wfuel 0.31962 FAR 0.02390 ETINOX ppm  
Nozzle

==== INLETS==== eRam 1.0000 Afs -----  
Inlet -----  
==== DUCTS==== dProrm MN  
Duct1 0.0000  
ICduct 0.0020  
Duct6 0.0000  
Duct43 0.0000  
ITduct 0.0000  
Duct12 0.0000  
==== SHAFTS==== Nmech  
HP\_Shaft 13445.9  
LP\_Shaft 10789.4  
LP\_Shaft 15000.0  
==== BURNERS==== TtOut 2849.06 efi 1.0000  
Burner  
==== NOZZLES==== PR 1.050 Cfg 1.0000 Cdth 1.0000 Wfuel 0.31962 FAR 0.02390 ETINOX ppm  
Nozzle

==== INLETS==== eRam 1.0000 Afs -----  
Inlet -----  
==== DUCTS==== dProrm MN  
Duct1 0.0000  
ICduct 0.0020  
Duct6 0.0000  
Duct43 0.0000  
ITduct 0.0000  
Duct12 0.0000  
==== SHAFTS==== Nmech  
HP\_Shaft 13445.9  
LP\_Shaft 10789.4  
LP\_Shaft 15000.0  
==== BURNERS==== TtOut 2849.06 efi 1.0000  
Burner  
==== NOZZLES==== PR 1.050 Cfg 1.0000 Cdth 1.0000 Wfuel 0.31962 FAR 0.02390 ETINOX ppm  
Nozzle

==== INLETS==== eRam 1.0000 Afs -----  
Inlet -----  
==== DUCTS==== dProrm MN  
Duct1 0.0000  
ICduct 0.0020  
Duct6 0.0000  
Duct43 0.0000  
ITduct 0.0000  
Duct12 0.0000  
==== SHAFTS==== Nmech  
HP\_Shaft 13445.9  
LP\_Shaft 10789.4  
LP\_Shaft 15000.0  
==== BURNERS==== TtOut 2849.06 efi 1.0000  
Burner  
==== NOZZLES==== PR 1.050 Cfg 1.0000 Cdth 1.0000 Wfuel 0.31962 FAR 0.02390 ETINOX ppm  
Nozzle

==== INLETS==== eRam 1.0000 Afs -----  
Inlet -----  
==== DUCTS==== dProrm MN  
Duct1 0.0000  
ICduct 0.0020  
Duct6 0.0000  
Duct43 0.0000  
ITduct 0.0000  
Duct12 0.0000  
==== SHAFTS==== Nmech  
HP\_Shaft 13445.9  
LP\_Shaft 10789.4  
LP\_Shaft 15000.0  
==== BURNERS==== TtOut 2849.06 efi 1.0000  
Burner  
==== NOZZLES==== PR 1.050 Cfg 1.0000 Cdth 1.0000 Wfuel 0.31962 FAR 0.02390 ETINOX ppm  
Nozzle

==== INLETS==== eRam 1.0000 Afs -----  
Inlet -----  
==== DUCTS==== dProrm MN  
Duct1 0.0000  
ICduct 0.0020  
Duct6 0.0000  
Duct43 0.0000  
ITduct 0.0000  
Duct12 0.0000  
==== SHAFTS==== Nmech  
HP\_Shaft 13445.9  
LP\_Shaft 10789.4  
LP\_Shaft 15000.0  
==== BURNERS==== TtOut 2849.06 efi 1.0000  
Burner  
==== NOZZLES==== PR 1.050 Cfg 1.0000 Cdth 1.0000 Wfuel 0.31962 FAR 0.02390 ETINOX ppm  
Nozzle

==== INLETS==== eRam 1.0000 Afs -----  
Inlet -----  
==== DUCTS==== dProrm MN  
Duct1 0.0000  
ICduct 0.0020  
Duct6 0.0000  
Duct43 0.0000  
ITduct 0.0000  
Duct12 0.0000  
==== SHAFTS==== Nmech  
HP\_Shaft 13445.9  
LP\_Shaft 10789.4  
LP\_Shaft 15000.0  
==== BURNERS==== TtOut 2849.06 efi 1.0000  
Burner  
==== NOZZLES==== PR 1.050 Cfg 1.0000 Cdth 1.0000 Wfuel 0.31962 FAR 0.02390 ETINOX ppm  
Nozzle

==== INLETS==== eRam 1.0000 Afs -----  
Inlet -----  
==== DUCTS==== dProrm MN  
Duct1 0.0000  
ICduct 0.0020  
Duct6 0.0000  
Duct43 0.0000  
ITduct 0.0000  
Duct12 0.0000  
==== SHAFTS==== Nmech  
HP\_Shaft 13445.9  
LP\_Shaft 10789.4  
LP\_Shaft 15000.0  
==== BURNERS==== TtOut 2849.06 efi 1.0000  
Burner  
==== NOZZLES==== PR 1.050 Cfg 1.0000 Cdth 1.0000 Wfuel 0.31962 FAR 0.02390 ETINOX ppm  
Nozzle

==== INLETS==== eRam 1.0000 Afs -----  
Inlet -----  
==== DUCTS==== dProrm MN  
Duct1 0.0000  
ICduct 0.0020  
Duct6 0.0000  
Duct43 0.0000  
ITduct 0.0000  
Duct12 0.0000  
==== SHAFTS==== Nmech  
HP\_Shaft 13445.9  
LP\_Shaft 10789.4  
LP\_Shaft 15000.0  
==== BURNERS==== TtOut 2849.06 efi 1.0000  
Burner  
==== NOZZLES==== PR 1.050 Cfg 1.0000 Cdth 1.0000 Wfuel 0.31962 FAR 0.02390 ETINOX ppm  
Nozzle

==== INLETS==== eRam 1.0000 Afs -----  
Inlet -----  
==== DUCTS==== dProrm MN  
Duct1 0.0000  
ICduct 0.0020  
Duct6 0.0000  
Duct43 0.0000  
ITduct 0.0000  
Duct12 0.0000  
==== SHAFTS==== Nmech  
HP\_Shaft 13445.9  
LP\_Shaft 10789.4  
LP\_Shaft 15000.0  
==== BURNERS==== TtOut 2849.06 efi 1.0000  
Burner  
==== NOZZLES==== PR 1.050 Cfg 1.0000 Cdth 1.0000 Wfuel 0.31962 FAR 0.02390 ETINOX ppm  
Nozzle

==== INLETS==== eRam 1.0000 Afs -----  
Inlet -----  
==== DUCTS==== dProrm MN  
Duct1 0.00

TABLE H.6.—75 PERCENT DESIGN SPEED CRUISE

\*\*\*\*\*  
Date:05/24/11 Time:12:57:35 Model: AHS 2010 Govt turbohaft engine - 75% speed turbine - Cruise converge = 1 CASE: 101  
Version: NPSS\_2.3 Gas Package: Janaf iter/pass/Jacob/Broy= 53/ 75/ 2150 Run by: tm1862 = 1 PC: 50

SUMMARY OUTPUT DATA

MN	alt	dts	W	BSFC	Wfuel	VTAS	OPR	T4	T41	T47	Dyn_P.
0.510	28000.0	0.00	11.45	0.3147	736.90	511.85	39.986	2895.8	2663.6	2191.6	0.0

FLOW STATION DATA

FL1	InletStart.F1_0	W	Et	tt	FAR	WC	Ps	Ts	Aphy	MN	gramt	grams
FL2	Inlet.F1_0	5.705	440.66	440.66	0.0000	27.18	4.776	418.82	104.63	0.510	1.4010	1.4011
FL22	Duct1.F1_0	5.705	440.66	440.66	0.0000	27.18	5.155	428.07	130.50	0.383	1.4010	1.4010
FL23	LPC.F1_0	81.120	1022.86	116.60	0.0000	2.91	73.121	437.41	243.22	0.193	1.4010	1.4010
FL24	ICduct.F1_0	80.957	1022.86	116.60	0.0000	2.92	72.975	594.03	13.85	0.391	1.3793	1.3811
FL25	HPC_axi.F1_0	91.306	1061.40	126.33	0.0000	2.64	86.095	594.03	13.85	0.391	1.3793	1.3811
FL26	Bld25.F1_0	10.67	1061.40	126.33	0.0000	2.64	82.327	1044.44	16.07	0.293	1.3769	1.3780
FL27	HPC_centri.F1_0	10.67	1061.40	126.33	0.0000	2.64	82.327	1031.69	11.69	0.300	1.3769	1.3780
FL28	Bld3.F1_0	8.09	228.102	1405.52	0.0000	1.13	214.211	1382.50	6.70	0.306	1.3556	1.3570
FL3	Duct6.F1_0	8.09	228.102	1405.52	0.0000	1.13	214.211	1389.48	6.00	0.254	1.3556	1.3566
FL4	Burner.F1_0	8.50	223.540	2895.77	0.0000	0.86	221.811	1395.23	7.41	0.203	1.3556	1.3562
FL42	Duct43.F1_0	10.87	106.607	2246.15	0.0000	3.12	100.693	2832.95	6.24	0.397	1.2819	1.2837
FL43	Duct4.F1_0	10.87	106.607	2246.15	0.0000	3.12	100.693	2816.24	19.27	0.297	1.2819	1.2837
FL44	LPT.F1_0	11.65	29.200	1684.74	0.0179	10.57	28.373	1672.74	15.02	0.386	1.3053	1.3071
FL45	ITduct.F1_0	11.65	29.200	1684.74	0.0179	10.57	28.373	1672.74	15.02	0.386	1.3053	1.3071
FL6	PowerT.F1_0	5.015	1154.21	-187.21	0.0179	50.93	4.652	1131.49	278.41	0.334	1.3588	1.3603
FL7	Duct12.F1_0	5.015	1154.21	-187.21	0.0179	50.94	4.652	1131.49	278.41	0.334	1.3588	1.3603
FL9	Nozzle.F1_0	5.015	1154.35	-187.21	0.0179	50.94	4.776	1139.55	338.39	0.269	1.3588	1.3597

TURBOMACHINERY PERFORMANCE DATA

LPC	PR	0.8472	11869.667	2.3312	TR	efPolY	SMN	SMW
HPC_axi	PR	2.92	1.128	0.8938	-2291.4	17.98	18.02	
HPC_cen	PR	2.46	2.498	0.8938	-155.9	19.48	11.70	
HPT	PR	1.29	0.8499	0.8744	-1329.0	23.31	22.04	
LPT	PR	3.12	3.651	0.8301	1485.0			
PowerT	PR	10.157	5.823	0.8474	2351.3			

TURBOMACHINERY MAP DATA

LPC	WCMap	PRmap	effMap	NcMap	R/Param	S_McDes	s_effDes	s_NcDes
LPC	28.95	8.831	0.8549	98.914	1.8864	0.938796	0.9911	0.8333
HPC_axi	29.52	1.201	0.8554	0.984	1.9166	0.098842	1.0414	0.0001
HPC_cen	29.51	3.060	0.8520	0.984	2.0277	0.083218	1.0077	0.0001
HPT	30.15	5.995	0.9287	99.905	5.9954	0.042746	0.9152	0.0176
LPT	149.63	6.424	0.9247	100.763	6.4237	0.020843	0.9163	0.0192
PowerT	10.78	5.823	0.8690	4481.571	5.8226	0.980704	1.0000	1.0000

===INLETS===

Inlet	eRam	Afs	Fram	BLEEDS - output	Wb/Win	hscale	Pscale	W	Tt	ht	Pt
===DUCTS===	dProrm	MN	Aphy	C_LPTCharg	Bl>	0.0180	1.0000	0.2059	1061.40	126.23	91.306
Duct1	0.0000	0.3830	130.50	C_HPTUncharg	Bl>	0.502	1.0000	0.5744	1061.40	126.23	91.306
ICduct	0.0020	0.3905	13.85	C_HPTUncharg	Bl>	0.0819	1.0000	0.8734	1405.52	214.29	228.102
Duct6	0.0000	0.2545	6.00								
Duct43	0.0000	0.2972	19.27								
ITduct	0.0000	0.2083	90.09								
Duct12	0.0000	0.3341	278.41								

===SHAFTS===

IP_Shaft	Nmsch	trg_in	Pwr_in
IP_Shaft	13423.1	581.1	1485.0
LP_Shaft	10940.7	1099.9	2291.3
LP_Shaft	8077.0	1528.8	2351.1

===BURNERS===

Burner	TtOut	eff	dProrm	Wfuel	FAR	ETINOx	ppm
===NOZZLES===	PR	Cfg	Cdth	Cv	Ath	MNth	Vact
Nozzle	1.050	1.0000	1.0000	1.0000	305.32	0.269	438.3
							158.7

TABLE H.7.—85 PERCENT DESIGN SPEED TAKE OFF

*****										
Date:05/24/11	Time:13:47:18	Model:	AHS 2010 Govt turboshaft engine	-65% speed turbine	- Takeoff	converge = 1	CASE: 100	*****		
Version:	NPSS_2.3	Gas Package:	Janaf	iter/pass/Jacob/Broy=	7/ 29/ 2/ 4	Run by:	tm1862	*****		
SUMMARY OUTPUT DATA										
MN	alt	dTs	W	BSFC	Wfuel	VTAS	OPR	T4	T47	Dyn P.
0.000	0.0	45.00	26.67	0.3130	2513.91	0.00	42.293	3748.4	3459.4	2876.7 0.0
FLOW STATION DATA										
	W	Et	Tt	fc	FAR	WC	Ps	ApHy	Ts	gramt
FL1 InletStart.FI_O	26.67	14.696	563.67	4.62	0.0000	27.80	14.696	--	563.67	1.3995
FL2 Inlet.FI_O	26.67	14.696	563.67	4.62	0.0000	27.80	13.161	128.83	546.19	1.3995
FL22 Duct1.FI_O	26.67	14.696	563.67	4.62	0.0000	27.80	14.292	240.10	559.20	1.3995
FL23 LPC.FI_O	26.67	213.240	1303.06	187.88	0.0000	2.91	191.489	13.66	1266.28	1.3640
FL24 ICduct.FI_O	26.67	212.813	1303.06	187.88	0.0000	2.92	191.106	13.69	1266.28	1.3640
FL25 HPC_axi.FI_O	26.67	239.578	1349.89	199.81	0.0000	2.64	225.463	15.87	1328.41	1.3602
FL26 Bid25.FI_O	24.89	239.578	1349.89	199.81	0.0000	2.46	215.196	11.56	1312.09	1.3611
FL27 HPC_centri.FI_O	24.89	621.533	1788.60	316.56	0.0000	1.09	585.493	6.62	1761.87	1.3378
FL28 Bid3.FI_O	18.97	621.533	1788.60	316.56	0.0000	0.83	596.254	5.96	1761.87	1.3378
FL3 Duct6.FI_O	19.67	609.102	3748.43	252.28	0.0368	1.28	605.186	7.36	1776.63	1.3372
FL4 Burreir.FI_O	25.59	290.574	2946.75	148.62	0.0281	3.08	274.578	19.04	2810.05	1.2528
FL42 Duct43.FI_O	25.59	290.574	2946.75	148.62	0.0281	3.08	262.861	14.84	2810.05	1.2808
FL44 LPT.FI_O	27.37	83.903	2267.29	-26.44	0.0262	10.02	81.746	89.36	2213.48	1.3001
FL45 ITduct.FI_O	27.37	83.903	2267.29	-26.44	0.0262	10.02	75.655	47.81	2213.48	1.3001
FL6 PowerT.FI_O	27.37	15.431	1561.63	-229.40	0.0262	45.23	14.527	272.82	1538.35	1.3305
FL7 Duct12.FI_O	27.37	15.431	1561.63	-229.40	0.0262	45.23	14.527	272.82	1538.35	1.3305
FL9 Nozzle.FI_O	27.37	15.431	1561.69	-229.40	0.0262	45.23	14.696	300.63	1542.91	1.3292
TURBOMACHINERY PERFORMANCE DATA										
LPC	PR	NC	TR	efPoly	FWR	SMN	SMW			
LPC	27.80	14.510	2.3118	0.8844	-6907.8	20.09	19.67			
HPC_axi	2.92	1.126	0.8867	0.8884	-457.5	19.95	12.51			
HPC_cen	1.28	2.594	0.8577	0.8737	-4111.6	20.02	18.35			
HPT	3.08	250.842	1.1363	0.8162	4569.1					
LPT	3.08	230.450	1.2595	0.8238	6908.0					
PowerT	10.102	3.463	0.9357	0.8238	7859.2					
TURBOMACHINERY MAP DATA										
LPC	WcMap	PrMap	effMap	NcMap	R/Param	s_PRdes	s_effDes	s_NcDes		
LPC	30.00	8.994	0.8509	100.000	2.0028	1.6901	0.9909	0.8333		
HPC_axi	29.94	1.200	0.8515	0.998	1.9904	0.6285	1.0413	0.0001		
HPC_cen	29.93	3.192	0.8514	0.998	1.9942	0.7773	1.0074	0.0001		
HPT	30.15	5.976	0.9281	100.172	5.9760	4.5393	0.9152	0.0175		
LPT	149.76	5.999	0.9281	100.389	5.9991	0.020596	0.9163	0.0191		
PowerT	10.44	5.437	0.9357	7174.453	5.4374	1.0000	1.0000	1.0000		
===INLETS===										
Inlet	eRam	Afs	Fram	BLEEDS - output	Wb/Win	hscale	Pscale	Tt	ht	Pl
Inlet	1.0000	----	0.0	C_LPTCharg Bl>	0.0175	1.0000	1.0000	1349.89	199.81	239.578
===DUCTS===										
Duct1	dProrm	eff	dProrm	C_LPTUncharg Bl>	0.0493	1.0000	1.0000	1349.89	199.81	239.578
ICduct	0.0020	MN	128.83	C_HPTUncharg Bl>	0.0805	1.0000	1.0000	1788.60	316.56	621.533
Duct6	0.0000	0.4001	13.66	C_HPTUncharg Bl>	0.1572	1.0000	1.0000	1788.60	316.56	621.533
Duct43	0.0000	0.2500	15.96							
ITduct	0.0000	0.3006	19.04							
Duct12	0.0000	0.2008	89.36							
Duct12	0.0000	0.2008	272.81							
===SHAFTS===										
HP_Shaft	Nmech	trg_in	Fwr_in							
IP_Shaft	15357.7	1562.6	4569.1							
LP_Shaft	12509.7	2900.2	6908.0							
LP_Shaft	15000.0	2751.8	7859.2							
===BURNERS===										
Burner	TtOut	eff	dProrm	Wfuel	FAR	ETINOx	ppm			
Burner	3748.43	1.0000	0.0200	0.69831	0.03681					
===NOZZLES===										
Nozzle	PR	Cfg	Cdth	Cv	Ath	MNth	Vact	Fg		
Nozzle	1.050	1.0000	1.0000	1.0000	299.10	0.272	510.0	433.8		



TABLE H.9—85 PERCENT DESIGN SPEED CRUISE

*****														
Date:05/24/11 Time:13:47:20 Model: AHS 2010 Govt turbohaft engine - 65% speed turbine - Cruise converge = 1 CASE: 101														
Version: NPSS_2.3 Gas Package: Janaf iter/pass/Jacob/Broy= 41/ 74/ 3/37 Run by: tml1862 PC: 50														
SUMMARY OUTPUT DATA														
MN	alt	dts	W	Power	BSPC	Wfuel	VTAS	OPR	T4	T41	T47	Dyn_P		
0.510	28000.0	0.00	11.38	-21.3	0.3207	751.16	511.85	40.624	2927.6	2695.8	2218.6	0.0		
FLOW STATION DATA														
	W	Et	FR	tt	ht	FAR	WC	Ps	Ts	Aphy	MN	gramt	grams	
FL1 InletStart.FI_O	11.38	5.705	440.66	-24.88	0.0000	0.0000	27.01	4.776	418.82	103.97	0.510	1.4010	1.4011	
FL2 Inlet.FI_O	11.38	5.705	440.66	-24.88	0.0000	0.0000	27.01	5.147	427.87	128.83	0.386	1.4010	1.4010	
FL22 Duct1.FI_O	11.38	81.168	1023.71	-24.88	0.0000	0.0000	27.01	5.557	437.36	240.10	0.194	1.4010	1.4010	
FL23 LPC.FI_O	11.38	81.168	1023.71	116.81	0.0000	0.0000	2.89	73.031	994.35	13.66	0.394	1.3793	1.3811	
FL24 ICduct.FI_O	11.38	81.249	1061.96	116.81	0.0000	0.0000	2.62	82.885	994.35	13.69	0.394	1.3793	1.3811	
FL25 HPC_axi.FI_O	10.62	91.249	1061.96	126.37	0.0000	0.0000	2.45	85.937	1044.32	15.87	0.296	1.3769	1.3779	
FL26 Bid25.FI_O	10.62	231.744	1413.48	126.37	0.0000	0.0000	1.11	82.122	1031.71	11.56	0.394	1.3769	1.3788	
FL27 HPC_centri.FI_O	8.09	231.744	1413.48	126.37	0.0000	0.0000	1.11	217.828	1390.69	6.62	0.303	1.3552	1.3565	
FL3 Duct6.FI_O	8.09	231.744	1413.48	182.05	0.0000	0.0000	0.85	221.977	1397.60	5.96	0.253	1.3552	1.3561	
FL4 Burner.FI_O	10.82	227.109	2927.51	182.05	0.0000	0.0000	3.09	225.438	1403.30	7.36	0.202	1.3552	1.3558	
FL42 HPT.FI_O	10.82	107.897	2273.72	91.74	0.0197	0.0197	3.09	101.892	2863.94	19.04	0.397	1.2807	1.2825	
FL43 Duct43.FI_O	10.82	107.897	2273.72	91.74	0.0197	0.0197	3.09	97.496	2219.80	14.84	0.397	1.3041	1.3059	
FL44 LPT.FI_O	11.58	30.139	1712.83	-45.12	0.0183	0.0183	10.26	27.005	1667.01	89.36	0.204	1.3268	1.3289	
FL45 ITduct.FI_O	11.58	30.139	1712.83	-45.12	0.0183	0.0183	10.26	27.005	1667.01	47.81	0.409	1.3268	1.3289	
FL6 PowerT.FI_O	11.58	5.015	1181.43	-188.56	0.0183	0.0183	51.23	4.650	1156.80	272.82	0.345	1.3567	1.3583	
FL7 Duct12.FI_O	11.58	5.015	1181.43	-188.56	0.0183	0.0183	51.23	4.650	1156.80	272.82	0.345	1.3567	1.3583	
FL9 Nozzle.FI_O	11.58	5.015	1181.43	-188.56	0.0183	0.0183	51.23	4.776	1166.42	340.30	0.269	1.3567	1.3577	
TURBOMACHINERY PERFORMANCE DATA														
	PR	NC	TR	efPolY	SMN	SMW								
LPC	27.01	11892.165	2.3231	0.8911	18.83	18.78								
HPC_axi	2.90	9626.512	1.0374	0.8906	153.8	12.08								
HPC_cen	2.45	9451.543	1.3310	0.8737	-1351.8	20.55								
HPT	1.28	249.951	1.1489	0.8294	1505.6									
LPT	3.09	229.904	1.2862	0.8251	2280.3									
PowerT	10.26	195.161	1.4500	0.8136	2351.0									
TURBOMACHINERY MAP DATA														
	WcMap	PrMap	NCMap	R/Parm	S_McDes	s_Prdes	s_effDes	s_NcDes						
LPC	29.15	8.827	99.101	1.5218	0.526742	1.6901	0.9909	0.8333						
HPC_axi	29.74	1.201	0.992	1.9515	0.097488	0.6285	1.0413	0.0001						
HPC_cen	29.74	3.117	0.991	2.0221	0.082277	0.7773	1.0074	0.0001						
HPT	30.15	6.015	6.0153	0.042317	4.5393	0.0152	0.0175	0.0175						
LPT	149.85	6.236	100.151	6.2361	0.020596	2.0295	0.9163	0.0191						
PowerT	10.69	6.010	0.8471	6.0097	0.959975	1.0000	1.0000	1.0000						
===INLETS===														
Inlet	1.0000	103.97	181.0	BLEEDS - output	Wb/Win	hscale	Pscale	W	Tt	ht				
===DUCTS===	dPnorm	MN	Aphy	C_LPTCharg	Bl>	1.0000	1.0000	0.1990	1061.96	126.37				
ICduct	0.0020	0.3861	128.83	C_LPTUncharg	Bl>	1.0000	1.0000	0.5606	1061.96	126.37				
Duct6	0.0000	0.3940	13.66	C_HPTCharg	Bl>	1.0000	1.0000	0.8547	1413.48	216.37				
Duct43	0.0000	0.2527	19.04	C_HPTUncharg	Bl>	1.0000	1.0000	1.6692	1413.48	216.37				
ITduct	0.0000	0.2979	19.04											
Duct12	0.0000	0.2038	89.36											
Duct12	0.0000	0.3446	272.81											
===SHAFTS===														
HP_Shaft	13524.2	584.7	1505.6	trg_in										
LP_Shaft	10961.4	1092.6	2280.3	trg_out										
LP_Shaft	8077.0	1528.8	2351.0											
===BURNERS===														
Burner	TtOut	2927.61	1.0000	eff	dPnorm	Wfuel	FAR	ETINOX	ppm					
===NOZZLES===	PR	1.050	1.0000	Cfg	Cdth	1.0000	Cv	Ath	MNth	Vact	Fg			
Nozzle									0.269	443.6	159.7			

## References

1. Snyder, C. A. and Thurman, D. R., "Gas Turbine Characteristics for a Large Civil Tilt-Rotor (LCTR)," NASA/TM—2010-216089, February 2010.
2. D'Angelo, M., "Wide Speed Range Turboshaft Study," NASA CR-198380, August 1995.
3. Welch, G.E., "Assessment of Aerodynamic Challenges of a Variable-Speed Power Turbine for Large Civil Tilt-Rotor Application," *Proc. American Helicopter Society 66<sup>th</sup> Annual Forum*, Phoenix, AZ, May 11-13, 2010.
4. Kacker, S. C., and Okapuu, U., "A Mean Line Prediction Method for Axial Flow Turbine Efficiency," ASME 81-GT-58, 1981.
5. Moustapha, S.H., Kacker, S. C., and Tremblay, B., "Improved Incidence Losses Prediction Method for Turbine Airfoils," ASME 89-GT284, 1989.
6. Smith, S. F., "A Simple Correlation of Turbine Efficiency," *J. Royal Aero. Soc.*, 69, 1965, p. 467–470.

REPORT DOCUMENTATION PAGE			Form Approved OMB No. 0704-0188		
<p>The public reporting burden for this collection of information is estimated to average 1 hour per response, including the time for reviewing instructions, searching existing data sources, gathering and maintaining the data needed, and completing and reviewing the collection of information. Send comments regarding this burden estimate or any other aspect of this collection of information, including suggestions for reducing this burden, to Department of Defense, Washington Headquarters Services, Directorate for Information Operations and Reports (0704-0188), 1215 Jefferson Davis Highway, Suite 1204, Arlington, VA 22202-4302. Respondents should be aware that notwithstanding any other provision of law, no person shall be subject to any penalty for failing to comply with a collection of information if it does not display a currently valid OMB control number.</p> <p>PLEASE DO NOT RETURN YOUR FORM TO THE ABOVE ADDRESS.</p>					
<b>1. REPORT DATE (DD-MM-YYYY)</b> 01-02-2012		<b>2. REPORT TYPE</b> Final Contractor Report		<b>3. DATES COVERED (From - To)</b> October 2010 to March 2011	
<b>4. TITLE AND SUBTITLE</b> Variable-Speed Power-Turbine for the Large Civil Tilt Rotor			<b>5a. CONTRACT NUMBER</b> NNC10BA15B		
			<b>5b. GRANT NUMBER</b>		
			<b>5c. PROGRAM ELEMENT NUMBER</b>		
<b>6. AUTHOR(S)</b> Suchezky, Mark; Cruzen, G., Scott			<b>5d. PROJECT NUMBER</b>		
			<b>5e. TASK NUMBER</b> NNC10TA76T		
			<b>5f. WORK UNIT NUMBER</b> WBS 877868.02.07.03.01.02.01		
<b>7. PERFORMING ORGANIZATION NAME(S) AND ADDRESS(ES)</b> Williams International Co. LLC 2280 E. West Maple Road Walled Lake, Michigan 48390-0200			<b>8. PERFORMING ORGANIZATION REPORT NUMBER</b> E-18111		
<b>9. SPONSORING/MONITORING AGENCY NAME(S) AND ADDRESS(ES)</b> National Aeronautics and Space Administration Washington, DC 20546-0001			<b>10. SPONSORING/MONITOR'S ACRONYM(S)</b> NASA		
			<b>11. SPONSORING/MONITORING REPORT NUMBER</b> NASA/CR-2012-217424		
<b>12. DISTRIBUTION/AVAILABILITY STATEMENT</b> Unclassified-Unlimited Subject Categories: 01, 02, 03, and 07 Available electronically at <a href="http://www.sti.nasa.gov">http://www.sti.nasa.gov</a> This publication is available from the NASA Center for AeroSpace Information, 443-757-5802					
<b>13. SUPPLEMENTARY NOTES</b>					
<b>14. ABSTRACT</b> Turbine design concepts were studied for application to a large civil tiltrotor transport aircraft. The concepts addressed the need for high turbine efficiency across the broad 2:1 turbine operating speed range representative of the notional mission for the aircraft. The study focused on tailoring basic turbine aerodynamic design design parameters to avoid the need for complex, heavy, and expensive variable geometry features. The results of the study showed that good turbine performance can be achieved across the design speed range if the design focuses on tailoring the aerodynamics for good tolerance to large swings in incidence, as opposed to optimizing for best performance at the long range cruise design point. A rig design configuration and program plan are suggested for a dedicated experiment to validate the proposed approach.					
<b>15. SUBJECT TERMS</b> Variable-speed power turbine; Turbine aerodynamics; Low pressure turbines; turbomachinery design; Rotordynamics; Turbine performance; Large civil tilt-rotor					
<b>16. SECURITY CLASSIFICATION OF:</b>			<b>17. LIMITATION OF ABSTRACT</b>  UU	<b>18. NUMBER OF PAGES</b> 100	
<b>a. REPORT</b> U	<b>b. ABSTRACT</b> U	<b>c. THIS PAGE</b> U			
			<b>19a. NAME OF RESPONSIBLE PERSON</b> STI Help Desk (email:help@sti.nasa.gov)		
			<b>19b. TELEPHONE NUMBER (include area code)</b> 443-757-5802		



